The role of the glutathione system in regulating the levels of ROS neutralisation in the endothelial cells of the blood-brain barrier

Hanan Abd Elwahab

3577259

A thesis submitted in fulfilment of the requirements for the degree of

Magister Scientiae in the Department of Medical Biosciences,

University of the Western Cape.

Supervisor: Prof. D. Fisher

November 2017

DECLARATION

I, **Hanan Abd Elwahab**, declare that *The role of the glutathione system in regulating the levels of ROS neutralisation in the endothelial cells of the blood-brain barrier* is my own work, that it has not been submitted before for any degree or assessment in any other university, and that all the sources I have used or quoted have been indicated and acknowledged by means of complete references.

Hanan Abd Elwahab: 2017

Date Signed:

i

ACKNOWLEDGMENTS

To God, for granting me the opportunity to complete my MSc degree.

To my parents, for being a great example of compassion and perseverance.

Much gratitude is paid to my supervisor, Prof. D. Fisher, for his academic support and professional input throughout this process. Thank you for all the motivation and encouragement; it is greatly appreciated.

To Dr. Olufemi Alamu for meticulously guiding me and for willingly sharing his knowledge in the lab work with me.

To my neurobiology colleagues, Shireen Mentor, Mariama Rado, Omar Zbeda, Dr. Jegede Ayoola Isaac, and the greater Department of Medical Biosciences at the University of the Western Cape, thank you for the support.

To my husband thank you for your patience and supporting me through this academic chapter of my life.

My brothers and sisters, for always encouraging me to do and be my best.

In conclusion, I would like to thank my country without whom none of my work would have been possible.

ABSTRACT

Brain endothelial cell types are frequently used as *in vitro* models to study the blood-brain barrier (BBB). Oxidative stress (OS) has been reported numerous times to cause BBB dysfunction which is crucial to the initiation and or propagation of several neurologic disorders.

Glutathione (GSH) plays a significant role in the defence against OS in the brain endothelial cells. Therefore, the brain endothelial cell line bEnd.5 was profiled as an endothelium model of the BBB because of its natural GSH content, and its reactive oxygen species (ROS)-neutralising capacity in the presence and/or absence of a modest concentration (25 µM) of a standard antioxidant, Trolox. Fluorescent microscopy with monochlorobimane (mBCl) as a fluorescent probe was used for cellular GSH targeting. Furthermore, the GSH Glo^{TM} assay kit (Promega) and the mBCl fluorescent probe were used for the fluorometric measurement of intracellular GSH content and hydrogen peroxide (H_2O_2) was added as a quantifiable source of ROS. The quantity of GSH depletion and changes in cellular morphology at varying concentrations of H_2O_2 were compared with untreated cells.

mBCl fluorescence indicating the presence of GSH was demonstrated in bEnd5 cells, and its intensity was variable among the cells which is suggestive of differences in individual cell redox status and viability. The cytoplasmic extensions of the cells showed the presence of GSH which underscores the dependence of its viability on the presence of GSH. Micrographs show that the nuclear membrane has a high localisation of GSH which could be indicative of the important role GSH plays in protecting Deoxyribonucleic acid (DNA) from OS. In a proliferation study,

iii

bEnd5 cell growth was shown to increase after 24 hours; its doubling time increased from 15.66 hours within the first 24 hours to 11 hours within the second 24 hours. This is important for the accurate estimation of cellular GSH after 24 hours that is allowed for attachment in culture. The normal GSH content in a bEnd5 cell-line was extrapolated to be 0.031 ± 0.00035 nmol.cell^{-1} and 0.00092 ± 0.00021 nmol.cell^{-1} for glutathione disulfide (GSSG). The basal thiol redox status GSH:GSSG ranged from 94:6 to 97:3 over an extended cell culture period of 24-96 hours. Cellular GSH content, with and without exogenous antioxidant, was well buffered and was neutralised at 50, 150, 250 and 500 µM H_2O_2 concentration. Cell growth up to this H_2O_2 concentration were comparable to controls but from 1 mM up to 2.5 mM H_2O_2 growth changes were observed, while the addition of the antioxidant Trolox allowed for the maintenance of normal cell growth to be extended up to 1 mM H_2O_2. *De novo* GSH synthesis was maximally initiated in a switch-like fashion at the slightest oxidative challenge. At the point of cellular growth compromise, approximately 30-35% of the total GSH remained unavailable for ROS neutralisation. In the study, we showed that bEnd5 cell line contains substantial amounts of GSH with the capability of neutralising a higher magnitude of ROS compared to several varieties of cells as shown in similar studies. Furthermore, factors that can facilitate the access to the latent GSH content of the cells will enhance cellular ROS-neutralising capacity.

KEYWORDS

Blood-brain barrier

Glutathione

bEnd5 mouse brain endothelial cells

Reactive oxygen species

Hydrogen peroxide

Monochlorobimane

Trolox

The role of the glutathione system in regulating the levels of ROS

neutralisation in the endothelial cells of the blood-brain barrier.

LIST OF SELECTED ABBREVIATIONS

A

AJ   -   Adherens junctions

AO   -   Antioxidant

ARE   -   Antioxidant response element

ATP   -   Adenosine triphosphate

B

BBB   -   Blood-brain barrier

BEC   -   Brain endothelial cell

bEnd5   -   Mouse brain endothelium

BM   -   Basement membrane

BMECs   -   Brain microvascular endothelial cells

C

CNS   -   Central nervous system

CO_2 -   Carbon dioxide

Cys   -   Cysteine

_D_

DABCO   -   (1, 4-diazabicyclo-[2,2,2]-octane)

ddH$_2$O   -   Double distilled water

DMEM   -   Dulbecco's modified eagle medium

DNA   -   Deoxyribonucleic acid

_E_

ECs   -   Endothelial cells

Enos   -   Endothelial nitric oxide synthase

EpRE   -   Electrophile response element

_F_

FBS   -   Fetal bovine serum

_G_

GCL   -   Glutamylcysteine ligase

GCLC   -   Glutamylcysteine ligase catalytic

GCLM   -   Glutamylcysteine ligase modulatory

GFAP   -   Glial fibrillary acid protein

GGT   -   γ-glutamyltranspeptidase

Glu   -   Glutamate

Glut   -   Glucose transporters

GLUT-1   -   Glucose transporter 1

Gly   -   Glycine

Gpx   -   Glutathione peroxidase

GS   -   Glutathione synthetase

GSB   -   Glutathione S-bimane

GSH   -   Glutathione

GSH_T -   Total glutathione

GST   -   Glutathione S-transferase

GSSG   -   Glutathione disulfide

_H_

H_2O_2 -   Hydrogen peroxide

_J_

JNK   -   Jun N-terminal kinases
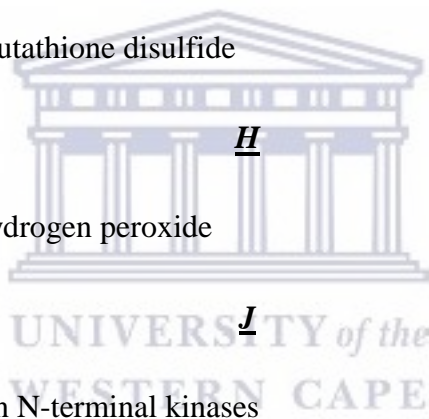
_K_

KH_2PO_4 -   Potassium phosphate (monobasic)

KOH   -   Potassium hydroxide

_L_

Luc-NT   -   Luciferin derivative

_M_

M   -   Molar

viii

mBCl	-	Monochlorobimane
MMPs	-	Matrix metalloproteinases

N

n	-	Sample number
NAC	-	N-Acetyl-L-Cysteine
NaCl	-	Sodium chloride
NADPH	-	Nicotinamide adenine dinucleotide phosphate
NEAA	-	Non-essential amino acids
NFkB	-	Nuclear factor Kappa B
Nrf2	-	Nuclear factor erythroid 2-related factor 2
NVU	-	Neurovascular unit

O

O_2^-	-	Superoxide
OS	-	Oxidative stress

P

P 38-MAPK	-	P38 mitogen-activated protein kinases
PBS	-	Phosphate buffer saline
Ph	-	"Power" of hydrogen (scale for measuring acidity and basicity)
pMBMEC	-	Primary mouse brain microvascular endothelial cell
PTKs	-	Protein tyrosine kinases

ix
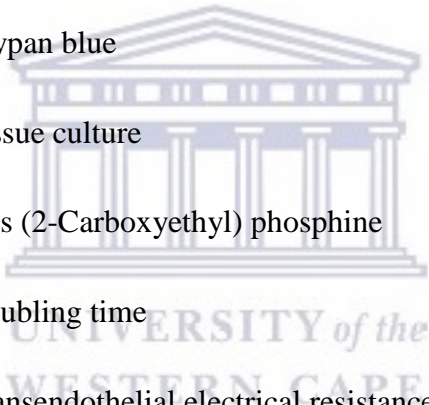
R

RLU   - Relative luminescence unit

ROS   - Reactive oxygen species

S

SDS   - Sodium dodecyl sulfate

SEM   - Standard error of mean

T

TB   - Trypan blue

TC   - Tissue culture

TCEP   - Tris (2-Carboxyethyl) phosphine

Td   - Doubling time

TER   - Transendothelial electrical resistance

TGF-ß   - Tissue growth factor beta

TJ   - Tight junction

TNF α   - Tumour necrosis factors alpha

Z

ZO   - Zonula occludens

ZO-1   - Zonula occludens-1

ZO-2   - Zonula occludens-2

x

ZO-3   - Zonula occludens-3

γ-GCS   - Gamma-glutamylcysteine synthetase

γ-GluCys   - Gamma-glutamylcysteine

TABLE OF CONTENTS

LIST OF FIGURES

LIST OF TABLES

CHAPTER ONE

Literature review

1.1   Glutathione

1.1.1   Discovery of glutathione

In 1888, glutathione (GSH) was discovered by de Rey Pailhade in yeast cells (Aoyama *et al*., 2008). He called GSH "philothione" (from the Greek words signifying "love" and "sulfur") because of its ability to reduce sulphur to hydrogen sulphide (Aoyama & Nakaki, 2013). In 1924, F.G. Hopkins reported this substance as a dipeptide comprising cysteine acid and glutamate, which he called "glutathione", but it is, in fact, a tripeptide, consisting of glutamate, cysteine, and glycine (Aoyama & Nakaki, 2013; Aoyama *et al*., 2008). In the 1930s its structure was identified and was later recognised as "the most important non-protein thiol" (Aoyama & Nakaki, 2013; Aoyama *et al*., 2008).

GSH's reaction to gluten in wheat was useful in weakening the strength of bread dough for baking. However, in living cells the significance of GSH function did not receive much attention until the 1970s, when a number of studies on GSH-related biochemical reactions and its metabolism emerged (Aoyama & Nakaki, 2013; Aoyama *et al*., 2008). Many studies on GSH have been published indicating its involvement in pivotal cellular physiological processes, e.g., antioxidant defence,

1

detoxication of xenobiotics, intracellular redox homeostasis, Cys carrier/storage, cell signalling, protein function, gene expression and cell differentiation/proliferation. GSH, L-γ-glutamyl-L-cysteinyl-glycine, is the predominant low-molecular-weight thiol compound present in almost all eukaryotic cells and is crucial to neutralise reactive oxygen species (ROS) molecules and to prevent cellular damage (Aoyama & Nakaki, 2013).

1.1.2 Glutathione synthesis

GSH is synthesised intracellularly from its amino acids in two consecutive steps by the consecutive action of two adenosine triphosphate (ATP)-dependent enzymes; γ-glutamylcysteine synthetase (γ-GCS, also known as a γ-glutamylcysteine ligase (γ-GCL) and glutathione synthetase (GS). Both enzymes are cytosolic. The first step in GSH syntheses is mediated by γ-GCS which utilise glutamate (Glu) and Cys as substrates forming the dipeptide γ-glutamylcysteine (γGluCys).

L-glutamate + L-cysteine + ATP $\xrightarrow{\text{GCL}}$ γ-L-glutamyl-L-cysteine + ADP + Pi.

[Reaction 1]

This reaction is the rate-limiting step in glutathione synthesis (Dringen, 2000; Li, *et al*. 2012). During the GCS reaction, the γ-carboxyl group of glutamate interacts with the amino group of Cys to form a peptidic γ-linkage, which shields GSH from hydrolysis by intracellular peptidases (Wu *et al*., 2004). The mammalian GCL is a heterodimer enzyme comprising approximately 73-kDa catalytic (heavy) subunit, GCLC, and approximately 28-kDa modulatory (light) subunit, GCLM. Only GCLC

2

has all the enzymatic activity which is subject to feedback from GSH. GCLM has no enzymatic action; on the other hand, the relationship of GCLM with GCLC diminishes the K_m value (concentration of the substrate which allows the enzyme to achieve half maximal reaction rate) for glutamate and increases the K_l value (inhibition constant, defined as the concentration of the inhibitor required to produce half maximal inhibition of a reaction rates) for the feedback hindrance of GSH (Aoyama & Nakaki, 2013). In the second step, the γGluCys is consolidated with glycine (Gly) in a reaction catalysed by GS to form GSH (Fig 1.1 and Reaction 2) (Wu *et al*., 2004). The GSH pathway occurs in virtually all cell types.

γ-L-Glutamyl-L-cysteine +Glycine+ ATP $\xrightarrow{\text{GS}}$ -L-glutamyl-L-cysteinyl-glycine + ADP + Pi (Dickinson & Forman, 2002)
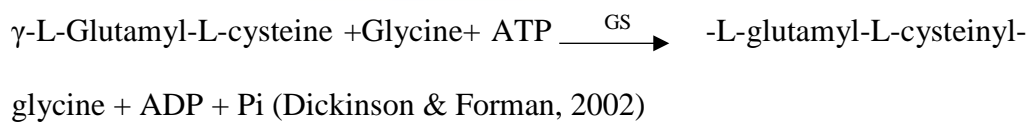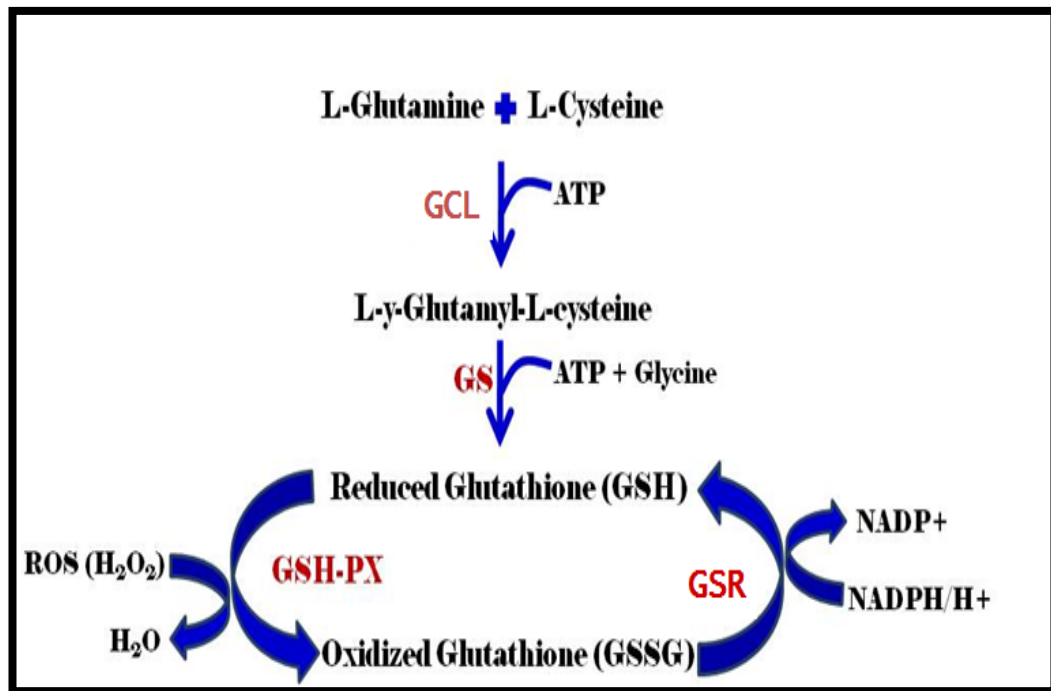
[Reaction 2]

Figure 1.1: Glutathione formation and recycling. The production of GSH occurs by two mechanisms. *De novo* synthesis which occurs in a two-step reaction catalysed by two separate enzymes, GCL and GS; and recycling of GSSG via the glutathione reductase (GSR) enzyme, a reaction requiring nicotinamide adenine dinucleotide phosphate (NADPH). During oxidative stress, GSH is utilised to neutralise reactive oxygen species leading to the formation of GSSG (Guilford & Hope, 2014).

1.1.3   Current concepts: structure and functions of GSH

Cellular glutathione exists in two forms: the thiol-reduced GSH and glutathione disulfide oxidised form (GSSG). Eucaryotic cells have three major repositories of GSH. Almost 90% of cellular GSH is found in the cytosol, while 10% is found in the mitochondria and an insignificant minute amount in the endoplasmic reticulum (Lu, 1999, 2009). In the endoplasmic reticulum, where GSH is implicated in protein

disulfide bond shaping the GSH to GSSG proportion is 3:1, while in the cytoplasm and mitochondria, proportions surpass 10:1 (Lu, 1999).

The peptide bond linking glutamate and Cys of GSH is through the γ-carboxyl group of glutamate instead of the routine α-carboxyl group (Fig 1.2). This unusual arrangement is subject to hydrolysis by only one known enzyme, called γ-glutamyltranspeptidase (GGT), which is just present on the external surfaces of certain cell types. As a result, GSH is resistant to intracellular degradation and is exclusively metabolised extracellularly by tissues with GGT (Lu, 1999). GSH serves several functions which include 1) detoxifying electrophiles; 2) scavenging free radicals; 3) maintaining the essential thiol status of proteins; 4) providing a reservoir for Cys; and 5) modulating critical cellular processes such as DNA synthesis, microtubule-related processes, and immune function (Lu, 2009).

At the blood-brain barrier (BBB) level, GSH has been revealed to play an important role in maintaining its integrity (Agarwal & Shukla, 1999). GSH has been shown to protect against the compromising tight junction (TJ) proteins (Song *et al*., 2014).
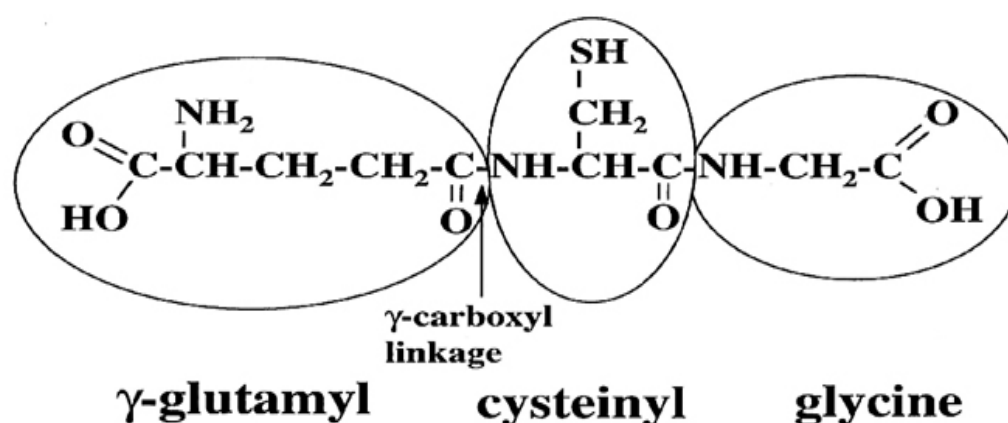
Figure 1.2: The structure of glutathione - γ-glutamyl cysteinyl glycine (Lu, 2009).

1.1.3.1 Detoxifying functions of GSH

Detoxification of xenobiotics or their metabolites is one of the significant functions of GSH. These compounds are electrophiles or electron-acceptor substances and they are structurally conjugated with GSH either spontaneously or enzymatically in interactions catalysed by GSH-S-transferase (Lu, 2009). The conjugates formed are usually excreted from the cell or into bile as in the case of hepatocytes.

The metabolism of GSH conjugates starts with cleavage of the γ-glutamyl moiety by GGT, leaving a cysteinyl-glycine conjugate. The cysteinyl-glycine bond is then severed by dipeptidase, resulting in a cysteinyl conjugate (Lu, 2009). This is followed by N-acetylation of the cysteine conjugate, forming a mercapturic acid (Fig 1.3), which starts either in the gall bladder, intestine, or kidney. However, the formation of the N-acetylcysteine conjugates mostly occurs in the kidney (Lu, 2009). Numerous endogenously formed conjugated compounds follow similar metabolic pathways as exogenous compounds. Most of the conjugated molecules that interact with GSH result in the detoxification of the compound, which could also be highly reactive (Lu, 2009).

http://etd.uwc.ac.za

$$X + \gamma\text{-Glu-CySH-Gly}$$

$$\downarrow \text{GSH S-transferase}$$

$$\gamma\text{-Glu-CyS-Gly}$$
$$|$$
$$X$$

$$\gamma\text{-Glu} \leftarrow \downarrow \gamma\text{-glutamyltranspeptidase}$$

$$\text{CyS-Gly}$$
$$|$$
$$X$$

$$\text{Gly} \leftarrow \downarrow \text{Dipeptidase}$$

$$\text{CyS-X}$$

$$\downarrow \text{N-acetylase}$$

$$\text{N-acetyl-Cys-X (mercapturic acid)}$$
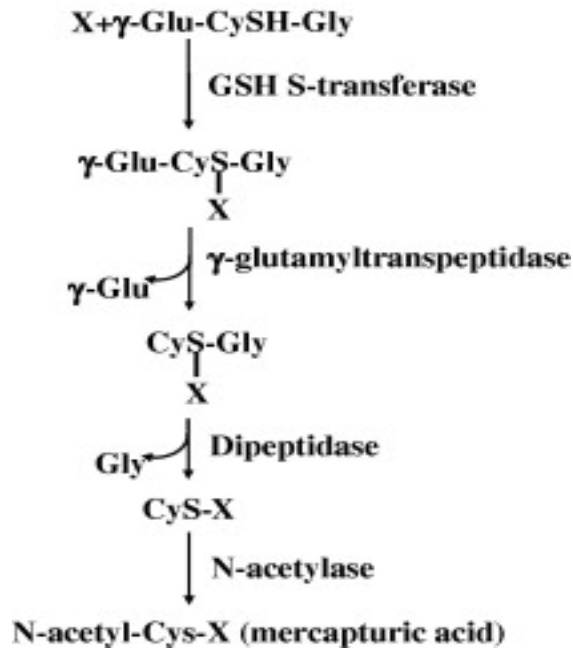
Figure 1.3: Detoxifying action of GSH through the mercapturic pathway (Lu, 2009).

1.1.3.2 Antioxidant function of GSH

All aerobic organisms are subject to a certain level of physiological OS from metabolic processes. The intermediates that are formed, such as superoxide (O_2^-) and hydrogen peroxide (H_2O_2), can prompt the generation of toxic oxygen radicals that can bring about lipid peroxidation and cell injury (Garcia-Ruiz & Fernandez-Checa, 2006). To prevent this, the endogenously produced H_2O_2 is lessened by GSH in the presence of selenium-dependent GSH peroxidase. In the process, GSH is oxidised to GSSG, which thus is reduced to GSH by GSSG reductase at the expense of NADPH, forming a redox cycle.

7

Hydrogen peroxide is catabolised and converted to water through the oxidation of GSH to GSSG by GSH peroxidase (Fig 1.4) (Lu, 2009). Either GSH peroxidase or GSH S-transferase can decrease organic peroxides. Hydrogen peroxide can likewise be decreased by catalase, which is available exclusively in the peroxisomes. In the mitochondria, GSH is especially important because there is no catalase. Thus, mitochondrial GSH is crucial in defending against physiologically and pathologically generated OS (Garcia-Ruiz & Fernandez-Checa, 2006).

Serious OS can exceed the ability of the cell to reduce GSSG to GSH leading to an accumulation of GSSG. To protect the cell from a detrimental shift in the redox equilibrium, GSSG can be actively exported from the cell or react with a protein sulfhydryl group (PSH) leading to the formation of a mixed disulfide (PSSG). Thus, severe OS exhausts cellular GSH (Lu, 2009).
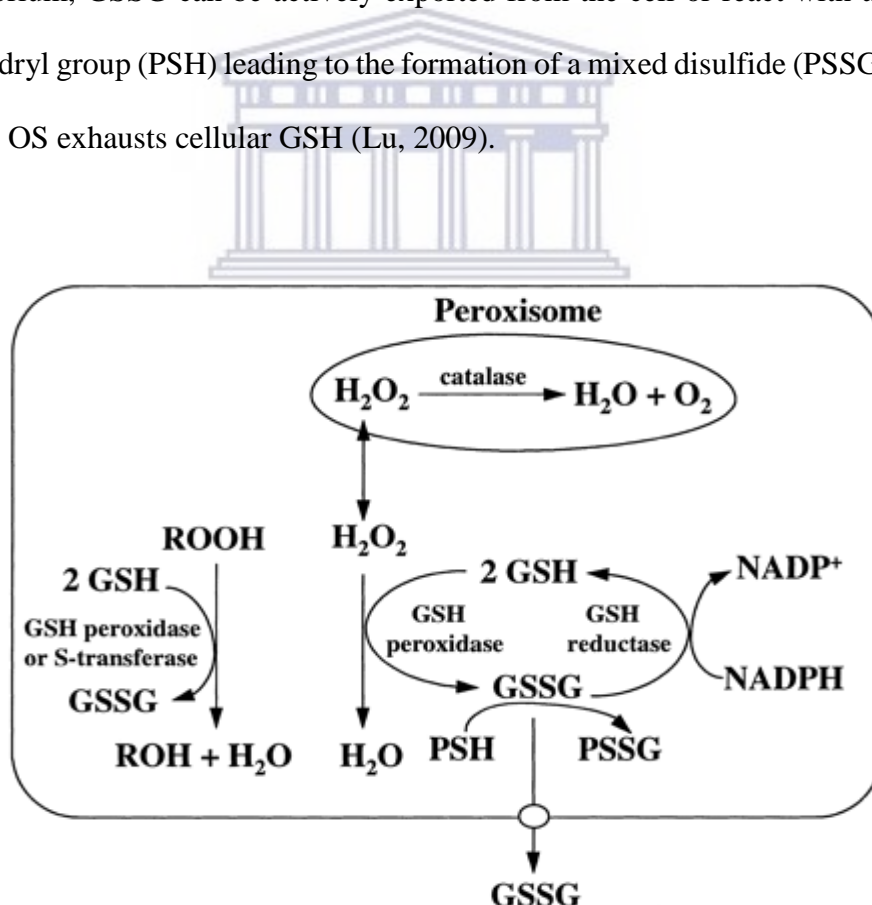
Figure 1.4: The antioxidant function of GSH **(Lu, 2009)**

1.1.3.3 Glutathione's role in cell proliferation

Glutathione plays a crucial role in the cell proliferation process and glutathione has been shown to be involved in the proliferation of many different cells, e.g., human fibroblast cells, hepatocytes, intestinal epithelial cells, lymphocytes, and mouse bone marrow cells (Ashtiani *et al*., 2013). GSH is able to affect cell proliferation in various ways, and as an intracellular antioxidant has a key role in factors activating regulation like P38 mitogen-activated protein kinases (P38-MAPK) and Jun N-terminal kinases (JNK). Also, this role has a direct relationship with intracellular GSH concentration. When the intracellular GSH concentration increases, activation of P38-MAPK and JNK can be inhibited (Cuadrado *et al*., 2003).

GSH acts as an inhibitor for alkyl agents, for example, N-methyl-N-nitro-N-nitrosoguanidine methyl and methane sulfonate. Through this inhibition, the activated P38-MAPK, JNK, and B-cell lymphoma 2 anti-apoptosis lead to apoptosis inhibition and increased proliferation (Cuadrado *et al*., 2003).

The relationship between the GSH and ROS is one of the most influential metabolic processes influencing cell proliferation. ROS, particularly O_2 and H_2O_2 play a key role in cellular death and proliferation (Ashtiani *et al*., 2013). These elements usually stimulates cellular growth in sub-micromolar concentration, whereas, at high concentrations (between 10 to 30 µM), they can result in apoptosis and necrosis (Ashtiani *et al*., 2013).

Indeed, the high concentration of this compound causes activation of transcription factors like the nuclear factors erythroid 2-related factor 2 and Kappa B (NF-κB)

9

and mitogen-activated protein kinases. Cellular death follows while low concentrations cause activation of different transcription factors, like antioxidant response element (ARE) (for example nuclear factor erythroid 2 Nrf2) (Day & Suzuki, 2005). The ARE transcription factor has a role in the enzyme γ-GCS gene expression regulation. This enzyme catalyses the rate-limiting step in GSH synthesis is in response to a xenobiotic. The result of this activation occurs after cellular proliferation, because of the increase of the GSH concentration (Day & Suzuki, 2005). GSH can affect tumour necrosis factor-α (TNF-α) too. TNF-α is a cytokine that is released by macrophage - monocyte cells which play an important role in infection and immunology. Cytokine TNF-α hasmany roles to play in biologics like antitumour and cellular proliferation inhibitor (Ashtiani *et al*., 2013).
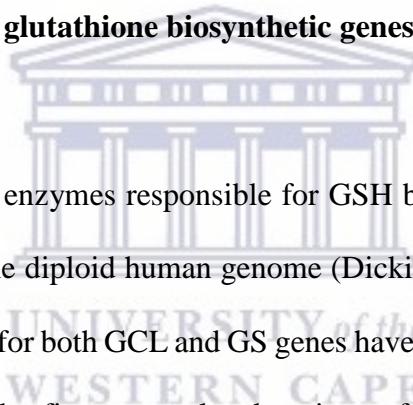
1.1.4 Endothelial GSH and S-glutathiolation in the control of vascular integrity
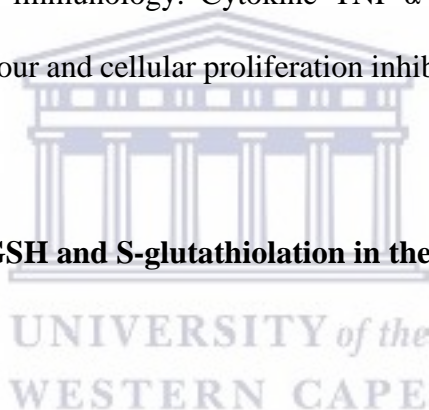
GSH influences vascular endothelial function, by affecting endothelial barrier permeability, angiogenesis, chemotaxis, cell apoptosis, constitutive and agonist-induced adhesion molecule expression, endothelial-dependent vasodilation and leukocyte-endothelial adhesion responses (Li *et al*., 2012). The modulatory impact of GSH is accomplished through the scavenging of ROS, a crucial second messenger in numerous endothelial functions. For example, GSH appeared to attenuate H_2O_2-induced decrease in transendothelial electrical resistance by means of the negative regulation of the p38-MAP kinase, which affects cell signalling with consequent cytoskeletal changes (Li *et al*., 2012).

10

Under different circumstances such as in the presence of non-radical toxic molecules, GSH acts as a substrate for the detoxification enzymes, GSH S-transferase and GSH peroxidase (Li *et al*., 2012). The role of S-glutathionylation in redox regulation of vascular function has been supported by a large body of evidence, ranging from cell signalling, protein folding and apoptosis, to cytoskeletal reorganisation. For example, in hypertensive vessels, the thiolation of endothelial nitric oxide synthase (eNOS) is essential in the redox control of vascular tone (Tousoulis *et al*. 2012).

1.1.5 Regulation of glutathione biosynthetic genes

Each of the three key enzymes responsible for GSH biosynthesis is encoded by a single-copy gene in the diploid human genome (Dickinson & Forman, 2002). The complementary DNA for both GCL and GS genes have been cloned, and sequenced (Gipp *et al*. 1995). The five untranslated regions of both genes have been also cloned, sequenced and further elucidated for regulatory components that could mediate transcription in response to a stimulus. (Moinova & Mulcahy, 1998).

Many elements, including those creating glutathione conjugates and those generating ROS, have been reported to stimulate GSH biosynthesis via increment transcription of GCL genes (Wild & Mulcahy, 2000). Sequence analysis and experimental manipulations employing reporter constructs of the five untranslated regions for human GCLC and GCLM genes have revealed several putative enhancer components. These could mediate, either alone or in combination, an

11

increase in transcription in reply to the binding of transcription factors, whose activity has been increased in response to a stimulus signalled by the presence of some element (Dickinson & Forman, 2002). The GCLC promoter contains numerous potential cis-acting compounds, including consensus recognition sites for binding of Sp-1, activator protein-1(TRE), TRE-like, activator protein-2, nuclear factor kappa B (NFkB), and the electrophile response element (EpRE, sometimes called the ARE) binding complexes (Dickinson & Forman, 2002). The GCLM promoter is activated by a large number of the same compounds, which also activate the GCLC promoter, with the notable exception of the kappa B compound. Of the above-mentioned enhancer components, those that have received the most attention have been TRE or TRE-like elements and EpRE elements. The part of these components in intervening GCL transcription in response to different stimuli has been reviewed previously (Dickinson & Forman, 2002).

GSH is one of the most abundant naturally occurring thiol-based antioxidant (AO) within mammalian cells. GSH play pivotal role in the cellular mitigation of OS among other functions such as oxidation-reduction reactions in metabolic pathways and redox signaling (Abegg *et al.*, 2012). Although, in some other cell types the presence of GSH, GSH content and its capacity to fight ROS has been established, it has not been scientifically reported in the brain endothelial cells or cell lines.
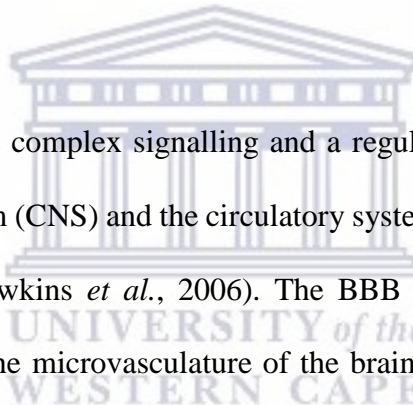
1.1.6 Trolox

Trolox (6-hydroxy-2,5,7,8-tetramethylchroman-2-carboxylic acid) is an exogenous antioxidant derived from water-soluble vitamin E, which penetrates biomembranes

12

and protects mammalian cells from oxidative damage. Trolox, a chain-breaking antioxidant, acts as a scavenger of radicals via the H-donating group in its chromanol nucleus. Furthermore, it is used in biochemical or biological applications to reduce OS or damage (McClain et al., 1995). Trolox, which has high AO potential, has been shown to reverse certain detrimental effects of EtOH on the BBB (Ramirez *et al*., 2009).

1.2 Blood-brain barrier

1.2.1 Overview

The BBB is an active complex signalling and a regulatory interface between the central nervous system (CNS) and the circulatory system, which insulates the brain from the plasma (Hawkins *et al.*, 2006). The BBB is a specialised endothelial structure that forms the microvasculature of the brain, also prohibits the entry of harmful blood-borne substances into the brain microenvironment, such as many toxic compounds and pathogens (Abbott *et al*., 2010). Furthermore, it functions by controlling the exchanges of substances such as molecules, ions and immune cells that take place between the brain and the blood circulation, and thus is primarily responsible for the maintenance of the CNS homeostasis.

The brain microvascular endothelial cells (BMECs) paracellular pathway is regulated by TJs (Furuse & Tsukita, 2006). Thus, barrier properties of the BBB are contributed mainly by the specialised endothelial cells (ECs) of the CNS microvasculature (Abbott *et al*., 2010). The BBB is indicative of a barrier that

demonstrates exceptionally regulatory epithelial and endothelial properties (Malaeb *et al*., 2012).

The BBB regulates the entry of water and ions, and a number of nutrients including small lipophilic molecules as well as regulated transported via receptor-mediated transcytosis (e.g. glucose, some amino acids, heparin, and transferrin). Under normal physiological conditions of the CNS, and because of the BBB permeability, plasma-borne macromolecules, and most cellular elements are restricted from crossing the BBB (Lossinsky & Shivers, 2004; Malaeb *et al*., 2012).

The BBB exists in all brain regions, excluding the circumventricular organs. These including the median eminence, neurohypophysis, pineal gland, sub-fornical organ, and lamina terminalis. These capillaries possess fenestrations which allow for diffusion of blood-borne molecules across the vessel wall. This allows the autonomic areas of the brain to sense variables of blood plasma, such as the concentrations of carbon dioxide (CO_2), H^+ ions glucose concentration, and lipostatic status of blood. These unprotected areas of the brain are an important interface (with the blood) responsible for the regulation of the autonomic nervous system and endocrine glands of the body. The latter allowing secretion of hormones into the blood to regulate distal anatomical and physiological systems (Cardoso *et al*., 2010; Malaeb *et al*., 2012).

14

1.2.2 Anatomical structure of the blood-brain barrier

The BBB endothelium of mammals, including humans, is created by thin, flat cells known as brain endothelial cells (BEC) that form walls of the cerebral capillaries (Pfeiffer *et al*., 2011). The layers between the blood and brain: consist of the EC capillaries, a basement membrane (BM) covering the outside capillaries, and specialised cells, called pericytes, between the endothelium and the BM, and astrocyte "foot-like" processes that are confined to the outside of the BM. Each of these components could potentially play a role in restricting the movement of solutes by regulating the trans endothelial permeability (Pfeiffer *et al*., 2011). The brain capillary endothelium interact with other cell types of the neurovascular unit (NVU), such as astrocytes, pericytes, perivascular microglia, and neurons to regulate the transport of substances across the BBB (**fig 1.5**) (Nakagawa *et al*., 2007; Yang *et al*., 2007).
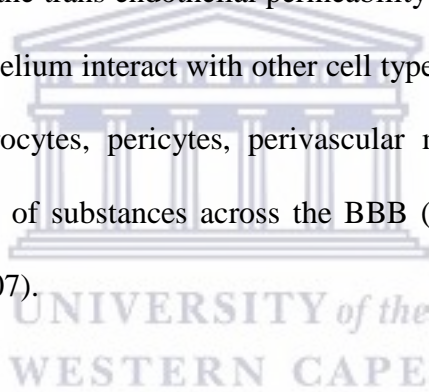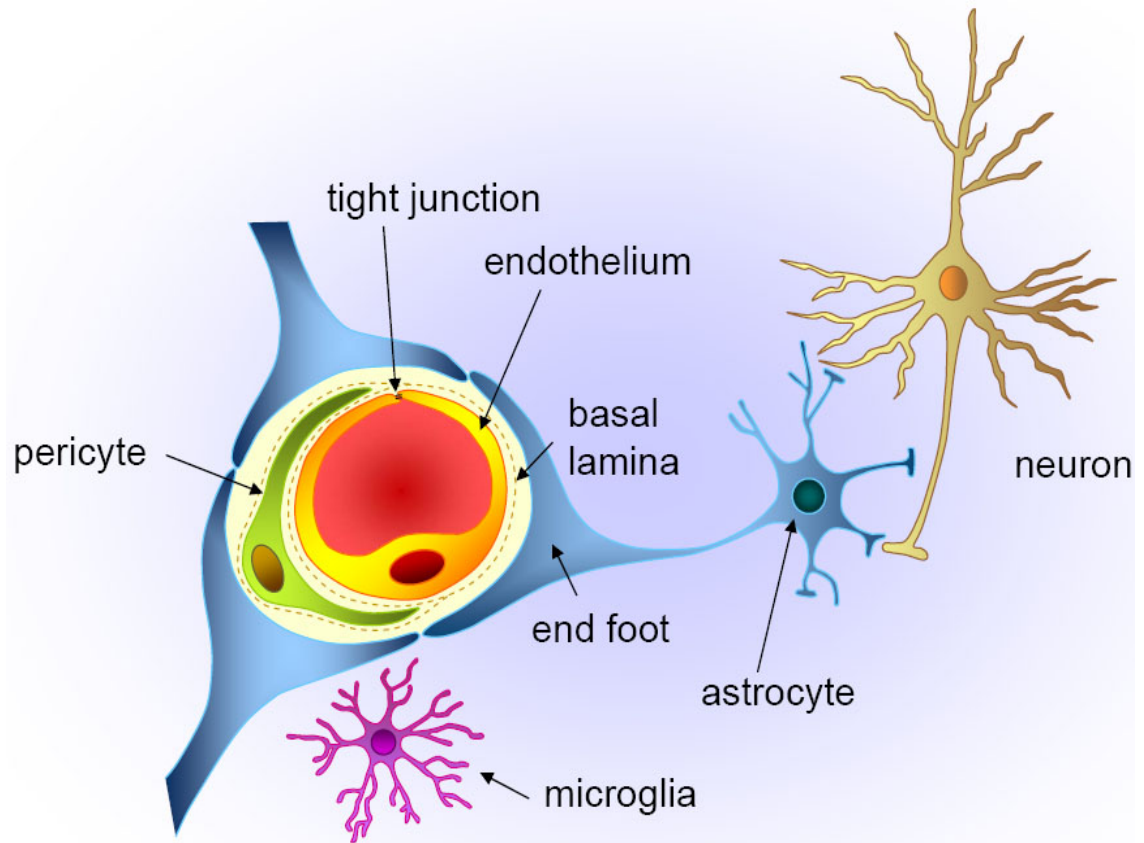
Figure 1.5: Schematic representation of the cross-section NVU of the BBB (Abbott *et al*., 2006). The NVU consists of the primary endothelial cells which are regulated by the astrocyte (end feet) and pericytes.

Brain endothelial cells are the key component controlling the BBB permeability, but interactions with astrocytes and pericytes are essential for the regulation of barrier function. For the explanation of these functions of the astrocytes and pericytes see Sections 1.2.2.3 and 1.2.2.4. (Kaur & Ling, 2008; Wolburg & Lippoldt, 2002).

1.2.2.1 Basement membrane

The BM is a thin, fibrous, a cellular element that separates pericytes, and astrocytes. The BM is the essential part of the BBB which appears in scanning electron microscopy as thin, tightly interwoven protein sheets (Engelhardt & Sorokin, 2009). The BM surrounds the vascular tube in two layers, the inner vascular layer and the outer parenchymal layer, also known as the vascular glia limitans perivascular (Daneman & Prat, 2015). The functions of the BM is to ensure anchorage of the NVU and establish a connection with the surrounding resident cells. The BM is crucial to the morphological and functional orientation of the BEC into apical and basolateral cellular domains (Daneman & Prat, 2015).
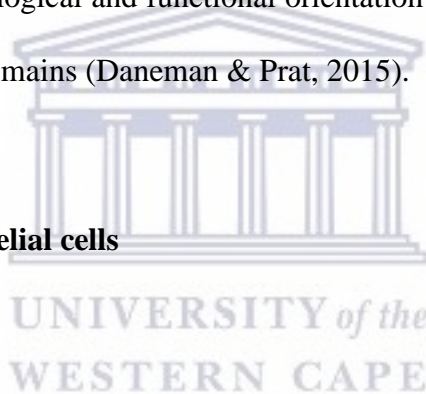
1.2.2.2 Brain endothelial cells

Brain endothelial cells are the most the most important component of the BBB, are shaped as simple squamous cells which are modified from the mesodermally derived cells (Daneman & Prat, 2015). Comparing the CNS ECs with those in other tissues, the CNS ECs are fundamentally different from other vascular endothelial in their ability to regulate the movement of molecules to and from the neural parenchyma (Cardoso *et al*., 2010). Also, they have higher amounts of mitochondria compared to other ECs. Moreover, CNS ECs express an extremely low level of leukocyte adhesion molecules, and they also lack pinocytic vacuoles, all of which contribute to the regulated permeability of the BBB (Daneman & Prat, 2015).

17

1.2.2.3 Pericytes

Pericytes are important cellular components of the NVU (Cardoso *et al*., 2010), which surround the abluminal surface of the cerebral capillaries of the endothelial tube and are completely enclosed by the BM. In the NVU, pericytes are thought to be responsible to synthesise growth factors and some BM components, and their association with the BEC, are essential for the structural maintenance of the BBB including junctional integrity (Cardoso *et al*., 2010; Daneman & Prat, 2015). Pericytes participate in the regulation of EC proliferation and migration and play an essential role in the mediation of inflammation as proposed by Cardoso *et al*. (2010).

1.2.2.4 Astrocytes

Astrocytes constitute the most numerous cell classes in the CNS. They have a stellate morphology and their end feet are structured to form a lacework of fine lamellae closely opposed to the exterior surface of the BBB endothelium and its respective BM (Abbott, 2002; Daneman & Prat, 2015). (Abbott, 2002; Daneman & Prat, 2015). At the BBB level, astrocyte end feet connect neurons and blood through close association, connecting the neurons in the brain to brain blood vessels (Bernacki *et al*., 2008). Astrocyte plays a critical role in the maintenance of the barrier properties, especially affecting the functions of the BEC. According to reports, they also have the ability to control the cerebral blood flow (Abbott *et al*.,

18

2010; Liebner, Czupalla *et al*., 2011). During development, astrocytes modulate angiogenesis and endothelial TJ formation by releasing neurotrophic and growth factors (Zhao *et al*., 2006). In addition, the astrocyte makes provision for essential modulatory factors, for example, tissue growth factor beta , interleukin-6, and glial fibrillary acidic protein (GFAP). Astrocytes with deficient GFAP are reported to have an inability in enhancing BBB properties (Wilhelm *et al*., 2011). Thus, the astrocytes' role is multifaceted, since it is included in the induction, repair, and maintenance of the BBB and in the angiogenesis of the brain capillaries (Weiss *et al*., 2009).

1.2.3   Inter-endothelial junctions

The BEC that form the BBB is stabilised by specialised cell junctions between adjacent cells (Cardoso *et al*., 2010). At the BBB level, there are two kinds of inter-endothelial junctions: TJs) and adherens junctions (AJ) (Fig 1.6).

19
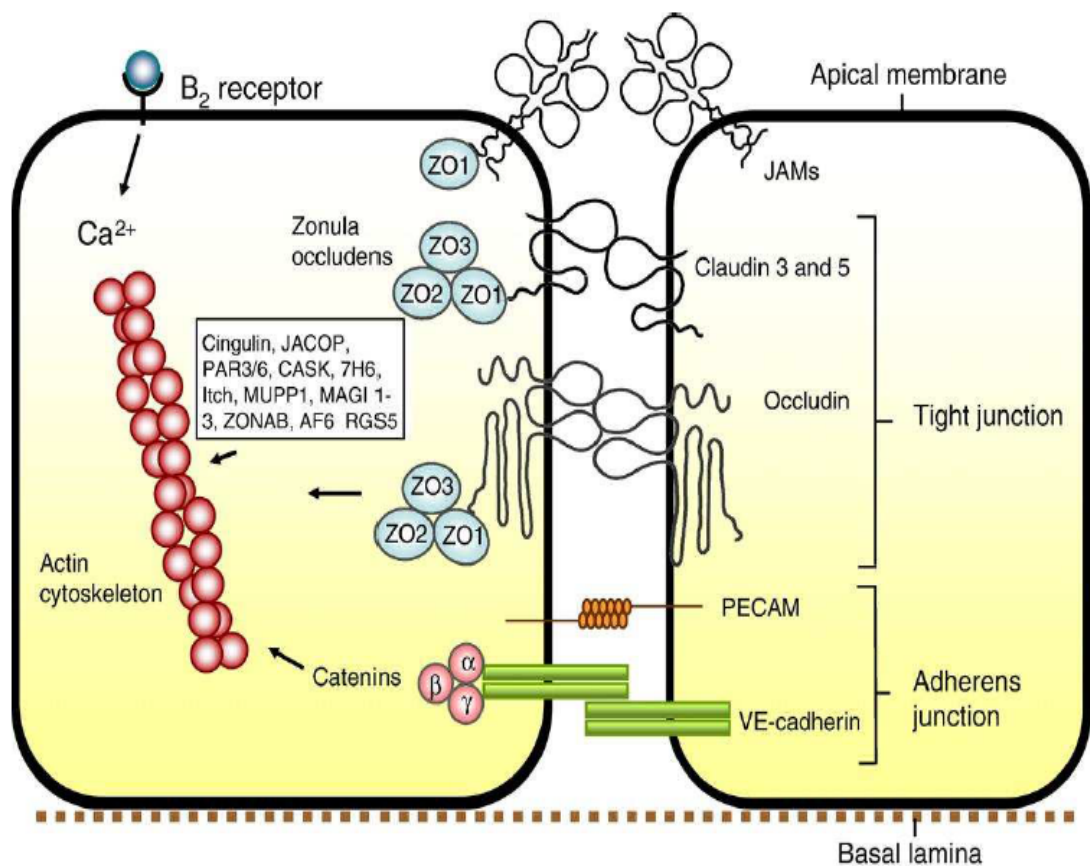
Figure 1.6: Structure of BBB inter-endothelial junctions (Abbott *et al*, 2010).

1.2.3.1 Tight junctions

Tight junctions have been identified as the main structures responsible for the barrier properties. They are molecular contacts between adjacent cerebral endothelial cells, set on the apicolateral sides of BEC. A TJ has the ability to seal the space between neighbouring cells allowing only limited passage of water but prevent other substances from entering the brain (Cardoso *et al*., 2010). Structurally, TJs consist of transmembrane proteins such as the claudins (3 but mainly 5), occludins, as well as a cytoplasmic of accessory and regulatory proteins

20

which include zonula occludens proteins (ZO-1/2/3) and cingulin (Cardoso *et al*., 2010).

These accessory or scaffolding proteins couple the junctional transmembrane proteins to actin filaments of the cytoskeleton, for the maintenance of the structural and functional integrity of the BEC. Transmembrane phosphoproteins consist of the major extracellular elements of TJs creating the paracellular barrier. They mediate cell-to-cell adhesion via homophilic interactions and might have a regulatory role related to BBB permeability and transendothelial migration of leukocytes (Lawther *et al*., 2011). A disrupted TJ could result in the uncontrolled entry of potentially damaging agents and transmit toxic effects to remote sites in the brain (Sambuy, 2009).

1.2.3.1.1 Claudin

Claudins belong to 20–28 kDa integral membrane phosphoproteins family comprising four transmembrane domains (Romanitan *et al*., 2010), and are genetically encoded by a multigene family of 24 distinct affiliates (Furuse & Tsukita, 2006; Malaeb *et al*., 2012). The belief is that claudins are the primary constructive component of TJs and responsible for their seal formation, and which regulate the specificity of TJ permeability. Their role in response to cellular stress were also suggested to play a part in the regulation of embryonic morphogenesis (Cardoso *et al*., 2010; Romanitan *et al*., 2010).

Claudins appear to be expressed in all tissue types, and although in mammalian BEC, the presence of claudin-1, -2,-3, -5, -11, -12 and -18 has been reported

21

(Cardoso *et al*., 2010; Romanitan *et al*., 2010). However, most dominant the claudins expressed by BEC is claudin-5 (Romanitan *et al*., 2010). Claudins bind to cytoplasmic proteins ZO-1, ZO-2, and ZO-3 by their carboxy-terminal. Moreover, claudins, as with occludins, extend over the plasma membrane four times, through two extracellular loops, with both -NH₂ and -COOH terminals in the cytosol. Claudins are homotopically bound to other claudins on neighbouring ECs which establishes the seal function of the TJs (Ballabh *et al*., 2004). At the BBB level, claudin-5 is one of the most studied members of the TJ, which has been shown to play one of the many important roles in the NVU. First, its ability to maintain normal BBB function (Vorbrodt & Dobrogowska, 2003) which is supported by the fact that down-regulation of claudin-5 expression is correlated with a breakdown of the BBB (Argaw *et al*., 2009), and second, it appears to play an important role during angiogenesis and in disease processes in regulating increased vessel permeability (Cardoso *et al*., 2010).
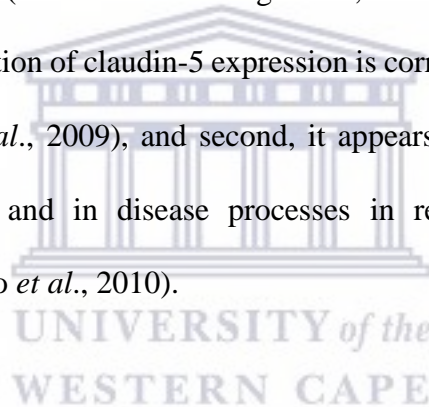
1.2.3.1.2 Occludin

Occludin is a 65 kDa integral membrane TJ protein, has four transmembrane domains (Hawkins & Davis, 2005), was the first tight junctional integral membrane protein discovered (Zlokovic, 2008). At the BBB level, occludin is not essential for the creation of TJ (Hawkins & Davis, 2005). Indeed, the results of many experiments have shown that loss of occludin can be compensated by normal expression and localisation of other junctional proteins (Zlokovic, 2008). Occludin function as an active regulatory protein, and has been assumed to be the physical

22

basis of the TJ barrier but has since been disputed. In addition, occludin-deficient mice are viable and exhibit normal barrier function (Findley & Koval, 2009). However, it has been suggested that occludin could act as an additional support structure with regulatory functions, which maintain electrical resistance and aqueous pore formation. In fact, high levels of occludin reduce paracellular permeability and high electrical resistance of the BEC monolayers, which underlines an active role of occludin in BBB function (Cardoso *et al*., 2010). The presence of occludin in the membrane is associated with augmented electrical resistance across the membrane and thus, diminished paracellular permeability (Huber *et al*., 2002).

1.2.3.2 Adherens junctions

Adherens junctions mediate the adhesion of ECs to each other to the BM. AJs consist of two fundamental adhesive units, cadherin/catenin, and nectin/afadin complexes(Lawther *et al*., 2011). These join the actin cytoskeleton via intermediary proteins (catenins) to create adhesive contacts between cells. Together TJ and AJ elements, especially ZOs and catenins are known to interact and further restrict permeability across the endothelium (Lawther *et al*., 2011).

1.2.4 Transport at the BBB

The passage of molecules across the EC of the BBB can occur between neighbouring cells (the paracellular pathway) or via the cells (the transcellular pathway) (Cardoso *et al*., 2010). Despite its barrier properties, lipophilic solutes can cross the BBB, as a result of their membrane solubility, (Schrot *et al*., 2005). Small inorganic molecules (e.g. oxygen, CO_2, nitric oxide, and water) diffuse across the endothelium membranes with ease as a result of their concentration gradient (Lawther *et al*., 2011). Other essential solutes necessary for brain function, such as glucose and amino acids, are transported by a specific carrier for example, Glut-1 and leucine-preferring or the L-type transport proteins, respectively.

Certain molecular elements with suitable molecular weight, charge as well as lipophilicity, might diffuse from the blood into the CNS (Fig 1.7) (Gabathuler, 2010). Various elements associated with the opening of the BBB are suggested to emerge as a result of receptor-mediated processes, by activating the signal transduction pathways within the endothelium (Abbott, 2002). Polar and lipid-insoluble molecules do not have the ability to cross the BBB (Cardoso *et al*., 2010). Some narcotic lipophilic molecules, such as alcohol, methamphetamine and nicotine can diffuse across the brain without restrictions. This ability to freely diffuse is governed by the transendothelial concentration, molecular size, charge, and lipophilicity (Gabathuler, 2010; Pardridge, 1995).

24
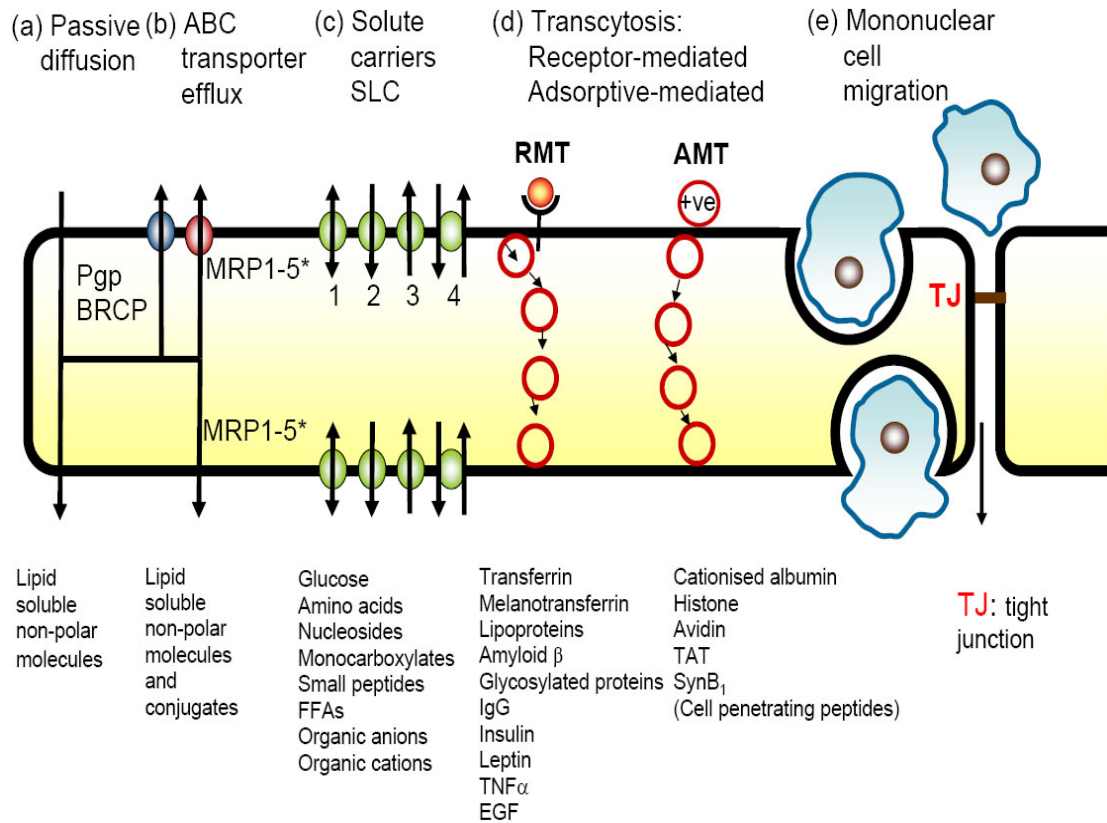
Figure 1.7: Routes of transport across the BBB (Abbott *et al*., 2010)

1.2.5 Permeability and pathophysiology of the BBB

Reactive oxygen species contributes to the disruption of the BBB as well as inflammation of the brain and induced cellular migration affecting BBB integrity by causing cytoskeletal rearrangements besides modifying the TJ proteins, claudin-5 and occludin (Schreibelt *et al*., 2007). The carboxy-terminal parts of occludin and claudins work together with the membrane-related recruiting proteins of the ZO protein family (Schreibelt *et al*., 2007). The proposed function of the ZO proteins is to connect transmembrane proteins to the actin cytoskeleton and may also be

25

involved in cellular signalling. During its contact with TJ molecules, the actin cytoskeleton plays a significant role in maintaining TJ integrity. Protein tyrosine kinases may possibly be activated in BEC which could progress to tyrosine phosphorylation of TJ proteins as a result of ROS (Schreibelt *et al*., 2007). Popescu (2013) hypothesised that Rho and other small Guanosine triphosphate influence the expression of TJ proteins, occludin and claudin-5 in various epithelial models. A chief mechanism influencing BBB permeability that has been shown, is the ROS-induced redistribution and down-regulation of claudin-5. Exogenous ROS transforms the organisation of occludin and ZO-1 in BEC (Schreibelt *et al*., 2007).

Experimentally-generated peripheral inflammation enhances BBB permeability and results in decreased occludin expression (Huber *et al*., 2002; Popescu, 2013) and augments expression of claudin-3 and -5 (Brooks *et al*., 2005; Popescu, 2013). The extravasation of plasma proteins associated with BBB dysfunction could occur through transcellular or paracellular routes, via the induction of fluid-phase or nonspecific pinocytosis and transcytosis, the formation of transendothelial channels, or disruption of the EC membrane TJ (Grant *et al*., 1998). Efflux transporters, such as P-glycoprotein, are important as they enhance barrier properties. They do this by returning the small lipophilic molecules that disseminate into the BEC, back to the bloodstream (Lippmann *et al*., 2012; Pardridge, 2003).

1.2.6   The BBB and diseases

There is a long list of CNS pathologies involving alterations in structural and functional elements of the BBB, including multiple sclerosis, hypoxia, ischemia, oedema, Parkinson's disease, Alzheimer's disease, epilepsy, tumors, glaucoma and lysosomal storage diseases (Abbott *et al*., 2010). Vascular leakage may possibly cause the disruption of the BBB, the chief pathophysiological mechanism of most CNS diseases (Brown & Davis, 2002). The barrier dysfunction can range from gentle and transient TJ opening to chronic barrier breakdown and changes in transport systems and enzymes can likewise occur (Abbott *et al*., 2010). Toxic agents and pathological conditions may compromise BBB function through an early change in its function which is mediated through direct effects on the ECs and associated with morphological changes in astrocytes (Cardoso *et al*., 2010). Microglial activation is increasingly recognised as an early indication of CNS inflammation, even in disorders not previously regarded as inflammatory (Abbott *et al*., 2010). The inflammation is a concern factor indicated in BBB alterations throughout CNS diseases. Indeed, in all the neurological disorders, the CNS show inflammatory features (Stolp & Dziegielewska, 2009).

1.2.7   The immortalised bEnd5 cell line as an *in vitro* blood-brain barrier

The immortalised mouse brain endothelial cell line (bEnd5) is composed of spindle-shaped cells (Steiner *et al*., 2011). It has been established as a cell line from isolated

27

mouse BEC by using polyoma virus middle T-antigen (Reiss *et al*., 1998; Steiner *et al*., 2011; Yang *et al*., 2007). This cell line expresses three junction proteins, occludins, claudin-5, and Zona occludins-1, besides von Willebrand factor, vascular endothelial-cadherin, platelet endothelial cell adhesion molecule-1, intercellular adhesion molecule-2, endoglin and transporters such as glucose transporter-1, P-glycoprotein, sodium-potassium chloride-/NKCC co-transporters, and most protein kinase C isoforms (Paolinelli *et al*., 2013; Yang *et al*., 2007).

The bEnd5 cells simulate the barrier properties of the BBB, similar to the primary mouse brain microvascular endothelial cell (pMBMEC) (Coisne *et al*., 2005; Röhnelt et al.,1997). The bEnd5 and pMBMEC cells are associated with the establishment of a highly restrictive barrier which minimises the permeability across the *in vitro* BBB model (Coisne *et al*., 2005; Röhnelt et al.,1997). A disadvantage of bEnd5 cells may include the observation that continuous sub-culturing of the cells could result in a change of occludin expression and incomplete TJ generation. On the other hand, immortalised bEnd5 cells, when compared to primary cell cultures, are more reproducible and require less time to culture (Lundquist *et al*., 2002).

1.2.8   The proposed *in vitro* blood-brain barrier model

A challenge to BBB research is the scarcity of reliable *in vitro* models to concentrate the cellular and molecular mechanisms of BBB function under pathological and normal conditions (Yang *et al*., 2007). The BBB *in vitro* models are composed of

28

EC culture systems derived from brain microvascular cells BMCs. Primary brain ECs are isolated by using an enzymatic digestion, typically using various sets of enzymes such as dispase or collagenase (Cecchelli *et al*., 1999). In earlier studies, the primary cultured ECs of brain capillaries which were retrieved by the utilisation of mechanical filtration and homogenisation were used (Cecchelli *et al*., 1999). Subsequently, there has been a significant advancement in cell culture, with choices of using well-established protocols for primary cell cultures or using commercially available immortalised cell lines.

Significant advantages of *in vitro* BBB models which utilise immortalised cell lines include decreased variability and also conceivable high throughput of experimental treatment (Coisne *et al*., 2005). The *in vitro* model is helpful in that it diminishes animal utilisation in experiments, and furthermore, BBB models can retrieve useful information about the transport mechanisms for a specific medication or treatments in a timeous manner (Weidenfeller *et al*., 2005). This is achievable because it features derivable information on basic mechanisms of individual components of the BBB eliminating other BBB elements, e.g. astrocytes or pericytes which could cloud the investigations, thus allowing for faster and greater profiling of treatments (Weidenfeller *et al*., 2005).

With reference to the immortalised bEnd5 cell line, not only does it express unmistakable cellular markers of ECs of the *in vivo* BBB of humans, and that of the mouse, but is also in alignment with the laboratory *in vivo* mouse model. Consequently, there is enough motivation to use this immortalised cell line in research studies (Mentor & Fisher, 2017).

1.3 Reactive oxygen species

ROS are small, extremely reactive, oxygen-containing molecules, naturally produced in minute quantities during metabolic reactions in the body (Wu *et al*., 2003). ROS consist of free radical atoms which contain an unpaired electron, therefore making them inherently unstable and highly reactive. Various kinds of ROS include O_2^-, H_2O_2 and the hydroxyl radical ($OH^.$) (Betteridge, 2000). The potential sources of ROS are from an assortment of cellular enzyme systems, including oxidase, arachidonic acid metabolising enzymes, including cytochrome P-450 enzymes, xanthine oxidase, uncoupled endothelial nitric oxide synthase, lipoxygenase and cyclooxygenase, and mitochondrial metabolic processes (Zhang & Gutterman, 2007). The mitochondrial metabolic process is a major source of ROS in most mammalian cell types. In mitochondria, the electron transport chain is the primary site of ROS production. In vascular ECs, ROS under normal physiological conditions, has the ability to regulate vascular tone, oxygen sensing, cell division and apoptosis, and inflammatory responses (Zhang & Gutterman, 2007).

OS is an expression used to depict various injurious processes consequent from an imbalance between an increase in the formation of ROS and/or reactive nitrogen species and its destruction by the limited capacity of antioxidant defences (Turrens, 2003). Uncontrolled increases in the steady-state concentrations of those oxidants lead to free radical-mediated chain responses that indiscriminately target proteins (Stadtman & Levine, 2000; Turrens, 2003), DNA, lipids and polysaccharides (Turrens, 2003). However, cells are equipped to check the oxidative assault with

many cellular antioxidant defences such as GSH, catalase and dismutases (Freeman & Keller, 2012). In the mitochondria and cytosol, H_2O_2 can be diminished by glutathione peroxidase, which utilises GSH to neutralise H_2O_2 and lipid peroxides to water and equivalent alcohols, respectively (Zhang & Gutterman, 2007).

The BBB endothelial cells have a high concentration of mitochondria, providing an increased opportunity for creating OS (Freeman & Keller, 2012). Under normal conditions, the integrity of the BBB is shielded from OS because BBB cells contain high levels of antioxidant enzymes (Plateel *et al*., 1995; Tobwala *et al*., 2014). Increased OS can lead to neurodegeneration and breakdown of the BBB through the disturbance of TJ proteins which can change flowing of the bloodstream (Freeman & Keller, 2012).

OS is one of the most important mechanisms responsible for the interruption of the BBB, which permits the entry of toxic substances into the brain, leading to the development of, and progression of several neurological diseases (Tobwala *et al*., 2014). During different disease stages and ageing, the antioxidant defence systems can be compromised leading to progressive oxidative harm and subsequent significant loss of function and/or cell death (Freeman & Keller, 2012). GSH decreases ROS levels and activates cellular OS responses using many mechanisms (Song *et al*., 2014).

At the point when OS occurs, cells neutralise the consequential oxidant impact to restore the redox equilibrium. All organisms have adaptive responses to OS, for example, activation of genes encoding defensive enzymes, transcription factors, and structural proteins (Emerit *et al*., 2004). Fortunately, the cell has its own internal defence mechanism to battle against OS. Principally, this is intervened by

31

the transcription factor NF-E2-related factor (Nrf2), which is responsible for controlling a series of antioxidant and cellular protective genes, in response to OS (Shelton & Jaiswal, 2013). Under OS, Nrf2 becomes activated and translocates from the cytoplasm to the nucleus and subsequently activates the transcription of antioxidant genes. The promoters of these AO genes contain the ARE and research evidence has shown that Nrf2 promotes cell survival by preventing expansion in ROS under different conditions of OS (Song *et al*., 2014).

In a few studies, GSH was found to inhibit cell death in OS (Abramov *et al*., 2007). In addition, Song *et al*., (2014) demonstrated that GSH protects DNA against OS, and also GSH neutralises the generation of ROS under OS.
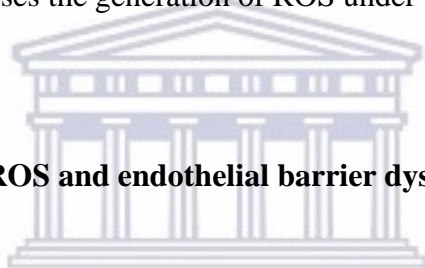
1.3.1   Influence of ROS and endothelial barrier dysfunction

There is abundant evidence to demonstrate that OS induced by ROS like O_2^-, H_2O_2, or HO^- can elicit endothelial barrier dysfunction (Lum & Roebuck, 2001). In addition, oxidant stress of the endothelium also increases the intracellular calcium concentration ([Ca2+]i) which correlates with expanded endothelial permeability (Fig 1.8) (Lum & Roebuck, 2001). Also, oxidants such as H_2O_2 appear to increase the phosphorylation of myosin light chain kinase indicating that ROS can contribute to endothelial barrier dysfunction and alter endothelial contraction (Hawkins & Davis, 2005). The paracellular permeability in the endothelium is controlled by the TJ and intercellular endothelial AJ (Hawkins & Davis, 2005). H_2O_2-induced barrier disruption appears to occur through rearrangement of β-catenin, the disruption of

32

β-catenin/cytoskeletal association and endothelial cadherin, but the signalling events remain to be resolved.

However, occludin phosphorylation and activation of ERK1/ERK2 signalling appeared to mediate the disruption of occludin-ZO-1 interactions on endothelial cell surfaces and cause the disorganisation of occludin (Li *et al*., 2012). ROS is able to activate signalling pathways, for example, may further regulate the phosphorylation state of TJ proteins and other AJ (Konstantoulaki *et al*., 2003).
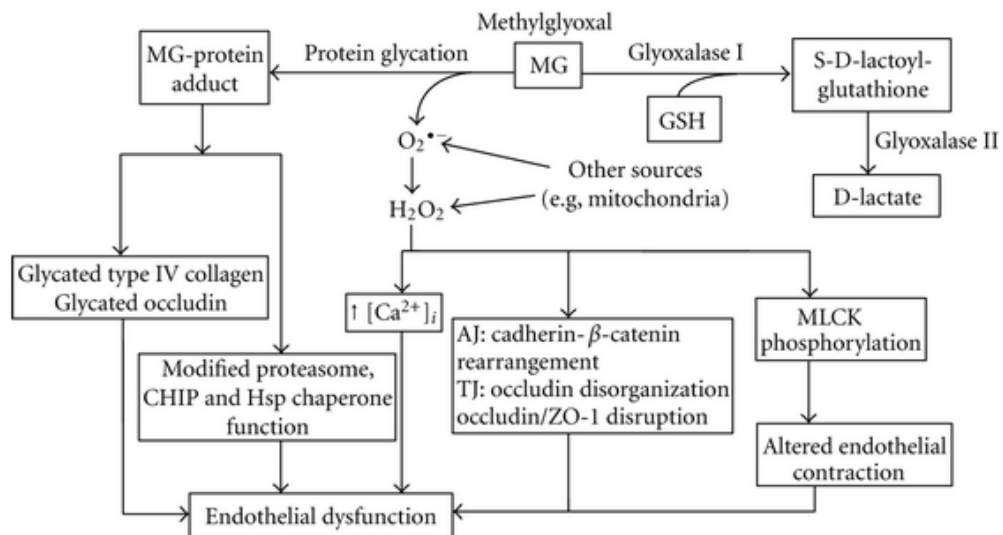
Figure1.8: Mechanisms of MG-mediated endothelial barrier dysfunction and its protection by GSH (Li *et al*., 2012)

From the foregoing discussion, it is apparent that GSH has an important role to play in the protection of the BBB against OS-induced dysfunction. It is rational to consider the use of antioxidant agents in the treatment of BBB dysfunction-linked neurological disorders. However, objective judgement regarding the point in the

33

progression of a disease that will justify the use of exogenous antioxidants, will depend on the capacity of the endogenous system to neutralise ROS. This study aims to detect the presence of the GSH system within bEnd5 endothelium model of the BBB and to determine its quantity as well as evaluate its capacity to neutralise ROS

1.4   Research aims and objectives

1.4.1 Aims

The aim of this study is to establish the presence of GSH in bEnd5 cells line model of the BBB, to quantify the amount of GSH in bEnd5 cells, and to evaluate functional capacity of the GSH content of bEnd5 cells.
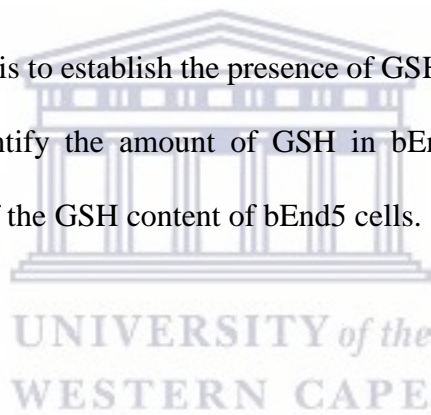
1.4.2   Objectives

- To establish the presence of GSH in bEnd5 cells by using mBCL a fluorometrically based assay.
- To quantify the amount of GSH and GSSH per cell in bEnd5 cells using a GSH-Glo^{TM} Glutathione assay kit.
- To evaluate the functional capacity of GSH in bEnd5 cell content by exposing the cell to increasing concentrations of H_2O_2.

- To determine if an exogenous treatment of an AO (Trolox) will increase the capacity of the endogenous antioxidant GSH.

1.5   Research question/hypothesis

The hypothesis for this study is that the GSH-based AO system of the bEnd5 cells have limited capacity to regulate the levels of ROS neutralisation in the *in vitro* model of the BBB.

35
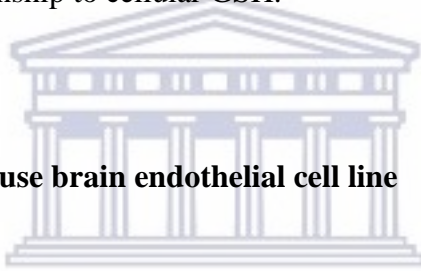
CHAPTER TWO

Methods and materials

An *in vitro* analysis was carried out to establish the presence of GSH in bEnd5 cells. This would be achieved by quantifying the amount of GSH and GSSG in bEnd5 cells. The final phase of the study was to evaluate the functional capacity of bEnd5 cells to OS (exposure to H_2O_2 over 24 and 48 hours as well as in combination with Trolox) and its relationship to cellular GSH.

2.1 Immortalised mouse brain endothelial cell line

The bEnd5 cell line was obtained from ECACC, (Sigma-Aldrich, 96091930), which was established from BECs of BALB/c mice. Cellular immortalisation was imparted by transfecting the primary cells with the retrovirus coding for the polyoma middle T antigen (Reiss *et al*., 1998). The bEnd5 cells have an endothelial-like morphology, and they also express endothelial-specific proteins, endoglin, PECAM-1, FIK-1, and MECA-32 (Reiss *et al*., 1998).

2.2 Mouse brain endothelial (bEnd5) cell culture procedure

2.2.1 Chemicals required for bEnd5 cells culture procedure

All reagents were obtained from Whitehead Scientific Pty Ltd, SA. The following chemicals were required for the culture of bEnd5 cells, foetal bovine serum (FBS) (biowest, S12010S181G), non-essential amino acids (NEAA) (Lonza, BE 13-114E), antibiotic Penicillin-Streptomycin Amphotericin B mixture (Lonza, DE17-602E), sodium pyruvate (Lonza, BE13-115E), Dulbecco's modified eagle medium (DMEM) (Lonza, BE 12-719F). The mouse brain endothelial (bEnd5) cell line (Sigma-Aldrich, 96091930) ECACC, trypsin-EDTA (Lonza, 5MB042), phosphate buffer saline (PBS) (by Life Technologies Corp., Gibco,20012-019), and Trypan blue (by Life Technologies, Gibco, 15250-061).

2.2.2 Brain endothelial (bEnd5) cell culture procedure

The bEnd5 cells were grown in complete media (DMEM) F-12, supplemented with 10% FBS, 1% sodium pyruvate, 1% Penicillin and Streptomycin, and 1% NEAA (Reiss *et al*., 1998; Steiner *et al*., 2011). The cells were grown in a 25 cm^2 (50 ml) tissue culture (TC) flasks containing the desired amount of supplemented DMEM. Cells were incubated at 37°C and 5% CO$_2$ at 95% humidity until the cell culture reached confluence. Every 24 hours cells were checked for media colour change, attachment and confluence, using an inverted-phase microscope. At 80-90% confluence, the bEnd5 cells were trypsinised and sub-cultured to routinely calculate

the required concentration of cells needed for the experiments. The bEnd5 cells used in this experiment were of passage numbers 17-25. These passage numbers were ensured by freezing away a large reserve of the low passage numbers.

2.3 Fluorescence targeting of GSH

2.3.1 Detection of glutathione in bEnd5 cells using the monochlorobimane fluorescence method

The use of fluorescent probes to confirm the presence and to assay for glutathione in cultured cells has been well-reported (Baxter *et al*., 2015; Chatterjee *et al*., 1999; Hartmann *et al*., 2003). Monochlorobimane (mBCl) is a non-fluorescent bimane that passively diffuses across cellular membranes into the cytoplasm, and selectively and enzymatically conjugates with GSH to form fluorescent glutathione S-bimane (GSB) (Fig 2.1), which can be fluorometrically assayed (Reiss *et al*., 1998; Steiner *et al*., 2011).
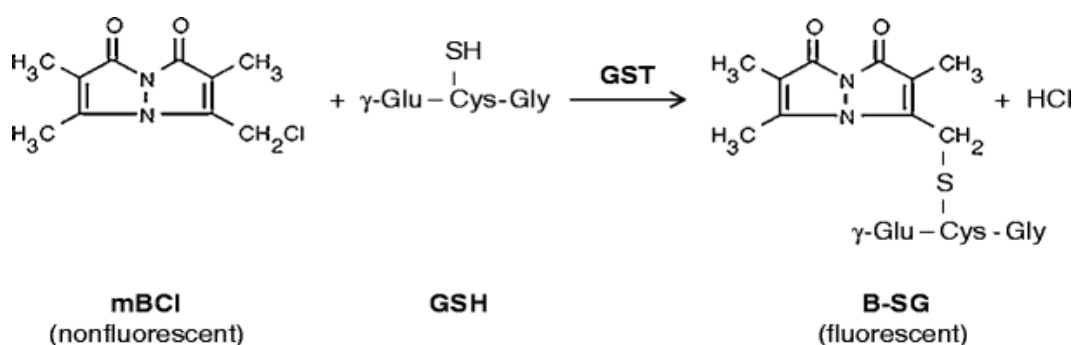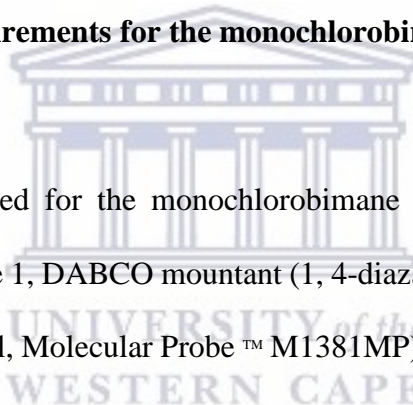
Figure 2.1: The reaction of monochlorobimane mBCl with glutathione (GSH)(Machado & Soares, 2012)

2.3.2 Coating tissue culture surface with collagen

Rat-tail collagen was harvested in our laboratory using standard procedures and used to coat (10 µg/ml) the microscopy slides to improve bEnd5 cells adherence to glass surfaces and to mimic a BM. This allowed for the bEnd5 cells to physiologically and functionally orientate themselves with regard to their apicolateral and basolateral morphology. Collagen coating was done only for the microscopy experiments in which cells were grown on glass slides.

2.3.3 Chemical requirements for the monochlorobimane fluorescence study

The chemicals required for the monochlorobimane (mBCl) fluorescence study included collagen type 1, DABCO mountant (1, 4-diazabicyclo-[2,2,2]-octane) and mBCl solution, (mBCl, Molecular Probe ™ M1381MP) that was prepared as a 33.3 mM stock solution by dissolving 25 mg of 226.66 g/mol of mBCl in 3.3 ml of DMSO this stock solution was stored in the dark at -20ºC. A working solution with a final concentration of 60 μM was used. This solution (60 μM) was prepared by diluting the stock solution in DMEM immediately before use and directly added to the bEnd5 cells cultures.

A solution of 4% paraformaldehyde and 0.2% glutaraldehyde in PBS, pH 7.4, was prepared and stored in the fridge. A 0.05 M PBS solution, pH 7.4, was prepared by using reagents that included 1 M Potassium Phosphate (Monobasic) solution (KH_2PO_4), 1 M Potassium Phosphate (Dibasic) solution (KH_2PO_4) Monobasic one

K and dibasic 2 K, and 5 M sodium chloride solution (NaCl). Additional stock solutions were prepared as follows: 10 ml of 1 M KH_2PO_4 (was prepared by dissolving 1.3609 g in 10 ml of double distilled water (ddH_2O)), 50 ml of 1 M KH_2PO_4 (was prepared by dissolving 8.709 g in 50 ml of ddH_2O) and 50 ml of 5 M NaCl (was prepared by dissolving 14.61 g in 50 Ml of ddH_2O). Stock solutions were then filtered.

Solutions of 0.05 M PBS, pH 7.4 stock were prepared by mixing 7.6 ml (1 M KH_2PO_4) with 42.4 ml (1 M dibasic KH_2PO_4) and 30 ml 5 M NaCl and then filled up to just under 1 liter with ddH_2O to allow for pH adjustments that were checked and adjusted to the desired pH by adding either hydrochloric acid or KOH.
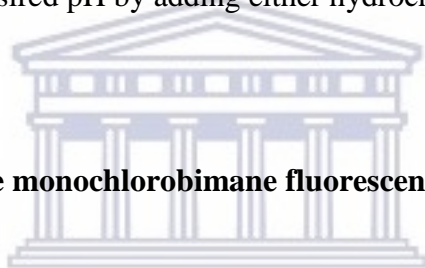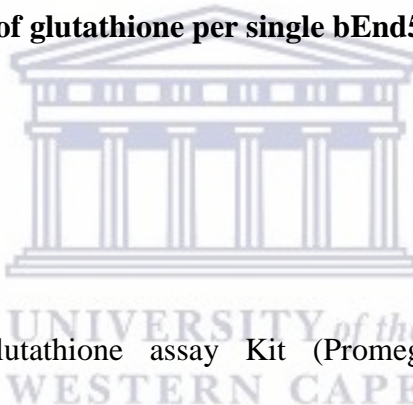
2.3.4 Protocol for the monochlorobimane fluorescence study

The microscopic glass slides which were first cleansed with 70% ethanol, wiped with tissue towel and then UV-sterilised were placed inside two groups of five Petri dishes (100*22 mm). The first group consists of plain glass slides while the second group consists of glass slides coated with rat-tail collagen (10 µg per ml), and each group has a control group and mBCl treated group. For the first group, an equal number of bEnd5 cells were seeded on the top of the glass slide in each of the Petri dishes, and cultures were incubated overnight at 37°C. For the second group, equal numbers of bEnd5 cells, as in the first group, were seeded on the top of the coated slide in each (100*22 mm) Petri dish, and cultures were incubated overnight at 37°C. The experiment was terminated in each group by aspirating the media. After aspiration, the cells on each slide were rinsed twice in PBS and then fixed.

40

Coverslips were mounted on each slide using 10 µl DABCO mountant. The mBCl treated samples were exposed to 10 ml of 60 µM mBCl solution which was pipetted into each Petri dishes and allowed to incubate for 30 minutes at 37ºC. The experiment was terminated by aspirating the mBCl solution following which the slides were rinsed twice in PBS and then fixed. Coverslips were then mounted on each slide using 10 µl DABCO mountant. Cells in each slide were viewed and imaged under a fluorescent microscope (Nikon Eclipse) at (ex: 365-400 nm, em: 450-490 nm). These experiments were carried out in triplicates.

2.4 Quantification of glutathione per single bEnd5 cell

2.4.1 Introduction

The GSH-Glo™ Glutathione assay Kit (Promega, cat no V6911/2, lot 0000155719), was used to quantify the amount of GSH in each cell. An equal number of bEnd5 cells were seeded in each well of the 96 well plate and were allowed to attach overnight. The quantity of GSH was measured in the total number of cells after a specific duration in culture, and this was divided by the total number of cells in the culture. However, cells multiply after they are seeded, and to accurately determine the quantity of GSH per unit cell, a pilot experiment was carried out to determine the number of bEnd5 cells after the selected culturing time frame.

41

2.4.2 Determination of bEnd5 cells proliferation rate

Cell proliferation is an increase in the number of cells after seeding them because of the healthy, normal processes by which cells grow and multiply. Determining cellular proliferation rate is necessary to approximate how many cells are in wells at a particular time after seeding. Trypan Blue (TB) was used in this experiment to count bEnd5 cells to determine bEnd5 cells proliferation.

Trypan Blue is a carcinogenic dye utilised for staining and identifying non-viable cells present in a sample with compromised membranes. This assay differentiates between dead and live cells (Strober, 2001). Non-viable cells absorb and retain the TB due to their non-selective permeability, whereas viable cells do not absorb the dye (Freshney *et al*., 2006; Mascotti *et al*., 2000). Non-viable cells were stained blue and the viable cells luminesced when viewed using standard light microscopy.

After a cell count, 1×10^6 cells were seeded into 25 cm^2 flasks in groups of five (n=3; day=0). Cells were incubated at 37°C and 5% CO_2. After the respective time intervals of the incubation bEnd5 cells were washed, trypsinated, centrifuged, resuspended in media in preparation to perform the TB staining for cell counting. Cells were counted, using the Neubauer hemocytometer after 24, 26, 28, 30 and 32 hours. The TB cell suspension was made up of 10 μl cells suspension and 10 μl TB. The 10 μl of TB cell suspension was added to the particular sections of the hemocytometer and was observed under an inverted- phase contrast microscope (Zeiss) to determine the total live and dead cells. This process was performed for each flask of cells at each time point to obtain a bEnd5 cells growth curve. Moreover, the bEnd5 cell doubling time (Td) was determined using the plot of the

rate of proliferation against duration of cells in culture. The experiment was performed in triplicate.

2.4.3 Quantification of cellular glutathione content using the GSH-Glo^TM Glutathione assay kit

2.4.3.1 Description for GSH-Glo^TM Glutathione assay

The GSH-Glo™ Glutathione assay is a luminescence-based assay for detecting and quantifying glutathione (GSH). The assay depends on the transition of a luciferin derivative (Luc-NT) into luciferin in the presence of glutathione, catalysed by glutathione S-transferase (GST) (Scherer *et al*., 2008) (Fig 2.2). The signal created during a coupled reaction with firefly luciferase is proportional to the quantity of glutathione present within the sample. Maximal luminescence is achieved in less than one hour. This assay (Fig 2.2) is suitable to detect and quantify GSH in cultured cells and different biological samples because of the ease with which cells can be grown, treated and lysed in the same plate and its generation of stable luminescence signal.

43
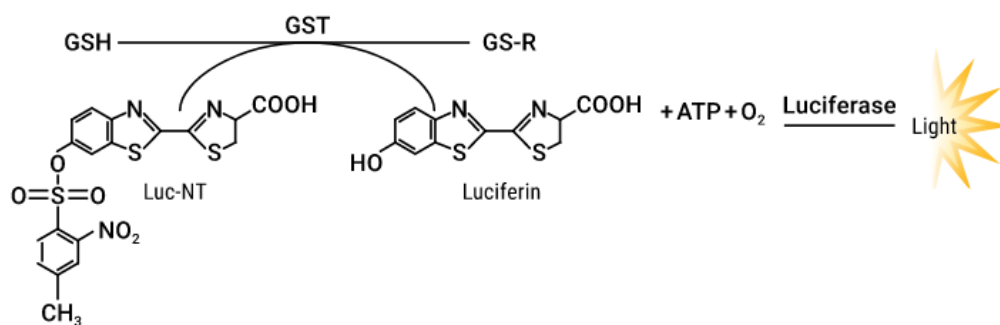
Figure 2.2: An overview of the GSH-Glo™ Glutathione assay. (**https://worldwide.promega.com**).

2.4.3.2 Chemical requirements and sample handling for the GSH-Glo™ Glutathione assay

The GSH-Glo™ Glutathione assay (Promega) included Luciferin-NT substrate, GST, GSH-Glo reaction buffer, 5 mM stock GSH solution, reconstitution buffer with esterase, lyophilised Luciferin detection reagent and 1 mM TCEP (Tris (2-Carboxyethyl) Phosphine) (Sigma C4706) to convert GSSG to GSH.

2.4.3.3 Reagents prepared

GSH-Glo Reagent 1X was prepared by transfer 35 µl of Luciferin-NT substrate, and 35 µl of GST and 3.5 ml of GSH-Glo reaction buffer to the Eppendorf tube. GSH Standards were prepared by diluting 5 mM stock GSH solution to (1:50). Then serial 1:1 dilutions was carried out to obtain a final range between 0 and 5 µM when 10 µl of each serial dilution product is mixed with 100 µl GSH-Glo reagent and 100

44

µl of luciferin detection reagent in each well. Luciferin detection reagent was prepared by transferring an equal volume of reconstituted buffer and esterase to the dark bottle of lyophilised Luciferin detection reagent and mixed by inversion until the substrate was dissolved. 174.43 mM stock of TCEP solution was prepared by dissolved 1 g of TCEP (Sigma C4706) in 20 ml of water and stored at -20ºC, to use at a final concentration of 1 mM.

2.4.3.4 Sample preparation

To quantify the content of GSH in bEnd5 cells, 4,000 bEnd5 cells were seeded in triplicate wells in columns eight to nine of a 96 well plate as per the instruction of the manufacturer. To facilitate referencing of the wells in a 96 well plate, the plate was annotated into columns eight to nine and rows A-E. The plate was incubated at 37°C and 5% CO^2 for 24 hours to allow for cell attachment. 10 µl of each diluted standard was transferred to triplicate was used wells in columns one to seven, of the same plate (preparing for final concentrations 5, 2.5, 1.25, 0.625, 0.3125, 0.15625 and 0.078 µM GSH). The culture medium was carefully removed from the cell-containing wells, and 100 µl of prepared 1X GSH-Glo reagent transferred to each well. Then 100 µl of 1 mM TCEP reagent were transferred to bEnd5 cells which were cultured in wells A-D in column nine. The plate was mixed briefly on a plate shaker and incubated at room temperature for 30 minutes. Of the reconstituted Luciferin detection reagent, 100 µl was transferred to each well, and the plate briefly mixed on a plate shaker. The plate was then incubated at room temperature

45

for 15 minutes, and luminescence was read using a GloMax–Multi Detection System (Promega).

Luminescence readings (in RLU) were converted to GSH concentration using the GSH standard curve obtained from readings in columns one to seven. Luminescence readings from column eight was divided by 10,000 to obtain the amount of GSH per cell. And total glutathione concentration obtained from readings in column nine was divided by 10,000 according to the bEnd5 cells proliferation rate to obtain the amount of total glutathione (GSH_T) per cell. The amount of (GSSG) glutathione per cell was derived from the difference between the GSH_T and GSH values. The values of GSH and GSSG was used to determine the GSH/GSSG ratio for the bEnd5 cells.
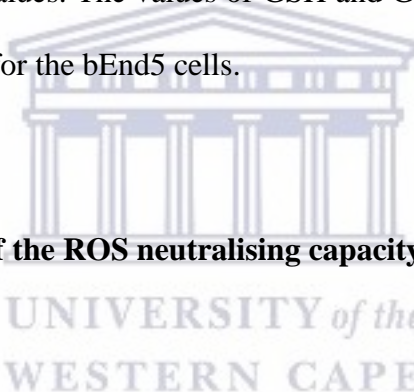
2.5 Determination of the ROS neutralising capacity of bEnd5 cells

To determine the GSH-mediated ROS neutralising capacity of bEnd5 cells, the GSH-Glo^{TM} Glutathione assay was used to relatively quantify and compare cellular GSH levels following treatment with increasing concentrations of H_2O_2.

2.5.1 Chemical requirements and sample handling for the determination of the ROS neutralising capacity of bEnd5 cells

The following stock solutions were used in the determination of the ROS neutralising capacity of bEnd5 cells. This included H_2O_2 that was serially diluted

46

into concentrations of 0.5, 1.0, 1.5, 2.0, 2.5, 5.0 mM and 50, 100, 150, 200, 250 and 500 µM. **(See Appendix).** Luciferin-NT substrate, GST, GSH-Glo reaction buffer, 5 mM stock GSH solution, reconstitution buffer with esterase, lyophilised Luciferin detection reagent and 1 mM TCEP (Sigma C4706) to convert GSSG to GSH were prepared as previously described (see Section 3.5.3.3).

2.5.2   Sample treatment with 0-5000 µM of H_2O_2

The bEnd5 cells were seeded in 96 well plates at a density of 4,000 cells per well. Cells were incubated overnight at 37°C and 5% CO_2 to allow for attachment after which the culture medium in each well was aspirated. Cells were treated in 12 columns of a 96-well plate using duplicate of four wells for each treatment group. They were treated with supplemented DMEM medium dosed with increasing concentrations (50, 100, 150, 200, 250, 500, 1000, 1500, 2000, 2500, 5000 µM) of H_2O_2 or supplemented DMEM alone (medium). An untreated set of four wells served as control (Fig 2.3). These experiments were set up in two 96 well plates with different duration of treatment lasting 24 and 48 hours for the different plates.

Following treatment for a specified time interval, cells in each well were viewed and imaged under an inverted-phase microscope, then growth media were removed, and 100 µl of prepared 1X GSH-Glo reagent was transferred to each well. Then 100 µl of 1 mM TCEP reagent was transferred to one column of each duplicate concentration, to convert the GSSG to GSH. The plate was mixed briefly on a plate shaker and incubated at room temperature for 30 minutes.

Of the reconstituted Luciferin detection reagent, 100 µl was transferred to each well, and the plate was mixed briefly on a plate shaker. The samples were incubated at room temperature for 15 minutes, and luminescence was read using a GloMax–Multi Detection System (Promega). Luminescence readings (in RLU) were converted to GSH concentration using the GSH standard curve. The GSH_T concentrations were obtained from readings in columns with TCEP. The amount of GSSG was derived from the difference between the GSH_T and GSH values. The values of GSH and GSSG were used to determine the GSH/GSSG ratio for the bEnd5 cell.
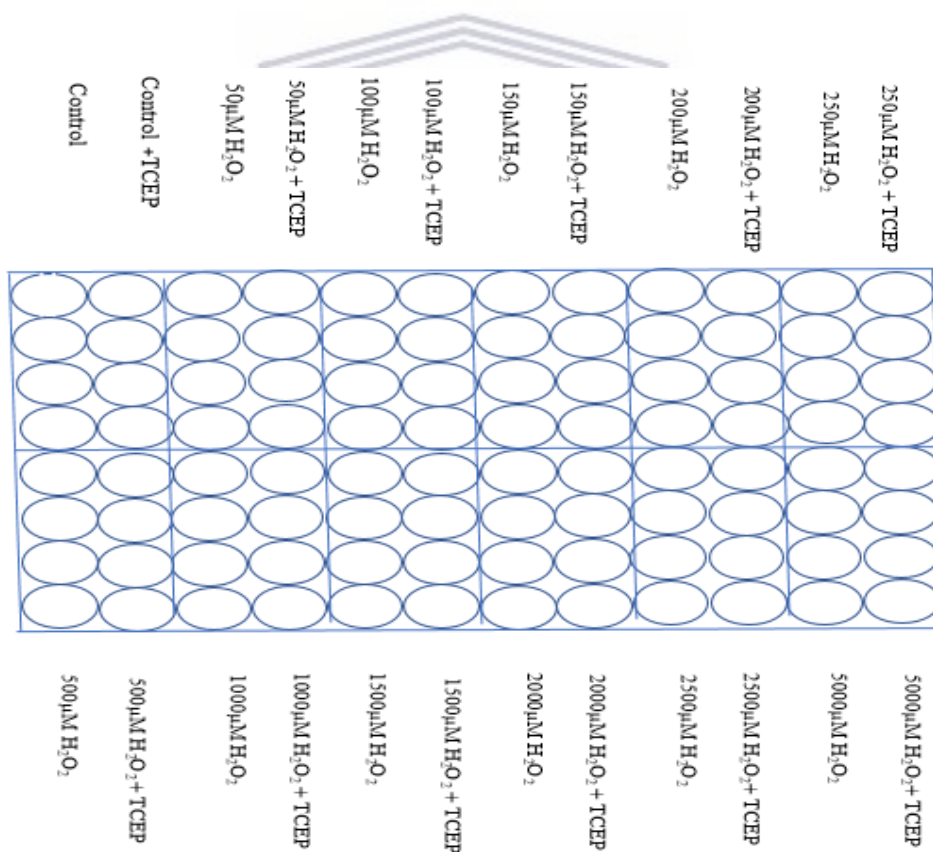
Figure 2.3: Treated cells in duplicate columns with supplemented DMEM medium dosed with increasing concentrations (50, 100, 150, 200, 250, 500, 1000, 1500, 2000, 2500, 5000 µM) of H_2O_2 or supplemented DMEM alone (medium)

2.6 Protective effect of Trolox against H$_2$O$_2$ toxicity and GSH depletion

Trolox (6-hydroxy-2,5,7,8-tetramethylchroman-2-Carboxylic Acid) (Fig 2.3) is a hydrophilic synthetic analog of vitamin E and a direct scavenger of alkoxyl radicals and peroxyl (Monticone *et al*., 2014). *In vivo* and *in vitro* studies have reported on its protective effects against oxidative damages, especially against lipid peroxidation in (Lee *et al*., 2005).
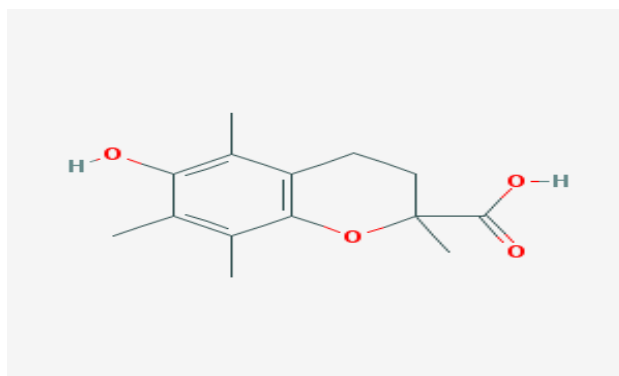
Figure 2.4: The molecular structure of Trolox (http://www.lookchem.com/Trolox-C/)

2.6.1 Chemical requirements and sample handling for the protective effect of Trolox against H$_2$O$_2$ toxicity and GSH depletion

A 100 mM Trolox solution was prepared. Of this, 25 µM of Trolox was prepared in combination with increasing concentrations of H$_2$O$_2$ 50, 100, 150, 200, 250, 500, 1000, 1500, 2000, 2500, and 5000 µM (11 experiment. groups) (See Appendix). Luciferin-NT substrate, GST, GSH-Glo reaction buffer, 5 mM stock GSH solution,

reconstitution buffer with esterase, lyophilised Luciferin detection reagent and 1 mM TCEP (Sigma C4706) to convert GSSG to GSH was prepared as previously described (see Section 3.5.3.3).

2.6.2 Treatment with combinations of Trolox and H_2O_2

The bEnd5 cells were seeded in 96 well plates at a density of 4,000 cells per well. Cells were incubated overnight at 37°C and 5% CO_2 to allow for attachment after which the culture medium in each well was aspirated. Cells in plates were then treated with a medium containing 25 µM Trolox in combination with increasing concentrations of H_2O_2 (50 to 5000 µM) (11 expermint. groups) or increasing concentrations 50 to 5000 µM for the control groups (11 groups). Both groups of cells were incubated for 24 hours, and then in the different groups , the exposure to H_2O_2 was repeated for a duration of 48 hours.

Following treatment for a specified time interval, cells in each well were viewed and imaged under an inverted-phase microscope, then growth media were removed, and 100 µl of prepared 1X GSH-Glo reagent was transferred to each well. The plate was mixed briefly on a plate shaker and incubated at room temperature for 30 minutes. Of the reconstituted Luciferin detection reagent, 100 µl was transferred to each well, and the plate was mixed briefly on a plate shaker. Then it was incubated at room temperature for 15 minutes, and luminescence read using a GloMax–Multi Detection System (Promega).

Luminescence readings (in RLU) were converted to GSH concentration using the GSH standard curve. The GSH_T concentration was obtained from readings in columns with TCEP. The amount of GSSG was derived from the difference between the GSH_T and GSH values. The values of GSH and GSSG was used to determine the GSH/GSSG ratio for the bEnd5 cell. The experiments were carried out in triplicate.

2.7 Statistical analysis

Results were expressed as the mean±SEM. GraphPad Prism (version 6.1) was used to analyse the data statistically. Significant differences between groups were determined by using the Holm-Sidak method for independent (unpaired) samples. A probability of $P < 0.05$ designated statistical significance and four samples were used in each treatment group (n=4) with each experiment done in triplicate unless otherwise stated.

CHAPTER THREE

Results

GSH is one of the most abundant naturally occurring thiol-based AO within mammalian cells. In the literature, it is reported to play a pivotal role in the cellular mitigation of OS among other functions such as redox signalling and oxidation-reduction reactions in metabolic pathways. The presence and concentration of GSH in BECs and in immortalised BECs used for studies of the *in vitro* BBB model have not been reported in the literature. Furthermore, the capacity of BECs to respond to OS and its relationship to cellular GSH content has not been investigated.

3.1 Monochlorobimane (mBCl) fluorescence

A monochlorobimane fluorescence microscopy assay was utilised to detect and localise GSH while fluorometric method using mBCl fluorescence was used to relatively quantify GSH in bEnd5 cells. Observation of a blue fluorescence from the cells was indicative of the presence of GSH which form a fluorescent GS-bimane adduct with mBCl. The intensity of the fluorescence observed correlate with amount of GSH in the cells (Fig 3.1 B-D). The control samples which were not treated with mBCl did not show blue fluorescence (Fig 3.1 A). The variable fluorescence intensity observed in the cells indicated a variable concentration of intracellular GSH content in the cells. GSH was found to be distributed throughout the cytoplasm and nuclear compartments of the cells. Also, the dendritic extensions of cells all contained GSH. However, higher magnification (X120) showed that

52

GSH was more concentrated in the nucleus than the cytoplasm part (Fig 3.1 D). Furthermore, the entire nucleus had the highest fluorescence which indicated the highest localisation of GSH.
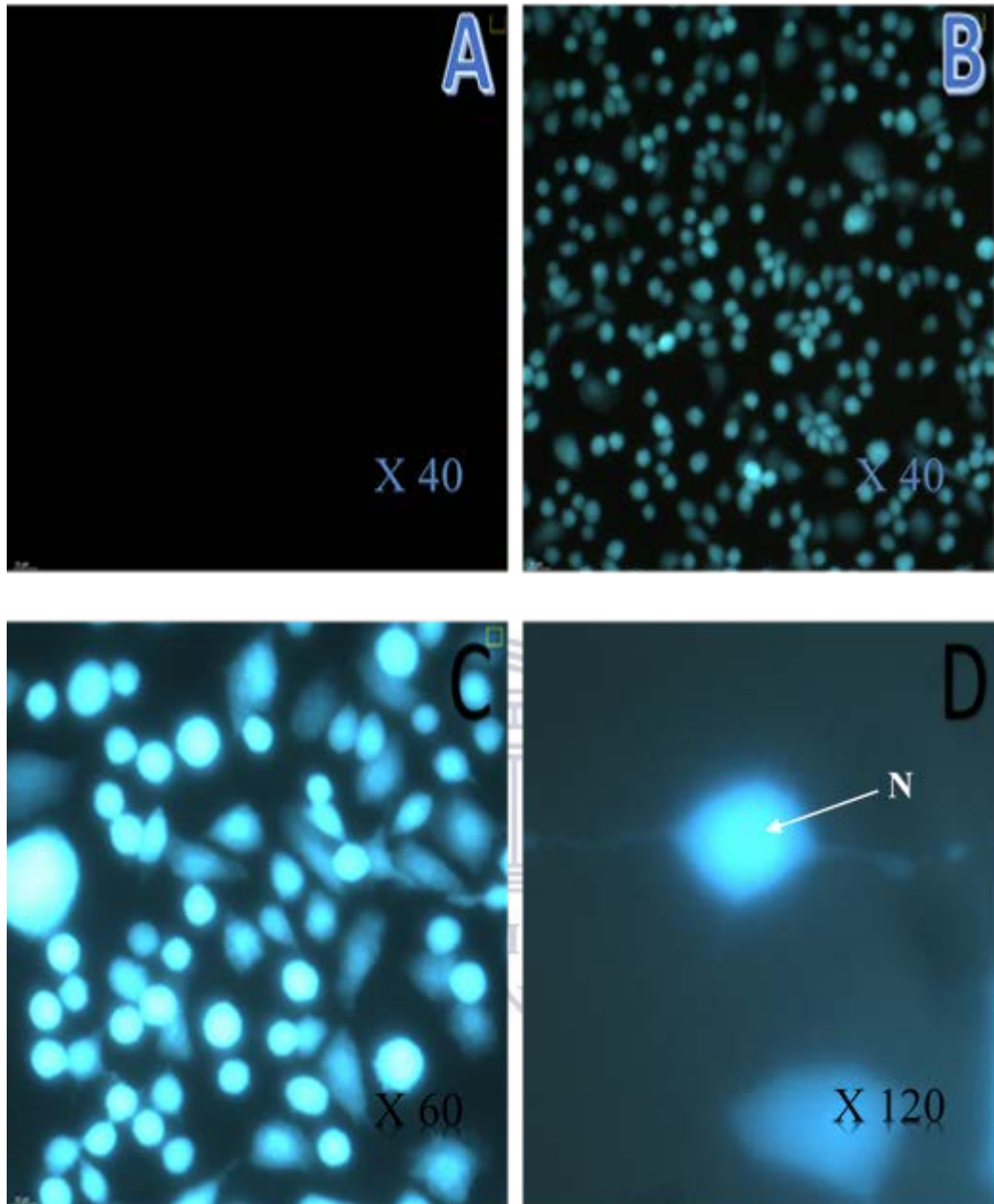
Figure 3.1 A-D: The above are fluorescent micrographs of bEnd5 cultures exposed to 60 µM mBCl. Fig A (X 40), the control group, was not exposed to mBCl. Fig B (X 40), the 60 µM mBCl group, shows fluorescence in all cells. The variable fluorescence between cells shows they contained different concentrations of GSH. Fig C, the higher magnification (X60), endorsed the varied concentration of GSH per endothelial cell. Fig D, the highest magnification (X120) shows two cells with varied fluorescence indicating the different concentrations of GSH within the two cells. N: represents the high localisation of GSH in the nucleus.

54

3.2 Rat-tail collagen and bEnd5 cells attachment

Slides were coated with rat-tail collagen (10 µg per ml) to improve the bEnd5 cells' adherence to slide surface and mimic an *in vivo* BM. This allowed the bEnd5 cells to physiologically and functionally orientate themselves regarding their apico-lateral and baso-lateral morphology.

Images obtained from the mBCl treated group showed blue fluorescence within the cells which localised the fluorescent GS-bimane adduct. While the images obtained from the control groups showed no fluorescence (Fig 3.2 A and C). Images for the second group (Fig 3.2 D), which was coated with rat-tail collagen, showed a higher number of bEnd5 cells attached to the slides than the first group which was not coated with collagen (Fig 3.2 B). This indicates that rat-tail collagen facilitated bEnd5 cell division and attachment to the slides.
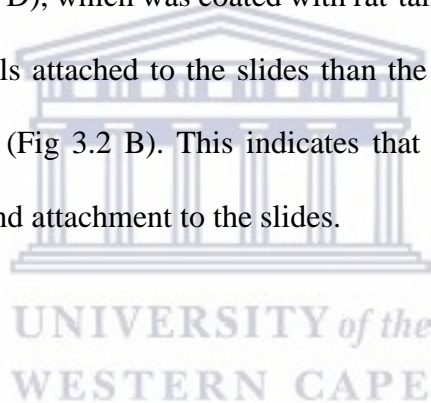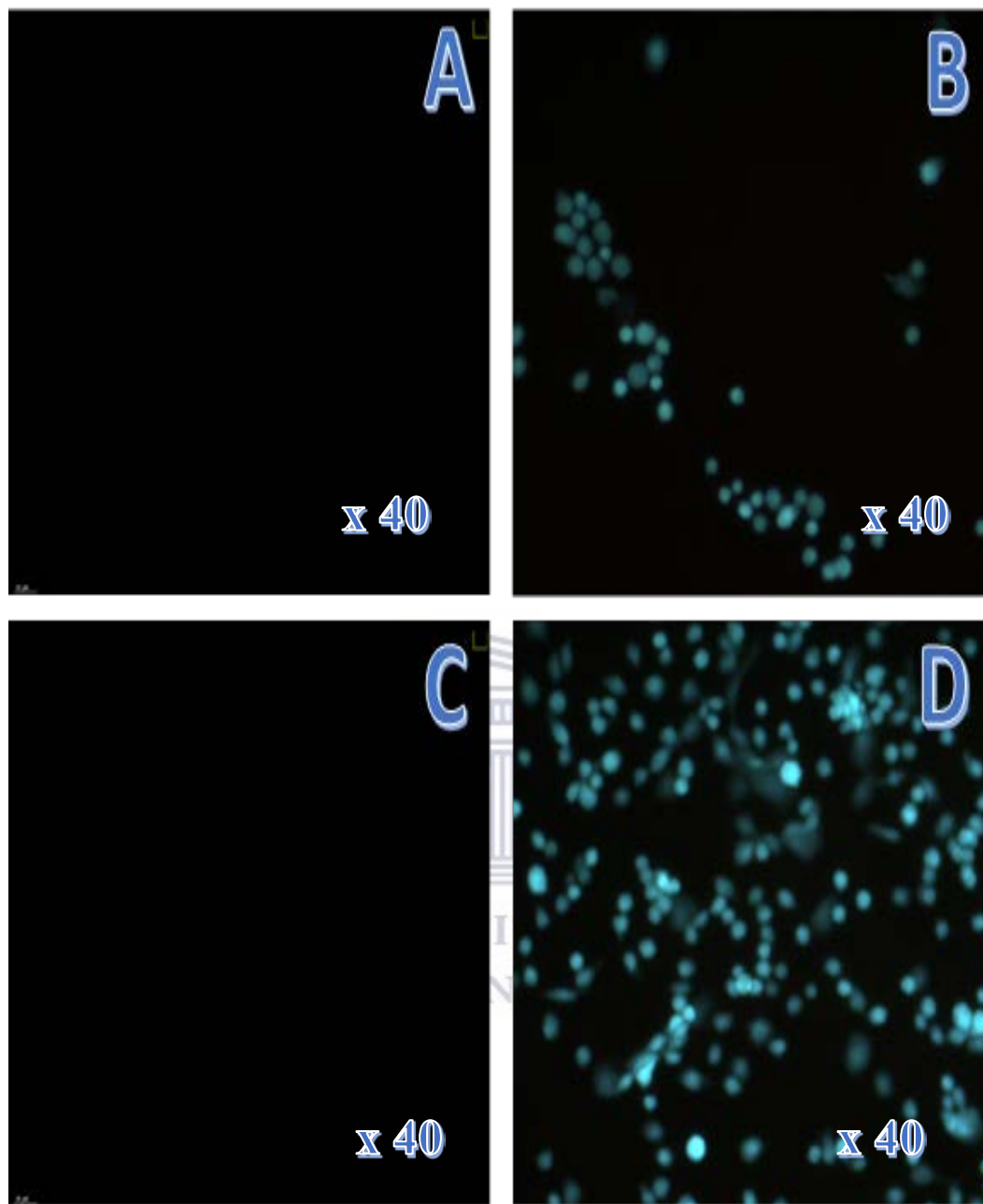
Figure 3.2 A-D: The above fluorescent micrographs show images of bEnd5 cultures exposed to 60 µM mBCl. Cells seeded on glass slides for the two groups: uncoated and coated with rat-tail collagen (Fig D collagen-coated group, and Fig B, uncoated group (X 40)). Figs A and C (control groups) were not treated with mBCl (X 40). B: the 60 µM mBCl uncoated group shows a lower number of bEnd5 cell attachment to the slide. C: the control group coated with rat-tail collagen. D: the 60 µM mBCl coated group showing a higher number of bEnd5 cells attached to the slide.

3.3 bEnd5 cells proliferation rate

To accurately determine the number of cells after they had been cultured for a defined period, it was crucial to determine the quantity of GSH per cell accurately.

The data, obtained over 35 hours are shown in Fig 3.3. Linear regression analysis indicated that the sloping line (rate of cell division) between 0 min and 24 hours and between 24 and 35 hours revealed the doubling time of cells as 15.66 hours over 24 hours, with 11 hours after that depicting the bEnd5 cell-growth curve.
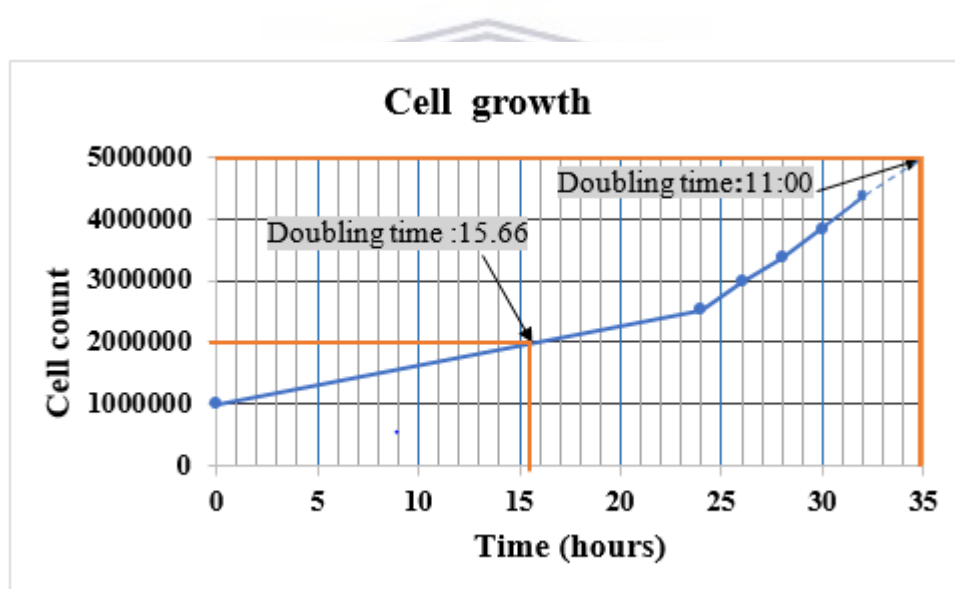
Figure 3.3: The bEnd5 cell-growth curve. The time of bEnd5 cells to double in culture over 24 hours is extrapolated in the graph to 15 hours 40 minutes. however, the slope of the graph changed after 24 hours to indicate an increased rate of cell division, with a doubling time of 11 hours between 24 and 35 hours. The experiment was done in triplicate.

3.4 Quantity of glutathione in bEnd5 cell

We also estimated the average basal quantity of GSH in a single bEnd5 cell using a GSH-Glo assay kit which utilises a luminescence method allowing for the quantification of GSH in 96 well plates. The redox status of the cell was investigated with respect to the GSH:GSSG ratio by using the GSH-Glo kit to quantify the amount of GSH per endothelial cell. We determined the basal GSH:GSSG status of the cells between 24 and 96 hours in culture to determine the effect of proliferation in culture on the basal redox status of the cells. The GSH-Glo kit does not allow the direct measurement of the GSSG fraction of the GSH_T.

We addressed this by recycling GSSG using 500 µM TCEP, to convert it to GSH, which then allows for the determination of the total amount of glutathione per cell. The concentration of GSSG per cell was quantified by subtracting the initial GSH concentration from the GSH_T concentration (GSH + GSH reduced from GSSG) (modification of the method of Tietze, 1969).

The analysis involved generating a glutathione standard curve according to the GSH-Glo™ Glutathione Assay Technical Bulletin #TB369. Briefly, this entailed serial dilutions of a 5 mM stock solution of glutathione in PBS (range 0–5 µM). GSH concentrations were calculated based on the GSH standard curve (Fig 3.4).

In subsequent calculations, we found that the approximate GSH concentration in each bEnd5 cell was 0.031±0.00035 nM, while the GSSG concentration was approximately 0.00092±0.00021 nM. Most of intracellular glutathione in bEnd5 cells was found in its reduced form where 97% of the glutathione pool is of reduced form (GSH) while 3% exists in the GSSG form (Fig 3.5).

GSH concentration standard curve

$y = 2E{+}06x + 273387$

$r^2 = 0.9987$
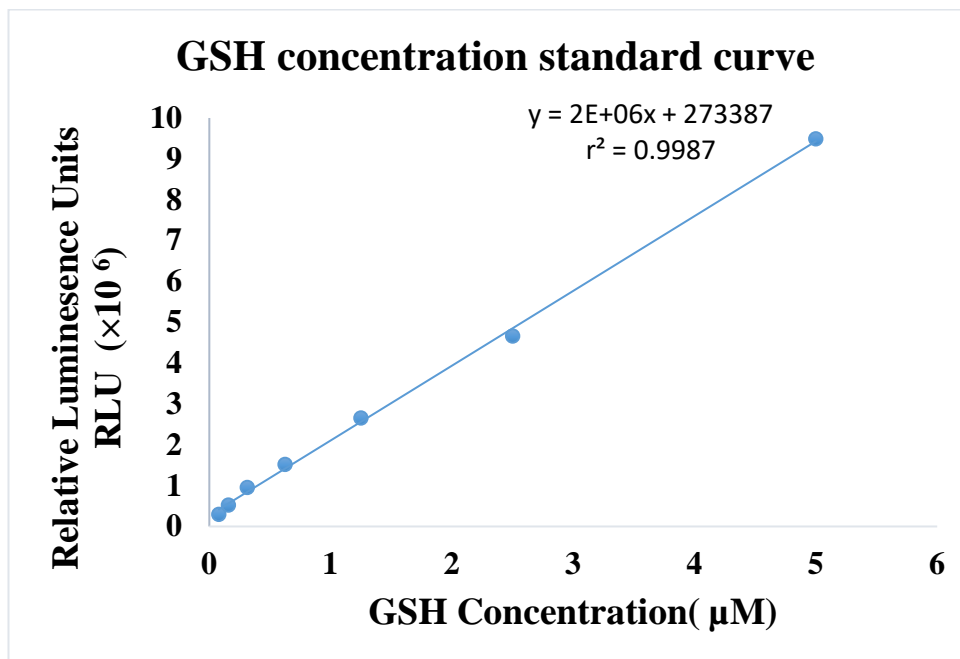
Figure 3.4: The GSH standard curve presented a linear correlation between the relative luminescence units (RLU) and the GSH concentration, with a r^2 value >0.9987.
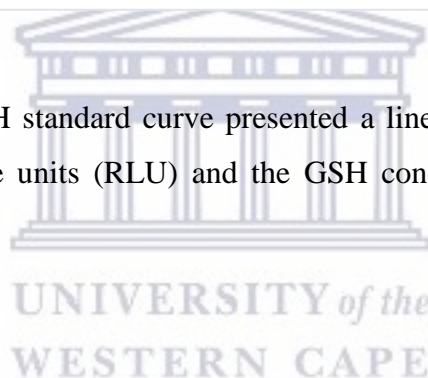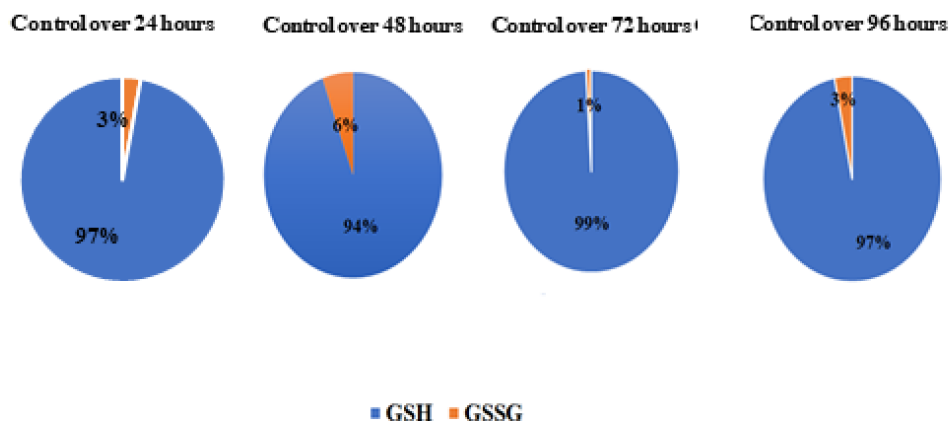
Figure 3.5: The ratio of GSH/GSSG in bEnd5 cells at 24, 48, 72 and 96 hours. The pie chart represents the GSH:GSSG ratio, in untreated bEnd5 cells which ranged between 99:1 and 94:6 over 96 hours. The bEnd5 cells showed an average 97% of the total glutathione pool in the reduced form (GSH) with 3% in the GSSG form.

3.5 ROS neutralising capacity of bEnd5 cells over 24 hours

3.5.1 GSH changes

GSH is one of the predominant intracellular AO used to neutralise cellular derived H_2O_2 (Fig 3.6). The possible ROS neutralising capacity was determined by treating bEnd5 cells with increasing concentrations of H_2O_2 (50-2500 µM) and measuring the relative concentrations of GSH_T and GSH over 24 hours. The assay enabled the measurement of the GSH_T and GSH. GSH_T represented the combined concentration of GSH and GSSG in the cells (Fig 3.6). Thus, GSSG was determined indirectly as the difference between GSH_T and GSH. (Chapter 2 p 49).

$$\text{GSH} + \text{H}_2\text{O}_2 \xrightarrow{\ \text{Gpx}\ } \text{GSSG} + \text{H}_2\text{O}$$
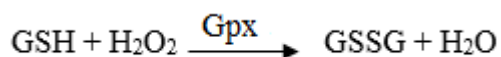
Figure 3.6: The above reaction represents the reduction of H_2O_2 by GSH and its subsequent conversion to GSSG and H_2O. The reaction is catalysed by glutathione peroxidase (Gpx).

H_2O_2 treatment was expected to reduce cellular GSH concentration because of its role in reducing H_2O_2 to H_2O through the oxidation of GSH to GSSG by Gpx (Fig 3.6).

Treatment of bEnd5 cultures with 50 to 150 µM H_2O_2 over 24 hours showed a significant increase (an average 34.89%) in GSH_T relative to control GSH_T concentrations (P <0.05). GSH_T were significantly (P <0.05) elevated between 50 and 500 µM H_2O_2 and significantly depressed between 1500 and 2500 µM H_2O_2 compared to the untreated bEnd5 cell Control group (Fig 3.7).

Several observations were surprising (Fig 3.7). First, the cellular level of GSH increased by (25.38 %) after treatment with 50 and 150 µM H_2O_2 relative to control. The cultures exposed to 250 and 500 µM H_2O_2, GSH concentrations showed a decrease of 8.79% to a new but stable level compared to the 150 µM H_2O_2. However, 1500 and 2500 µM H_2O_2 GSH dropped by 71.14% compared to the 500 µM H_2O_2.

Second, GSSG increased from the control level by 144.58% at 50 µM H_2O_2. At 150 and 500 µM H_2O_2, GSSG increased by an average of 39.57% to a new but constant level. At the doses of 1500 µM and 2500 µM H_2O_2, GSSG levels further increased

by an average of 77.05% compared to the 500 µM H_2O_2 and remained statistically constant across these treatments of H_2O_2.

Third, a dose-dependent decrease in GSH_T to a new level which remained sustained was then observed at 1500 and 2500 µM H_2O_2 compared to the 500 µM H_2O_2. GSH_T reflected the levels of intracellular GSH throughout the experiment (Fig 3.7). The latter drop in GSH_T at high levels of H_2O_2 and could be attributed to the decrease in GSH RLU because of the decline in cell numbers.

The average GSH:GSSG ratio at 50 and 500 µM H_2O_2 was 13:87 and the average GSH:GSSG ratio at 1500 and 2500 µM H_2O_2 was 48:52.
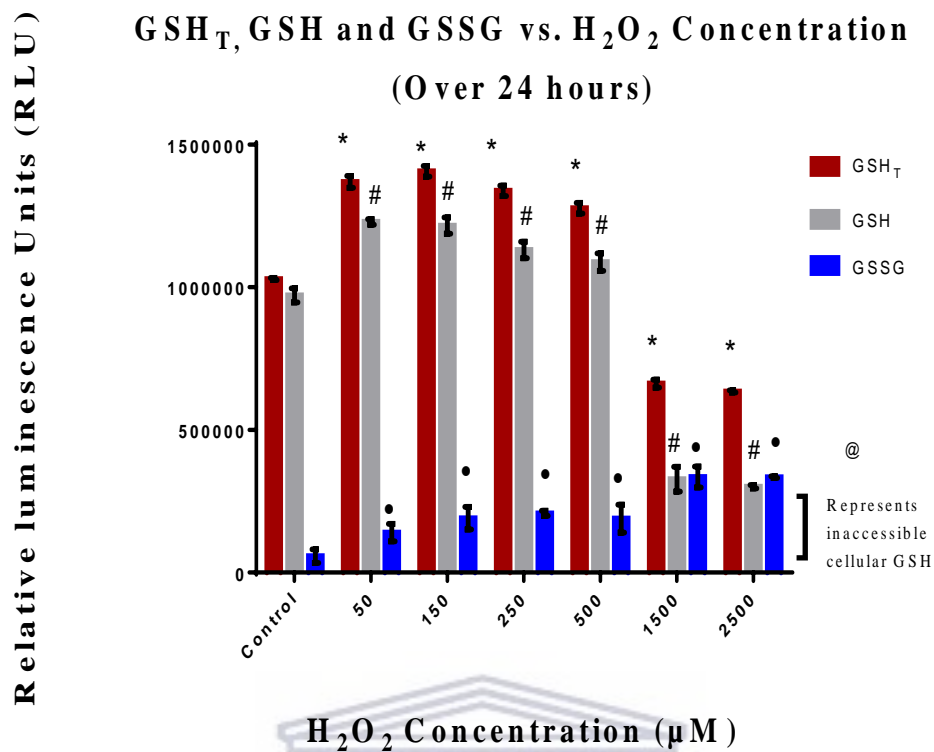
Figure 3.7: Relative reduced glutathione (GSH), glutathione disulphide (GSSG) and total glutathione (GSH_T) levels in bEnd5 cells following incubation with H_2O_2 over 24 hours. Control bEnd5 cells were incubated for 24 hours without any addition of H_2O_2, while other bEnd5 cells were treated with increasing concentrations of H_2O_2 (50 to 2500 µM) before determining the levels of GSH, GSSH, and GSH_T. The asterisk (*) denotes statistically significant differences between control GSH_T and H_2O_2 treated cells; the hash (#) denotes statistically significant differences between the GSH control and H_2O_2 treated group of bEnd5 cells; while the bullet (●) denotes statistically significant differences between control GSSG and the H_2O_2 treated groups of bEnd5 cells. The @ denotes that at high levels of H_2O_2 treatment (1500-2500 µM). Although the high levels of oxidative stress (OS) caused cells to begin to die, they were still not able to access available GSH. Data are represented as means ± SEM (n=4). Statistical significance at level P <0.05 was determined (see Appendix B). The experiment was performed three times.
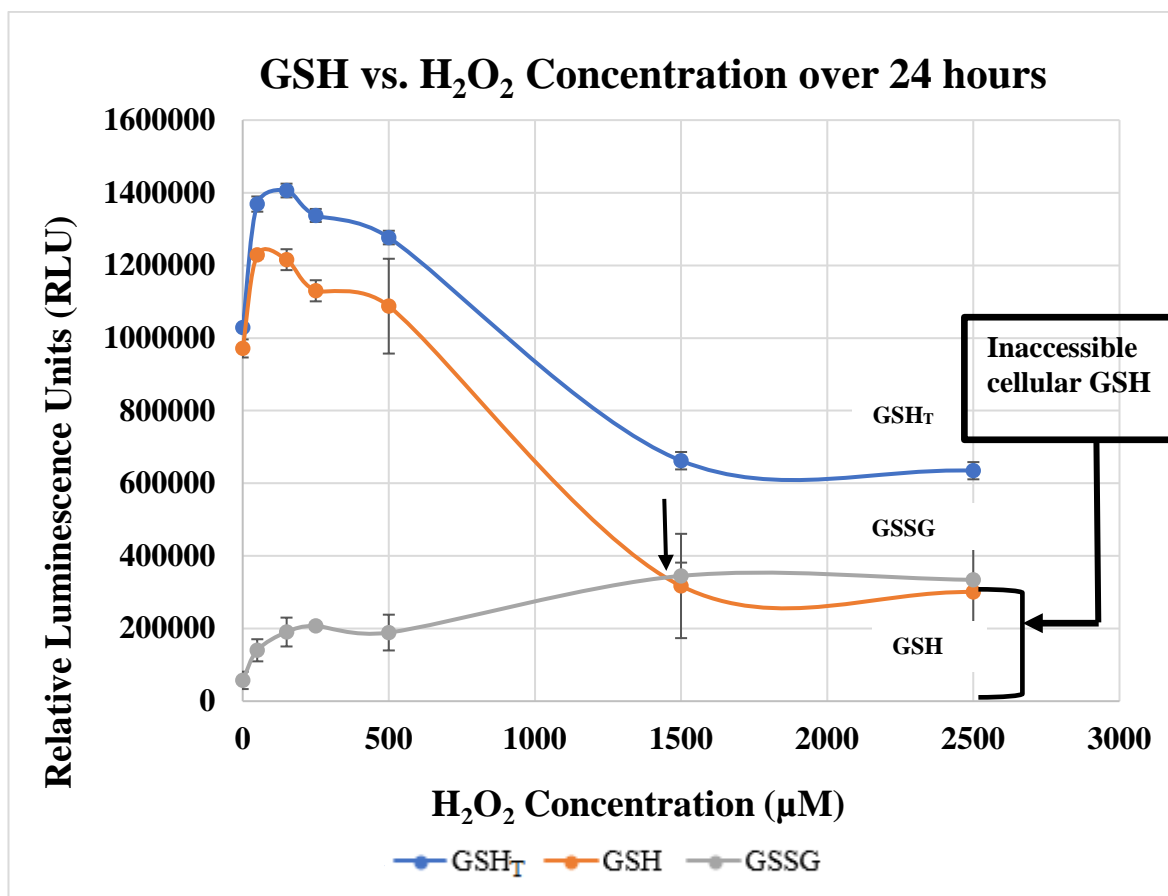
Figure 3.8: The data show a trend in relative cellular GSH_T, GSH and GSSG content of bEnd5 cells exposed to varying concentrations of H_2O_2 over 24 hours using a linear horizontal axis. A steep and maximal rise in the GSH was observed from 50 to 150 µM H_2O_2 which decreased at a concentration of 250-2500 µM H_2O_2. At the extrapolated H_2O_2 concentration of 1400 µM (see arrow), the reduced GSH and oxidised glutathione (GSSG) concentrations equalised. This point indicates the level of OS (H_2O_2) from which the cells appeared to change shape and enter a necrotic phase. GSH linearly decreased in concentration between 50 and 1500 µM H_2O_2 and then remained constant. GSSG linearly increased in concentration between 50 and 1500 µM and then remained statistically constant. Between 1500 µM and 2500 µM of H_2O_2, GSH and GSSG concentrations did not statistically change, and the decreases of GSH_T reflected the decreases of GSH.

3.5.2 GSH/GSSG ratio in bEnd5 cells after being treated with H₂O₂
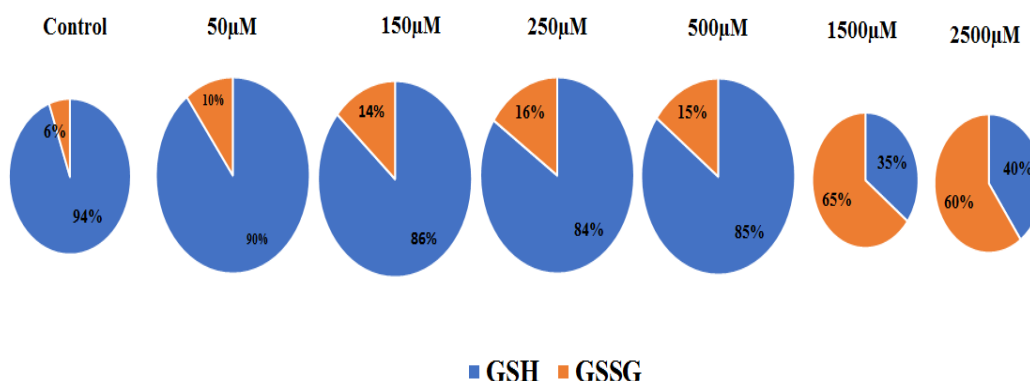
Figure 3.9: The ratio of GSH:GSSG in bEnd5 cells after being treated with increasing concentrations of H_2O_2 (50-2500 µM) over 24 hours. The diameter of the pie chart represents the GSH_T which increases and remains stable after treatment with 50-500 µM H_2O_2. However, it decreases with 1500-2500 µM H_2O_2 after treatment. The ratio of GSH:GSGS <1 between 1500 and 2500 µM in Fig 3.8, shows that at 1400 µM H_2O_2 the GSH:GSSG ratio is <1.

3.5.3 Cell growth changes at 24 hours

After treatment with increasing concentrations of the H_2O_2 (50-5000 µM) for 24 hours, the bEnd5 cells were observed and recorded. No observable cell growth and size changes in bEnd5 cells occurred between the control and exposed groups between 50-500 µM H_2O_2. Only at higher concentrations of H_2O_2 (1-5 mM) did cells appear to be smaller and less observable (Fig 3.10 H-L).

http://etd.uwc.ac.za
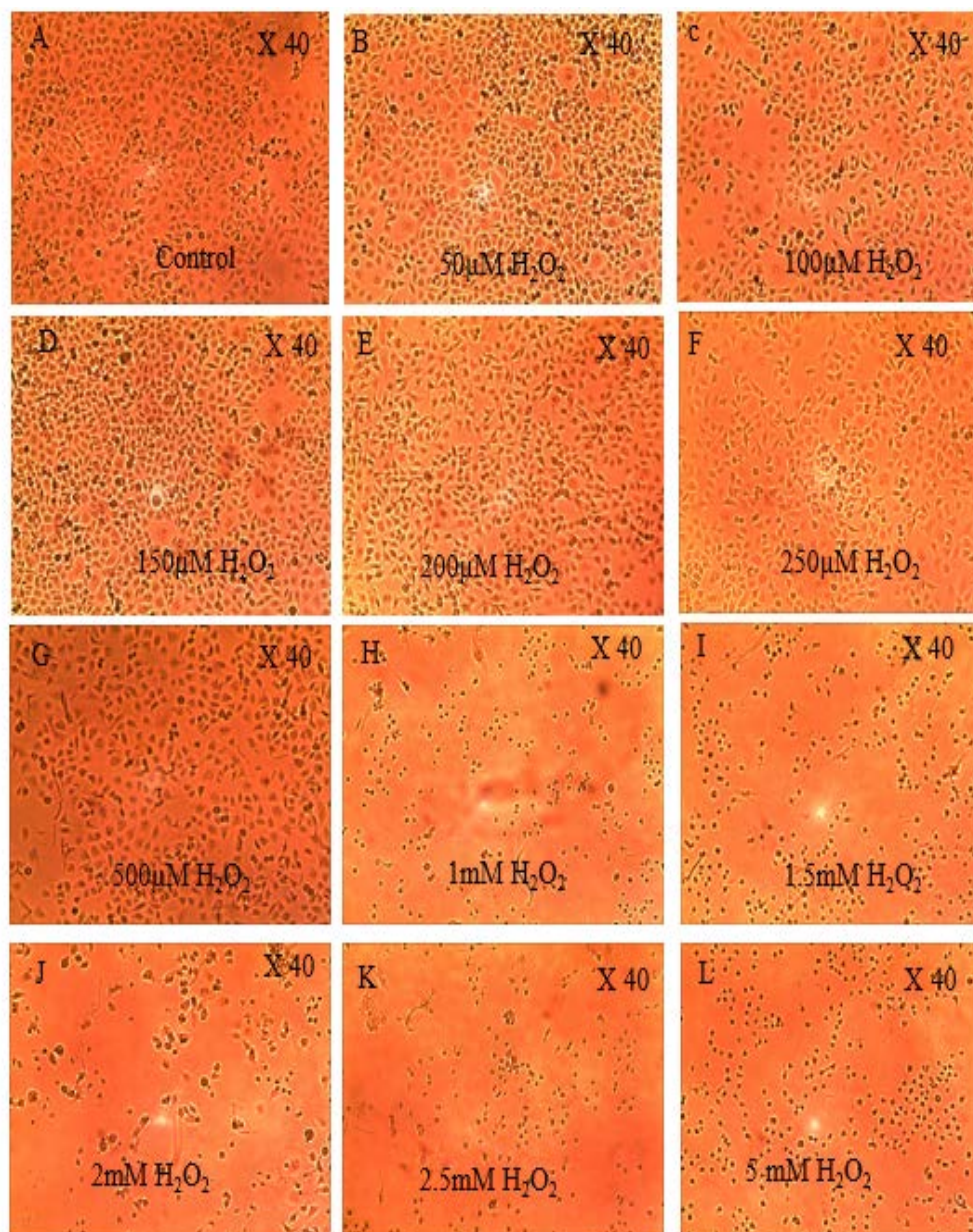
Figure 3.10 A-L: Observed bEnd5 cell growth at X 40 after being treated with increasing concentrations of H_2O_2 (0-5 mM) over 24 hours. Growth remained unchanged after treated with 0-500 µM H_2O_2. All higher concentrations (1-5 mM) showed a change in the cell growth (H-L).

3.6 ROS neutralising capacity of bEnd5 cells over 48 hours

3.6.1 GSH changes

The treatment of another group of cells was allowed to proceed for 48 hours to investigate if prolonged exposure to H_2O_2 would affect cellular concentrations of GSH/GSSG. Treated cells were exposed with H_2O_2 for 24 hours after which media were aspirated and replaced with fresh H_2O_2-dosed media and allowed to incubate for a further 24 hours. Doses of H_2O_2 (between 50 µM and 500 µM) continued over 48 hours to significantly elevate the levels of GSH_T.

Several observations were surprising. First, at 50 µM H_2O_2, GSH increased significantly compared to that of the control, then the GSH level decreased after treatment with 150, 250 and 500 µM H_2O_2. Second, at a dose of 1500 and 2500 µM H_2O_2, the GSH_T concentration dropped and remained statistically constant. However, at 1500 and 2500 µM H_2O_2 the GSH level decreased to a new (RLU <0.5 x 10^6) but relatively stable level, which did not differ statistically. Third, GSSG increased at 50 µM H_2O_2 compared to the control (P < 0.0001). The GSSG level increased to a new stable level at 150 and 250 µM H_2O_2, and then decreased and remained statistically constant at 1500 and 2500 µM H_2O_2 (Fig 3.11).

GSH_T reflected the levels of intracellular GSH throughout the experiment (Fig 3.11). The drop in GSH_T at 1500 and 2500 µM could be ascribed to a possible decrease in cell number (Fig 3.14).

The GSH to GSSG ratio at 50, 150, 250, 500 µM H_2O_2 was 75:25, which changed dramatically at 1500-2500 µM H_2O_2 to 51:49.
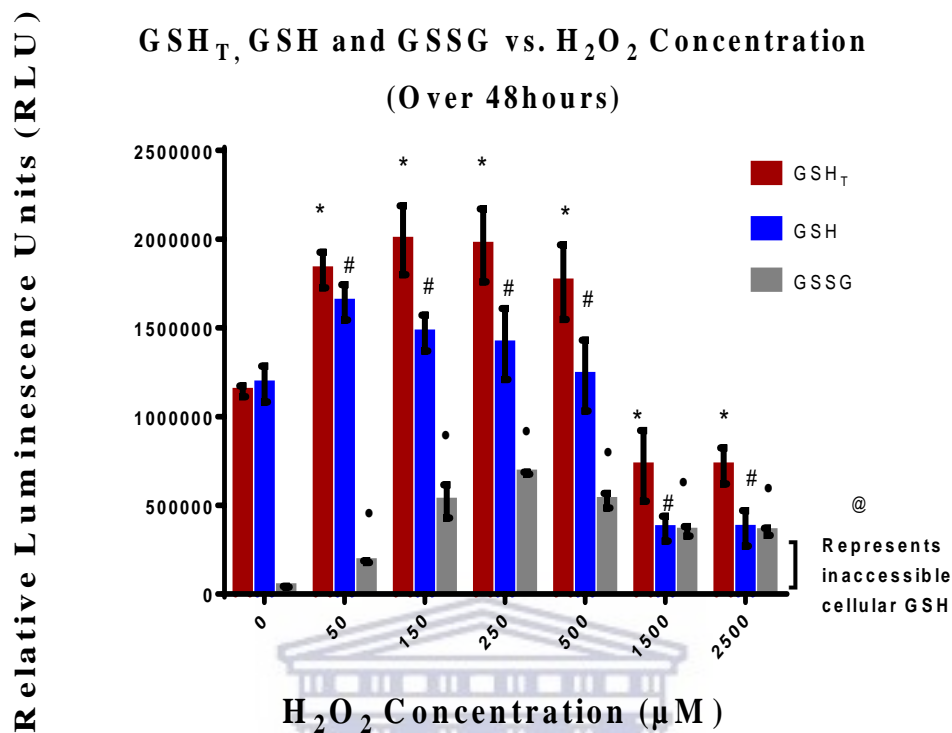
Figure 3.11: GSH, GSSG and GSH$_T$ levels in bEnd5 cells following incubation with H$_2$O$_2$ over 48 hours. The bEnd5 cells were incubated with increasing concentrations of H$_2$O$_2$ (50 µM to 2500 µM) before determining the levels of GSH, GSSH and GSH$_T$. The asterisk (*) denoted statistically significant differences between the control and experimental GSH$_T$ concentrations, and the hash (#) denoted statistically significant differences between the control and experimental GSH levels, while the bullet (●) denoted statistically significant differences in GSSG levels in bEnd5 cells between the experimental samples relative to controls. The @ denotes high levels of H$_2$O$_2$ treatment (1500 and 2500 µM), although GSH was still present in the cells, it appeared inaccessible and was not available to further protect the cells against the ravages of OS.

68
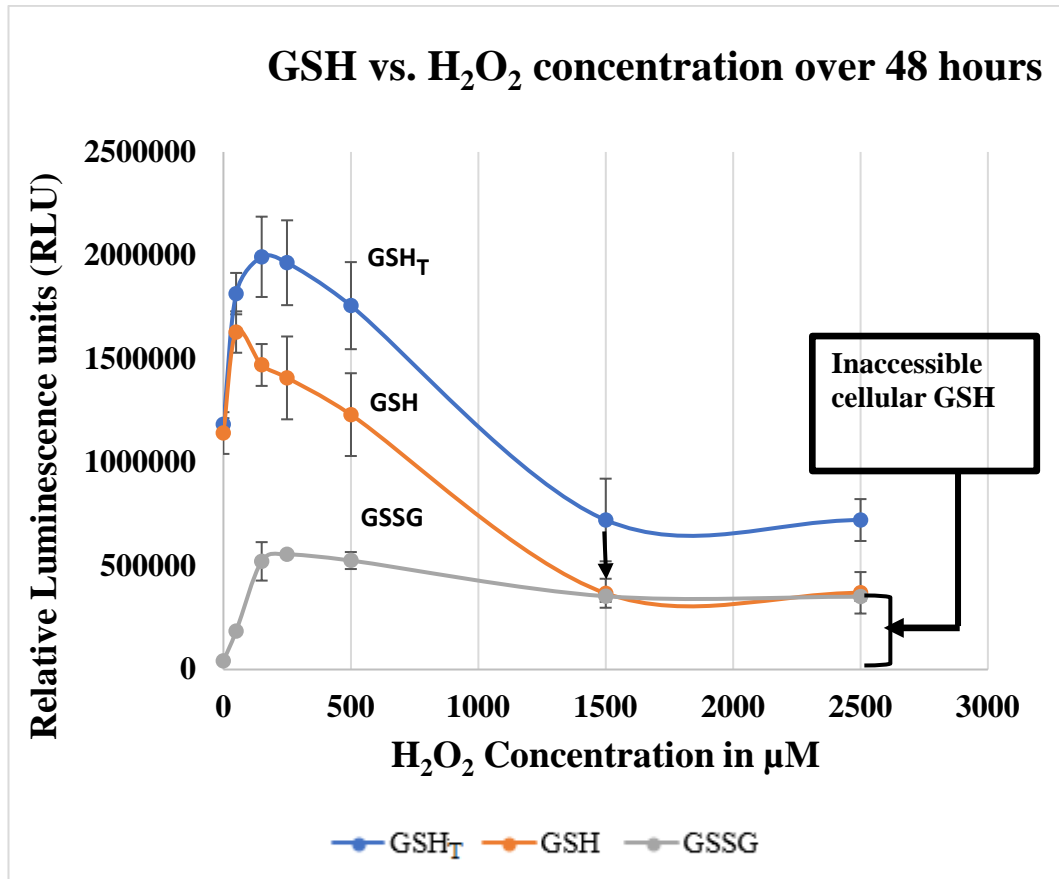
Figure 3.12: The above graph uses trend lines to depict changes in cellular glutathione content of bEnd5 cells exposed to varying concentrations of H_2O_2 over 48 hours. Between 50 and 100 µM H_2O_2 resulted in a steep and maximal rise in the GSH_T, which then decreased and plateaued at 1500-2500 µM H_2O_2. A similar decrease in GSH mirrored the GSH_T decrease. At H_2O_2 concentrations of 1500 µM (see arrow) reduced GSH and oxidised glutathione GSSG concentrations equalised. This point indicates the level of OS (H_2O_2) at which the cell numbers visible appeared to decrease. GSH maximally increased in concentration from 0-50 µM H_2O_2 which thereafter decreased in cells exposed to 1500 µM H_2O_2 and plateaued at 2500 µM H_2O_2. During 0-100 µM H_2O_2 exposure, GSSG increased maximally at 100 µM H_2O_2 and then plateaued at 2500 µM H_2O_2.

3.6.2 H₂O₂ treated cells at 48 hours

The ratio of GSH/GSSG in bEnd5 cells was found to increase after treatment with increasing concentrations of H_2O_2 (50-2500 µM) over 48 hours. The GSH:GSSG ratio was >1 for five of seven experimental treatment groups, while it was <1 in the other two groups indicating that bEnd5 cells were under OS (Fig 3.13).
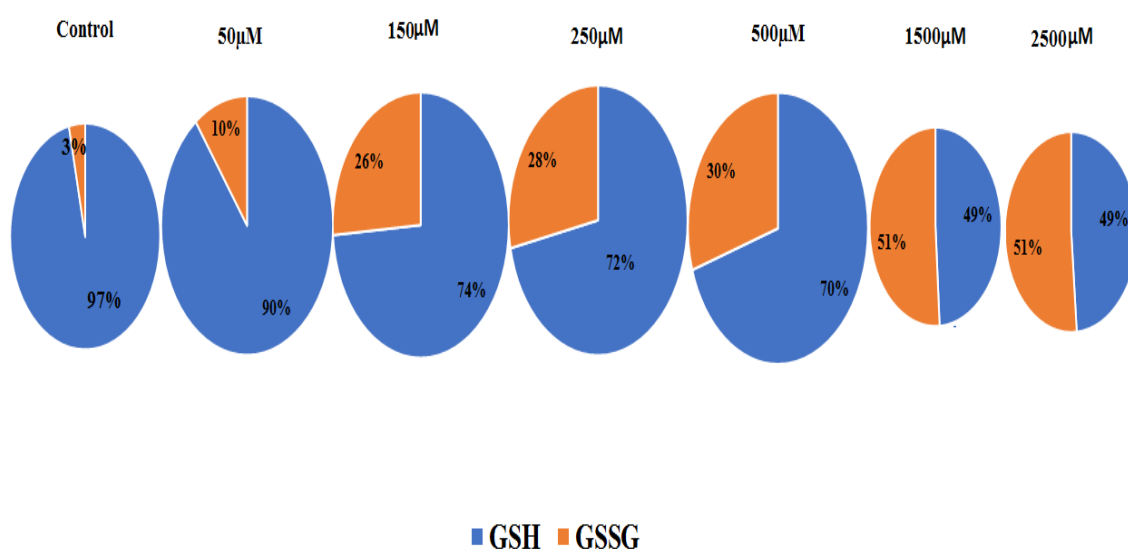
Figure 3.13: The longitudinal diameter of the pie charts reflects the relative GSH_T in bEnd5 cells. The pie chart also indicates the GSH:GSSG ratio in bEnd5 cells after being treated with increasing concentrations of H_2O_2 groups (50-2500 µM) over 48 hours. Except for 1500 and 2500 µM H_2O_2, the GSH:GSSG ratio of all the other groups was >1. Ratios of <1 typifies cellular population in redox stress.

3.6.3 Cell growth changes at 48 hours

After being exposed to increasing concentrations of the H_2O_2 (0-5 mM) over 48 hours, bEnd5 cell growth was observed with an inverted microscope (Zeiss) (Fig 3.14). No observable changes in the bEnd5 cell growth were noted between the control and the experimental groups of 50-500 µM (Fig 3.14 A-G). At higher concentrations (1-5 mM) cells became fewer and smaller than usual (Fig 3.14 H-L).
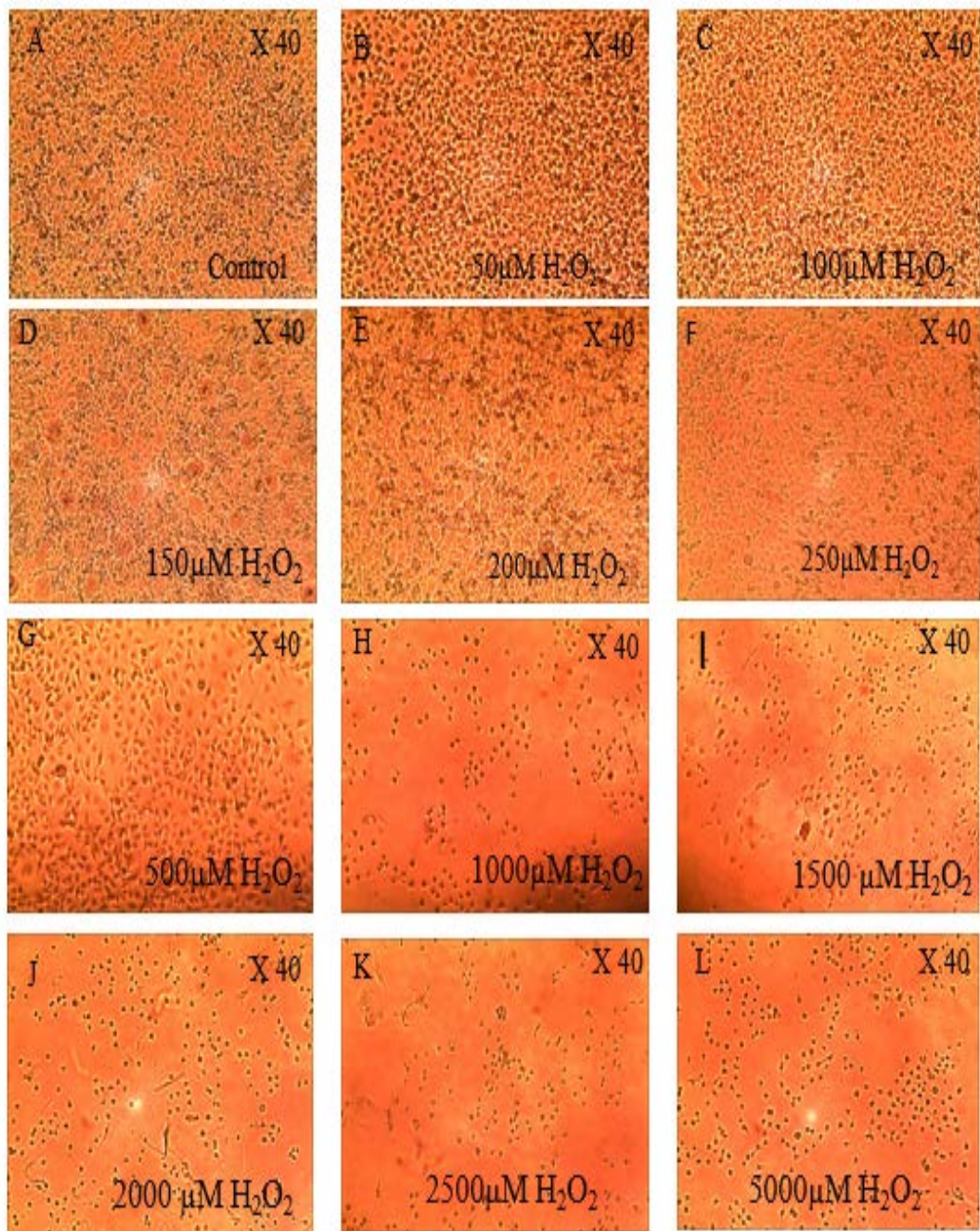
Figure 3.14 A-L: Micrographs at X 40 show bEnd5 cells after being exposed to increasing concentrations of H_2O_2 (0-5 mM) over 48 hours. No observable difference is seen until 500 µM (A-G). At higher concentration (1000-5000 µM) fewer cells were observed (H-L).

3.7 Protective effect of Trolox against H$_2$O$_2$ toxicity and GSH depletion over 24 hours

3.7.1 GSH changes

In view of the evidence in the literature, it was postulated that Trolox would alleviate the effects of H$_2$O$_2$. Therefore, the effects of the combinations of H$_2$O$_2$ and Trolox on the bEnd5 cells were investigated. The effect of the increasing concentrations of H$_2$O$_2$ (50-2500 µM) alone (control) was compared with the combined effect of the increasing concentrations of H$_2$O$_2$ (50-2500 µM) with 25 µM Trolox (test) for 24 hours. Simultaneous treatment of cells with H$_2$O$_2$ and Trolox was observed to have no effect on the GSH$_T$ - GSH - GSSG profile (P >0.05) in response to H$_2$O$_2$ treatment.
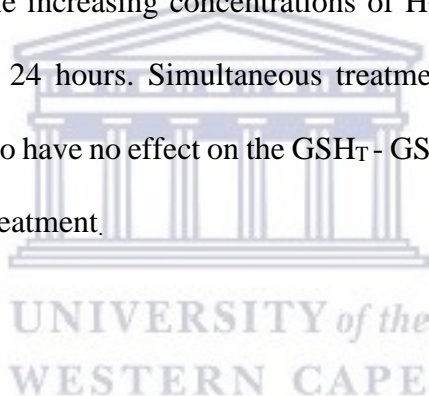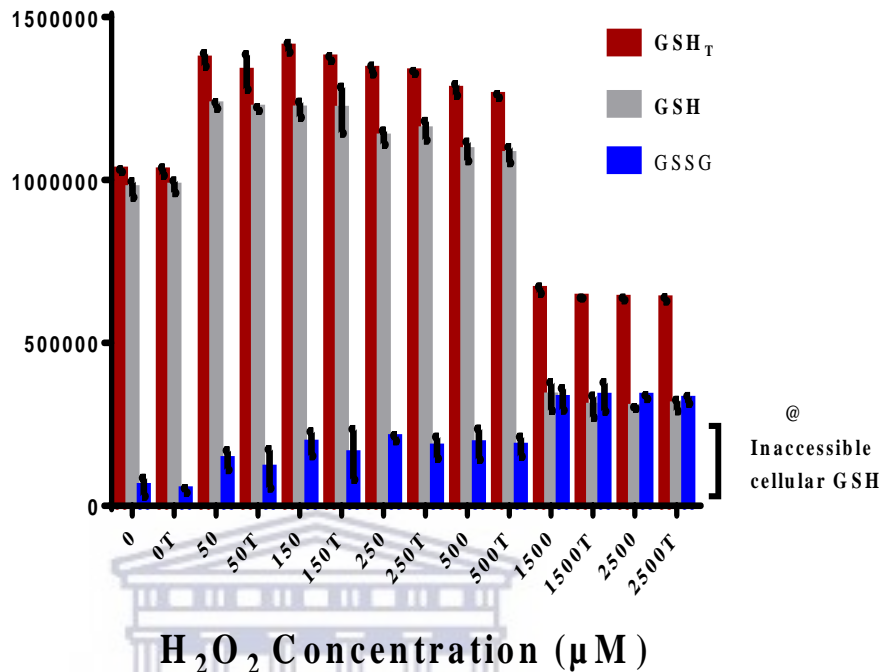
Figure 3.15: Shows changes in the GSH level in bEnd5 cells following incubation with increasing concentrations of H_2O_2 alone or in combination with 25 µM Trolox for a 24-hour exposure period. bEnd5 cells were incubated for 24 hours in supplemented DMEM medium dosed with increasing concentrations of H_2O_2 (50-2500 µM) alone (control groups) or combined with 25 µM of Trolox treated groups before determining the GSH_T level. The 'T' denotes the addition of 25 µM Trolox to the selected concentrations of H_2O_2. The data show there were no statistically significant differences in GSH_T, GSH and GSSG levels between cells exposed to H_2O_2 alone and those with added Trolox, P >0.05 (see Appendix E). The @ denotes that high levels of H_2O_2 treatment (1500-2500 µM) cells begin to die, yet were not able to access available GSH present in the cytoplasm.

74

3.7.2   Cell growth changes: Effect of Trolox

The bEnd5 cell growth was observed and recorded after being exposed to increasing concentrations of the H_2O_2 (50 µM-5 mM) or in combination with 25 µM Trolox over a 24 hour period (Fig 3.16). There was no observable difference between the cells exposed to H_2O_2 (50-500 µM) (Figs 3.16 A and C) and those that were exposed to both (50-500 µM) H_2O_2 and 25 µM Trolox (Figs 3.16 B and D).

There was a distinct difference observed between cells exposed to 1 mM H_2O_2 and those that were exposed to both 1 mM H_2O_2 and 25 µM Trolox (Figs 3.16 E & F). The cells became fewer and smaller (Fig 3.16 E). While in Fig 3.16, the cells exposed to both 1 mM H_2O_2 and Trolox appeared viable and healthy. There was no distinct difference observed between cells exposed to H_2O_2 at 5 mM and those that were exposed to both 5 mM H_2O_2 and 25 µM Trolox. Here both sets of cells became fewer and smaller (Figs 3.16 G & H). In general, cells exposed to Trolox exhibited a healthier appearance and appeared to have a pronounced protective effect against the OS effects of H_2O_2.

.
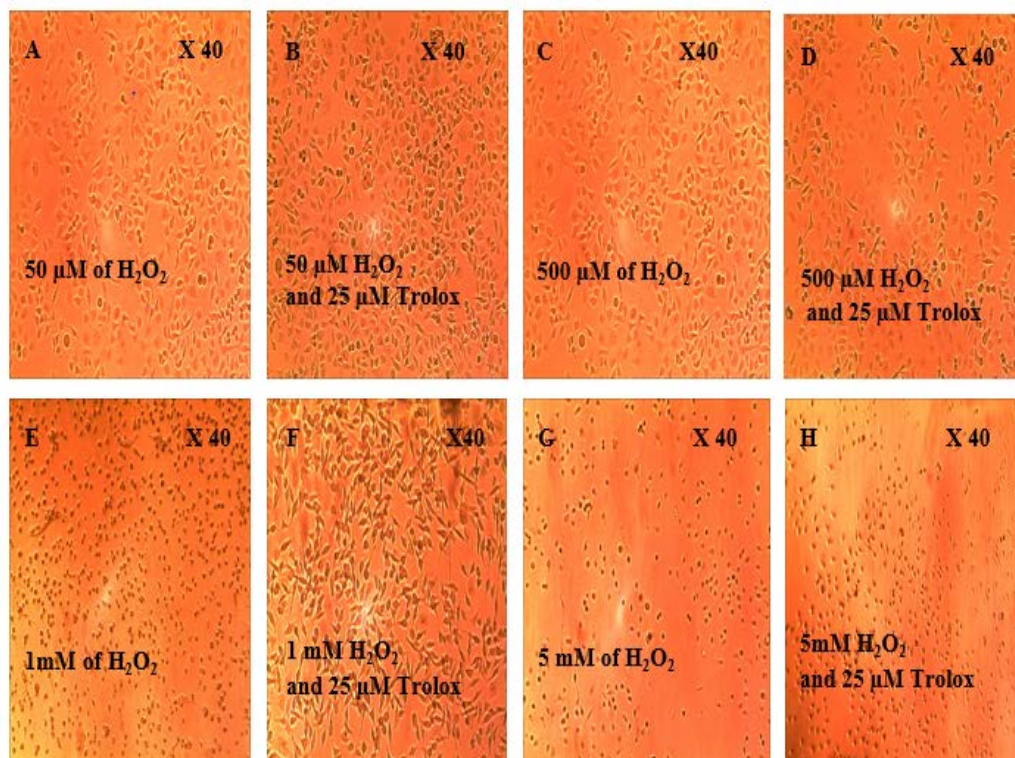
Figure 3.16 A-H: Exposure of bEnd5 cell growth to increasing concentrations of the H_2O_2 (50 µM-5 mM) alone or combined with 25 µM Trolox over 24 hours. Micrographs A and C represent cells exposed to 50 µM-500 µM H_2O_2, and B and D represent cells exposed to both H_2O_2 and 25 µM Trolox. In micrographs E-F there were distinct differences observed between cells exposed to 1 mM H_2O_2, where cells appeared fewer and small, but those that were exposed to both 1 mM H_2O_2 and 25 µM Trolox appeared viable and healthy. Cells exposed to 5 mM H_2O_2 were fewer and smaller (G), and the affect of Trolox did not protect the cells (H).

3.8 Protective effect of Trolox against H₂O₂ toxicity and GSH depletion over 48 hours

3.8.1 GSH changes

Extending the above study (Protective effect of Trolox against H_2O_2 toxicity and GSH depletion over 24 hours), the effect of the increasing concentrations of H_2O_2 (50-2500 µM) alone (control) was compared with the combined effect of the increasing concentrations of H_2O_2 (50-2500 µM) with 25 µM Trolox (test) for 48 hours. When evaluating the combination of increasing concentrations of H_2O_2 and 25 µM Trolox for 48 hours, the previously described GSH_T, GSH and GSSG profile for H_2O_2 treatment on bEnd5 cells was repeated. The data confirmed that treatment with Trolox and H_2O_2 had no effect on the GSH_T - GSH - GSSG profile.

UNIVERSITY *of the*

WESTERN CAPE

77
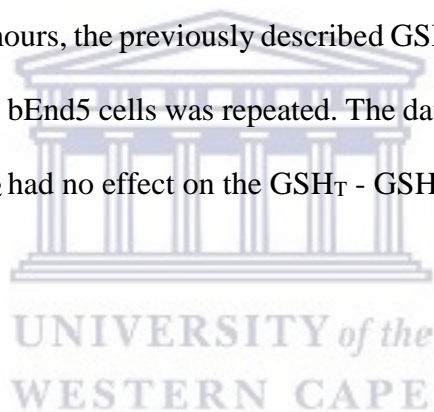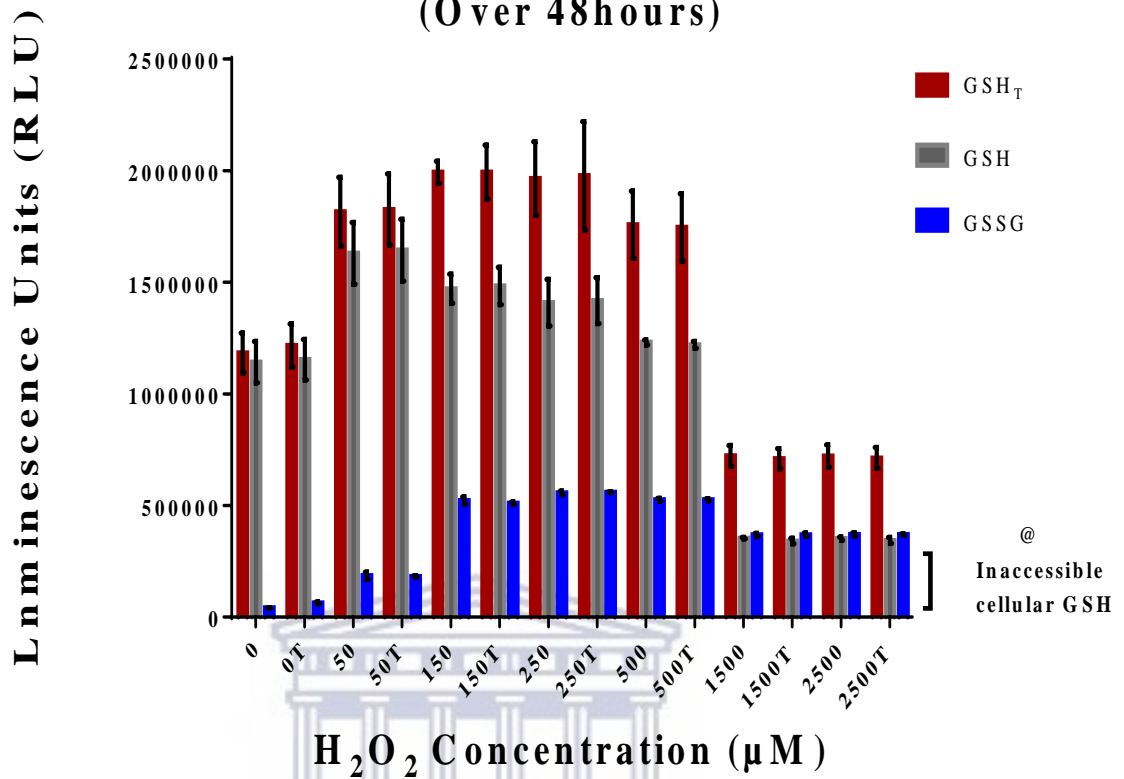
Figure 3.17: Changes in GSH level in bEnd5 cells following incubation with increasing concentrations of H_2O_2 alone or a combination of increasing concentrations of H_2O_2 and 25 µM Trolox for 48 hours are shown. bEnd5 cells were exposed to increasing concentrations of H_2O_2 (50-2500 µM) alone (control groups) or combined with 25 µM Trolox (treated groups) before determining the levels of GSH. The 'T' denotes the combination of increasing concentrations of H_2O_2 and 25 µM Trolox. The data showed there were no statistically significant differences in GSH_T, GSH and GSSG levels in bEnd5 cells between the experimental samples and controls (P >0.05) (see Appendix F). The @ denotes that high levels of H_2O_2 treatment (1500-2500 µM) cells begin to die, yet were not able to access available GSH present in the cytoplasm.

3.8.2 The effect of Trolox and H₂O₂ on cell growth over 48 hours

The bEnd5 cell growth was observed and recorded after being exposed to increasing concentrations of the H_2O_2 alone (50 µM-5 mM) or H_2O_2 (50 µM-5 mM) combined with 25 µM Trolox after a 48 hour exposure period (Fig 3.18). There was no observable difference between cells exposed to H_2O_2 (50-500 µM) (Fig 3.18 A and C) and the cells that were exposed to both (50-500 µM) H_2O_2 and 25 µM Trolox (Fig 3.18 B and D). There was a distinct difference observed between cells exposed to 1 mM H_2O_2 and those that were exposed to 1 mM H_2O_2 and 25 µM Trolox (Fig 3.18 E and F). Micrograph E represented the effect seen throughout the experiment with smaller and fewer cells between 1 mM-5 mM H_2O_2 (Fig 3.18 E), while Fig 3.18 F, the protective effects of Trolox are shown. However, there was no distinct difference observed between cells exposed to 5 mM H_2O_2 and those that were exposed to 5 mM H_2O_2 and 25 µM Trolox (Fig 3.18 G and H), which represented the effects seen throughout the experiment, presenting a decreased number of cells that were smaller than control cells.
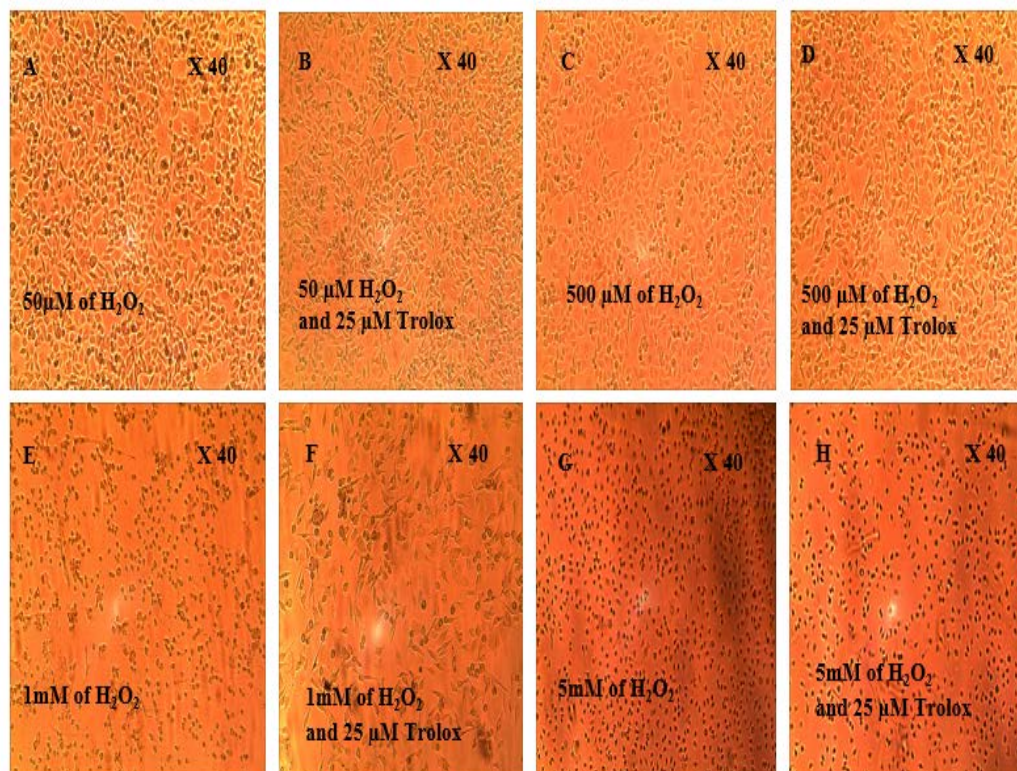
Figure 3.18 A-H: The effects of increasing concentrations of the H_2O_2 (50-5000 µM) alone or combined with 25 µM Trolox over a 48 hours exposure period. Micrographs X 80 A and C represent cells exposed to 50-500 µM, and micrographs B and D represent those cells exposed to both H_2O_2 and 25 µM Trolox. There was no observable difference between cells exposed to H_2O_2 (50-500 µM) and those that were exposed to both 50-500 µM H_2O_2 and 25 µM Trolox. Micrographs E and F show a distinct difference observed between cells exposed to 1 mM H_2O_2 (E) and those that were exposed to both 1 mM H_2O_2 and 25 µM Trolox (F), while E represents the effect seen throughout the experiment with smaller and fewer cells between 1 mM and 5 mM H_2O_2 Micrograph F showed that Trolox protects the cells against OS. There was no distinct difference observed between cells exposed to 5 mM H_2O_2 (G) and those that were exposed to both 5 mM H_2O_2 and 25 µM Trolox (H). In micrograph H the effect seen throughout the experiment shows smaller and fewer cells.

80

CHAPTER FOUR

Discussion

4.1 Introduction

The BBB is a structural and metabolic partition between the CNS and the peripheral blood circulation, which regulates the fluxes of molecules and cells *en* route to the CNS from the blood and *vice versa* (Huber et al., 2001). Thus, it is crucial to the maintenance of CNS homeostasis. Complex interactions between many cell types form the BBB, which is a dynamic interface capable of reactive responses to signals within the blood circulation and the CNS (Huber et al., 2001).

Primarily, the cell types include a monolayer of brain capillary endothelial cells as an interface with the blood and a perivascular set of cells on the brain side of microvessels, the astrocytes and pericytes (Abbott *et al.,* 2010). The primary function of the BBB is to keep the brain parenchyma undisturbed by changes in the plasma composition, as can occur following meals or exercise, and to protect from xenobiotics that are capable of altering neural functions. Also, to protect against peripherally circulating substances with neurotransmitter capabilities (Abbott et al., 2010).

The mechanical barrier is characterised by a lack of fenestrations in the endothelial junctions and very low rate of transcytosis (Wolburg & Lippoldt, 2002). Furthermore, the TJ between them is stronger than any endothelial TJ found elsewhere in the body as evidenced by its P-face strand association in freeze-

fracture replica electron microscopic studies (Wolburg & Lippoldt, 2002). This serves to restrict the paracellular diffusion of hydrophilic solutes such that only small molecules such as O_2, CO_2, and small lipophilic molecules (e.g., methamphetamine and alcohol) can freely diffuse across the lipid membranes of the endothelium (Fisher et al., 2015).

The BBB acts as a metabolic interface which contains specific carriers for essential molecules, such as the glucose transporter GLUT-1 occurring on both the luminal and abluminal membranes of the endothelial cells (Abbott *et al*., 2010). Another example of the role of the BBB is the P-glycoprotein transporter expressed on the endothelial luminal surface which protects the brain from xenobiotics and the potentially excitotoxic glutamate (Li *et al.,* 2012). Furthermore, the presence of endothelial degradation enzymes, such as peptidases and nucleotidases, which metabolise peptides and ATP, respectively, and the intracellular enzymes monoamine oxidase and cytochrome P450 1A and 2B which inactivate blood-borne neuroactive compounds (Li *et al*., 2012) provide an enzymatic barrier. Thus, multiple functions of the BBB regulate the brain microenvironment to ensure homeostatic balance.

Involvement of the BBB has been implicated in the development and propagation of several neuropathological conditions (Gilgun-Sherkiet *et al*., 2001). Hypoxic-ischemic disorders such as stroke, neurodegenerative disorders such as Parkinson's disease, Alzheimer's disease and multiple sclerosis have all been invariably linked to the compromise in the integrity of the BBB (Deane & Zlokovic, 2007; Stolp & Dziegielewska, 2009). Furthermore, many of the conditions leading to BBB dysfunction do so by way of inducing oxidative stress either within cells of the BBB

or tissues in the BBB microenvironment. On this basis, several clinical trials have been sanctioned to investigate the rational use of antioxidants in alleviating several neurological diseases (Moosmann & Behl, 2002; Rao & Balachandran, 2002).

Therefore, it was judicious to investigate how the BBB endothelial cells respond to OS and in particular look at the role of GSH, a naturally occurring intracellular antioxidant. As we were using an immortalised brain endothelial cell-line, bEnd5, we first had to establish whether GSH actually exists within the cell-line of study before investigating its physiological role in the BBB further.

4.2   Glutathione profile of bEnd5 cell line

In this study, we profiled, for the first time, the GSH content at the brain endothelial cell using the bEnd5 cell as a model to gauge the capacity of its innate GSH content to reactively neutralise ROS presented in the form of hydrogen peroxide. ROS is a known cause of BBB dysfunction (Lehner *et al.*, 2011), while GSH is an important cellular antioxidant (Lu, 2009).

Although bEnd5 cells are routinely used in the experimental modelling of the BBB (Steiner *et al.,*2011), information regarding its antioxidant capacity has not been previously reported in scientific literature. Our objectives, therefore, were first to demonstrate the presence of GSH in bEnd5 cells, estimate the quantity of this important antioxidant in a single endothelial cell (bEnd5) and determine the capacity of these cells in culture to neutralise OS (H_2O_2) and thereby protecting the cell from oxidative damage. Lastly, the impact of exogenous AOs and its impact on the endogenous GSH AO capacity of the bEnd5 cell was studied.

4.2.1   Detection of glutathione in bEnd5 endothelial cell line

The presence of GSH in bEnd5 cells was demonstrated by using a cell-permeable fluorochrome, mBCl. This compound has the ability to combine with thiol groups to form a fluorescent bimane adduct which can be detected and quantified fluorometrically. However, many of the bimane compounds bind with thiol groups in cellular proteins thereby contributing to the intensity of detected fluorescence and, therefore, is not specific for GSH.

Our choice of mBCl in this study was based on its specificity for the thiol group in GSH with negligible binding to protein thiols (Chatterjee et al., 1999). Ordinarily, mBCl alone does not fluoresce, but when in combination with the thiol group of GSH, it is converted to a fluorescent molecule that can be viewed under a fluorescent microscope. Cells that were incubated with 60 µM mBCl showed blue fluorescence, while untreated control experimental cells without mBCl showed no fluorescence (Fig 3.1 A and B). This confirmed that the observed fluorescence was attributable to the presence of the glutathione-bimane adduct in the mBCl-treated cells. The fluorescent intensity observed varied among the cells which suggest varying concentrations of GSH in the cellular content.

Differences in the redox and/or metabolic status of the cells may have imparted the differential fluorescent intensities. Furthermore, this observed variation in fluorescent intensities among the cultured cells may indicate differences in the redox status of individual cells in culture. Also, observed are slight differential density in the fluorescence between the nuclear and cytosolic compartments. The blue fluorescence observed in the cytosolic compartments showed increased

84

brightness around the nuclear compartments of the cells which suggest higher concentrations of GSH in the nuclear compartment of these endothelial cells (Fig 3.1 C). Also, the higher fluorescence found within the nucleus indicates a higher nuclear concentration of GSH than the cytosol. This points to the role of GSH as the primary AO protecting DNA against ROS (Fig 3.1 D), which agrees with previous reports of intracellular compartmentalisation of GSH distribution (Li et al., 2012).

In culture, bEnd5 cells are adherent cells which proliferate and also grow in size by projecting cytoplasmic extensions upon the substratum. This explains why the bEnd5 cells showed improved attachment and also with more conspicuous cytoplasmic extensions when they were grown on collagen-coated microscopic slides. We observed the presence of GSH-induced fluorescence in every strand of cytoplasmic extension, an observation which further underscores the antioxidative importance of GSH in every segment of the cells for their viability (Fig 3.1 D).

4.2.2 Proliferation rate of bEnd5 cells

The quantity of GSH in a single bEnd5 cell was estimated by calculating the average amount of GSH in a specific number of cells cultured under standard culture conditions and dividing the estimated amount of GSH by the number of cells in culture. The bEnd5 cells, being adherent cells, needed to be cultured under standard conditions and allowed to attach in culture to closely mimic their basal status in the BBB at the time of estimation of their GSH content. However, these cells while

attaching also multiply thereby challenging our determination of cell number at the time of estimation of GSH contents.

These challenges were addressed by performing a proliferation assay to determine the rate of proliferation of bEnd5 cells in culture over the period of hours covering our time of estimation. Cell numbers were counted and rate of proliferation studied over 35 hours. Cultured bEnd5 cell numbers were found to double at approximately 16 hours within the first 24 hours and 11 hours within the second 24 hours which indicate an increased, but constant rate of proliferation in the second 24 hours.

The graph of cell numbers plotted against duration of cultures revealed two different rates of growth before and after 24 hour (Fig. 3.3), with the slope of the growth curve assuming an overtly steeper slope from 24 hour and beyond which is an evidence in support of an increased growth rate. The increased rate of growth with advancing duration of culture is suggestive of paracrine stimulation of growth by contiguous cells now in close contact. The more the number of cells in culture at a time, the faster their rate of proliferation appears to be a valid rule for the bEnd5 cells. This important finding is being reported for the first time for any BEC model in the scientific literature.

4.2.3   Estimation of glutathione content of bEnd5 cell line

We estimated the quantity of GSH and GSSG in 1×10^4 bEnd5 cells using the GSH-Glo Assay Kit method and the modified GSH recycling method of Tietze, respectively (Tietze, 1969). The data allowed for the calculation and extrapolation of the cellular GSH content which averaged 0.031 ± 0.00035 nmol.cell^{-1} (31 ± 0.35

86

pmol.Cell^{-1}) while that of glutathione disulfide (GSSG) amounted to 0.00092±0.00021 nmol.cell^{-1} (0.92±0.21 pmol.cell^{-1}) in bEnd5 cells. This puts the resting redox status of bEnd5 cells at a percentage GSH:GSSG ratio of approximately 97:3.

Aggressive cancer cells have been reported to contain a relatively higher quantity of GSH than normal cells which correlates with their resistance to oxidative chemotherapeutic agents (Lash, Putt, & Jankovich, 2015). Indeed the intracellular thiol redox state which depends on the GSH content has been noted to be an important effector in regulating the mitochondrial permeability transition pore complex, which makes thiol oxidation a potential causal factor for a mitochondrial-based mechanism for cell death (Ortega *et al.,* 2011).

The content of GSH in bEnd5 cells is relatively higher when compared with values obtained in certain cancer cells which are reported to contain high GSH levels. For example, HepG2 human liver cancer cells have GSH concentrations of 0.00299 pmol.cell^{-1} (Yuan *et al*., 2013), while the ME180 cell-line (epithelial cells of human cervical carcinoma origin) have a GSH level of 0.017 pmol.cell^{-1} (Lee *et al.,* 1988).

Given the correlation of elevated GSH levels in various types of neoplastic tissues to increased resistance of these tissues to oxidative chemotherapy, a comparatively higher GSH content as found in the bEnd5 cells, position BECs for increased protection against ROS. This is not unexpected given that the BBB is regularly exposed to OS from various sources such as inflammation/pro-inflammatory cytokines, amyloid deposits as occur in the ageing process and Alzheimer's disease, excessive alcohol consumption and hypoxic states.

Earlier cellular GSH estimation methods reported cellular GSH in the range of 230-440 nmol.cell^{-1} for normal human erythrocytes which were much higher than the levels obtained in this study. Cellular GSH values reported in human erythrocytes was 440 nmol.cell^{-1} (Ellman, 1959), 230 nmol.cell^{-1} (Hardin *et al.,* 1954), and 240 nmol.cell^{-1} (Tietze, 1969). We suggest that the current values are more accurate given the recent advances in the methods of estimation.

4.2.4   Effects of proliferation over 96 hours on the GSH:GSSG profile

The quantity of GSH and GSSG in 1×10^3 bEnd5 cells was measured over 96 hours using the GSH-Glo Assay Kit method and the modified GSH recycling method of Tietze, respectively (Tietze, 1969). A considerable amount of energy in the form of ATP is required for the process of cell division (Lu, 2009), and therefore, cultured cells which are actively dividing are expected to produce high levels of OS (Ashtiani *et al*., 2013).

Data from our experiments showed that cells under OS had a much higher ratio of GSH:GSSG with GSSG levels of 10% to 30%, under stress of 50-500 µM H_2O_2 (Fig 3.9 and 3.13). Thus, it was surprising to find that over a period of 96 hours, the cell's GSH:GSSG ratio was fairly stable compared to control group cells (non-H_2O_2 stressed group) throughout the 96 hours of culture. GSH depletion has been scientifically reported to cause impairment of cellular proliferation in fibroblasts (Markovic et al., 2009). Our data indicated that dividing cells endogenous antioxidants must be up-regulated during the proliferation of bEnd5 cells, therefore, no significant OS is generated during proliferation of bEnd5 cells.

4.3　ROS neutralising capacity of bEnd5 cell line at 24 and 48 hours

When the bEnd5 cell line in culture was exposed for 24 and 48 hours to varying concentrations of H_2O_2, ranging from 50 µM to 5 mM, we observed that starting at 50 µM, there was a switch-like resetting of the GSH_T content of the cells to a maximum value of about 37% above the basal value. This increment remained sustained through until 500 µM, and then dropped rapidly at higher doses of H_2O_2.

At 150 µM H_2O_2, the GSH_T peaked at about 37% above resting cellular content and without a significant difference from values obtained at other H_2O_2 concentrations between 50 µM and 500 µM. This appears to be the maximum capacity of the bEnd5 cells for GSH synthesis and has not been reported in scientific literature previously.

However, between 50 µM and 500 µM H_2O_2, the increments in the value of the GSH_T varied within the range of 26.5-37% above resting intracellular content. This persistent indifference in the increased amount implies a definite switch in the transcriptional control of GSH biosynthesis sensitive to low concentrations of reactive oxygen species.

The maximum increase in the GSH level was at 150 µM H_2O_2 beyond which a slight but significant reduction was seen until 500 µM. At the same concentrations, the levels of GSSG showed a slight but steady increase. The GSH:GSSG ratio in the control group which was initially approximately 95:5 varied between the 50-500 µM H_2O_2 in the range of 90:10 to 85:15 which implied a minimal change in the thiol redox status of the bEnd5 cells at treatment concentrations of 50-500 µM H_2O_2 (Fig 3.7 and 3.8).

89

Regulation of the thiol redox status of the cell depends largely on the *de novo* synthesis of GSH, the rate of which is governed by the activity of the GCL enzyme. Our findings suggest that the bEnd5 cell reacts to slight oxidative challenges by switching to its maximal capacity for GSH synthesis and maintaining such until the demand for GSH oxidation exceeds its capacity for synthesis. At H_2O_2 concentrations above 500 µM, the values of GSH_T fell rapidly and there was a rapid decrease in the GSH:GSSG ratio until the concentration of the GSSG fraction approximately equalled or exceeded that of the GSH (Fig 3.7 and 3.8).

Scientific evidence supports the existence of plasma membrane transporters for the export of GSSG (Ballatori, Krance, Marchan, & Hammond, 2009; Brechbuhl et al., 2010; Leier et al., 1996). The decrease in the values of GSH_T observed at higher H_2O_2 concentrations appears to be attributable to GSSG export as well as the decrease in the total number of cells because of ROS-induced cell death

90
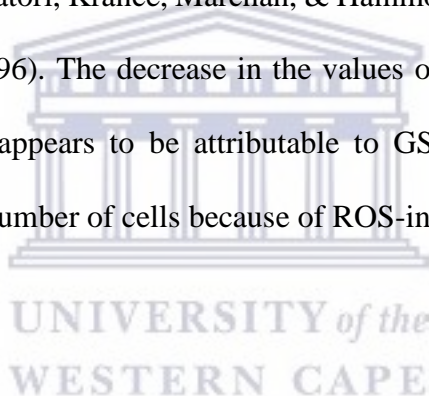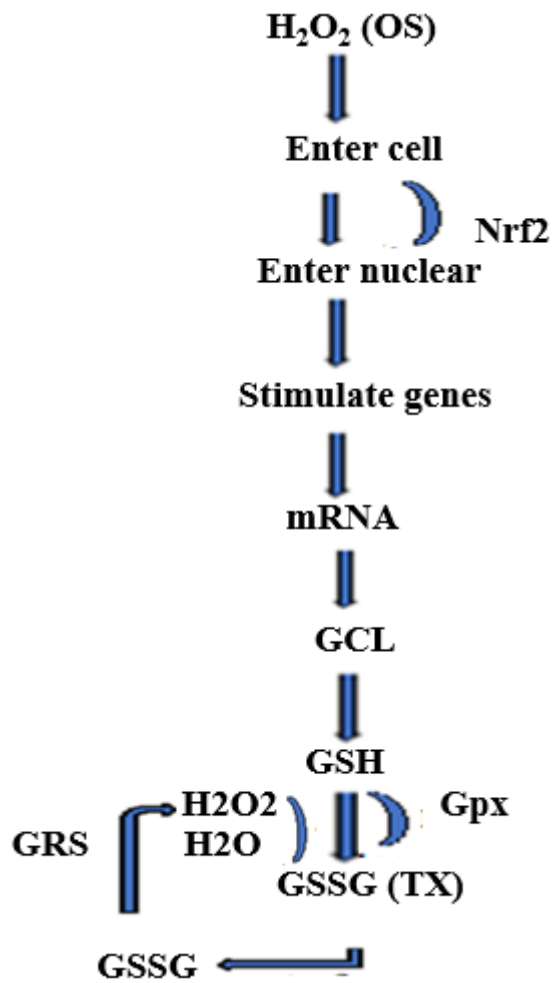
Figure 4.1: H_2O_2 diffuse across cell membranes, which regulates directly or indirectly a number of transcription factors, especially Nrf2. Nrf2 under OS becomes activated and translocated from the cytoplasm to the nucleus subsequently activating the transcription of antioxidant genes which up-regulate L-cysteine transport and glutathione biosynthesis that increase GSH levels. GSH is able to convert H_2O_2 to H_2O and O_2 in the presence of GSH peroxidase. In the process, GSH is oxidised to GSSG, which is either reduced back to GSH by GSH reductase at the expense of NADPH, forming a redox cycle, or excretion from the cell by ATP-dependent, multidrug resistance protein-related GSSG transporter (Ballatori et al., 2009; Brechbuhl et al., 2010; Leier et al., 1996).

4.4   Effects of H$_2$O$_2$ on cell growth

Observations of the changes in cell growth support those of a well-maintained thiol redox status for the cells between H$_2$O$_2$ concentrations of 50-500 µM. Cell growth apparently appeared normal concerning the control group of cells until H$_2$O$_2$ concentrations exceeded 500 µM. These results were similar for the 24 and 48 hour studies. The bEnd5 cells remained well adherent with well-spread cytoplasmic extensions. The maintenance of cell shape depends largely on cell cytoskeleton, and cell-cell adhesion in the BBB and these characteristics of the brain endothelial cell is crucial to the regulation of BBB permeability (Lum & Malik, 1994).

Specifically, actin cytoskeleton has been reported to be a target for oxidative stress which acts by remodelling of the actin filament network with consequent loss of cell shape and cell rounding (Lum & Roebuck, 2001). The observations in this study underscored the pivoting dynamics of the *de novo* GSH synthesis and GSSG recycling mechanism in regulating GSH homeostasis during the oxidative challenge to keep the cell at redox equilibrium.

However, it was assumed the cells were viable at these concentrations based on the intact morphological features observed. At H$_2$O$_2$ concentrations of 1 mM and above for 24 and 48 hours, GSH$_T$ values fall sharply to a new level about 65% of the resting value and remain so at all concentrations of H$_2$O$_2$ above 1.2 mM. The redox status of the cell viewed as the GSH:GSSG ratio changed to 1:1 at 1.2 mM H$_2$O$_2$ concentration. At H$_2$O$_2$ values above 1000 µM, cells decreased in size and were fewer in number.

4.5   Effects of H_2O_2 and Trolox on cell growth and GSH_T/GSSG/GSH levels

Combined treatment with the antioxidant, Trolox ((±)-6-Hydroxy-2, 5, 7, 8-tetram-ethylchromane-2-carboxylic acid), and H_2O_2 produced similar results with respect to the cellular GSH content. However, while Trolox does not ameliorate the cellular depletion of GSH (Fig 3.15), it protected the cell growth at a concentration of H_2O_2 up until 1 mM.

Cells treated with 25 µM Trolox showed intact growth up to 1 mM H_2O_2 which implies a level of protection is provided by the antioxidant properties of Trolox, a water-soluble analog of vitamin E. However, this concentration of Trolox 25 µM had no effect on the cellular GSH:GSSG content suggesting that it provides protection against ROS using a mechanism which are independent of glutathione mechanisms. The signal for the decrease in cell growth is apparently maximal at H_2O_2 concentrations of about 1 mM and higher in the absence of Trolox. In the presence of Trolox 25 µM the signal for the decrease in cell growth is averted and extended to 1 mM H_2O_2.

This signal for decrease in the cell growth is averted with antioxidant treatment but above ROS of 1 mM H_2O_2 cell death will ensue with or without antioxidant supplementation 25 µM Trolox. Therefore, it follows that GSH not only is important for cellular anti-oxidation but more importantly as a signal transducer for cell survival or death. This is exemplified by findings of elevated GSH levels in neoplasms that are resistant to oxidative chemotherapeutic drugs (Traverso *et al*., 2013).

4.6 GSH unassailable at high OS levels

Approximately 32% of resting cellular GSH remained unassailable within the cell (Fig 3.7 and 3.12). The utilisation of GSH in the presence of H_2O_2 challenge depends mainly on the availability and activity of the Gpx enzyme (Fig 3.6). This unreachable GSH reserve could be because of the limitation in the amount of cellular Gpx available to the cell in the presence of such levels of ROS. Whether such latent GSH reserve exists is not clearly known, in the *in vivo* situation. If it does exist, this implies any cellular manipulation directed at the upregulation of the Gpx enzyme will increase cellular antioxidant capacity by making latent GSH reserve available to neutralise more ROS. Furthermore, an antioxidant that supports the cellular capacity for increased GSH biosynthesis, such as N-acetyl-L-cysteine (NAC) would probably help protect the integrity of the endothelial cells of the BBB in situations of severe OS (metabolic pathways of Gpx in Fig 4.1).
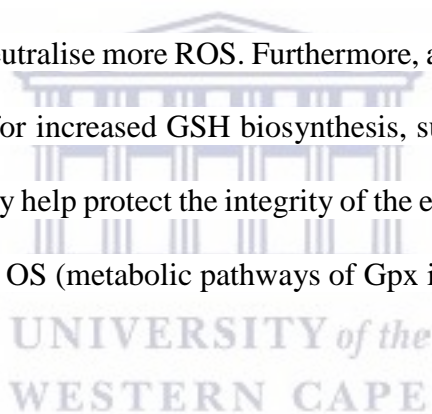
CHAPTER FIVE

5.1 Conclusion

The BBB insulates the brain from the plasma with its specialised endothelial structure that forms the microvasculature of the brain, prohibiting the entry of harmful blood-borne substances into the brain microenvironment. Thus, the transport of substances in and out of the brain is regulated, as is homeostasis. Therefore, understanding the function of the endothelial cells of the brain is of the utmost importance.
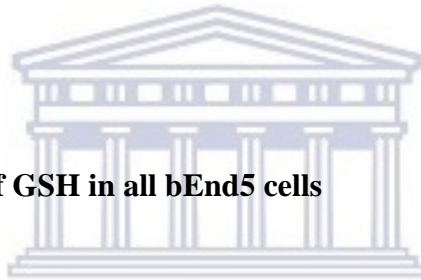
5.1.1 The presence of GSH in all bEnd5 cells

In this study, it was established that GSH is present in bEnd5 cells and distributed throughout the cytoplasm including the nuclear compartment. Variable fluorescence intensity observed in the cells indicated that bEnd5 cells have variable intracellular concentrations of GSH. The high localisation of GSH at the level of the nuclear membrane is indicative of the important role it plays in protecting DNA from OS.

5.1.2 Rat-tail collagen and bEnd5 cells attachment

Our technique studied endorsed the methodology that slides coated with rat-tail collagen facilitate bEnd5 cell attachment to the slides.

5.1.3 Proliferation rate of bEnd5 cells

The growth of cultured bEnd5 cells increases after 24 hours: cultured bEnd5 cell numbers were found to double at approximately 15.66 hours within the first 24 hours and 11 hours within the second 24 hours. This established that cells growing in close proximity to each other undergo accelerated cell division.

5.1.4 Estimation of glutathione content of bEnd5 cell line

For the first time, BEC were profiled in terms of their GSH_T/GSH/GSSG concentration:

- We established that the average amount of cellular GSH content is 0.031 ± 0.00035 nmol.cell^{-1} (31 ± 0.35 pmol.Cell^{-1}), while GSSG amounted to 0.00092 ± 0.00021 nmol.cell^{-1} (0.92 ± 0.21 pmol.cell^{-1}) in the bEnd5 cell line.
- The GSH:GSSG ratio at resting redox status of bEnd5 cells was found to be approximately 97:3 at 24 hours in culture.
- Cultured bEnd5 cells' basal redox status given as the GSH:GSSG ratio ranged from 94:6 to 97:3 over an extended cell culture period of 24-96 hours. These experiments established that cell growth under culture conditions did not produce excess ROS throughout the passage of 96 hours.

5.1.5 ROS neutralising capacity of bEnd5 cell line

- When comparing the concentration of GSH per cell to other cell lines, it was found that bEnd5 cells contain a relatively greater amount of GSH per cell, which indicates the enhanced capability of BEC to neutralise more ROS compared to several other varieties of cells.

- The GSH fraction of glutathione represents more than 95% of the total resting pool which confers a very stable resting redox status to these cells. The natural ROS neutralising capacity of bEnd5 cells is equivalent to 500 µMol H_2O_2, and further increases in OS is not able to deplete the cells of GSH before cellular compromise, leaving a level of GSH which appears inaccessible in cultured cells at the high level of OS.

- The redox status of the cell viewed as the GSH:GSSG ratio changed from 97:3 (GSH:GSSG) to 1:1 at 1.4 mM H_2O_2 concentration. In future, the GSH:GSSG profiling will allow for the level of OS to be monitored in cultured cells, and understood as to how it triggers necrosis or apoptosis.

- Combined treatment with antioxidant, Trolox and H_2O_2 produced similar results to treatment with H_2O_2 only, with respect to the cellular GSH:GSSG ratio and concentration.

- Trolox does not ameliorate the cellular level of GSH nor does it change the GSH_T/GSH/GSSG profile of cells under various stages of OS.

- Trolox did not affect cellular GSH/GSSG content suggesting that it provides protection against ROS using a mechanism which is independent of glutathione mechanisms.

- In conclusion, GSH not only acts in its capacity as an antioxidant but as the key signal transducer for cellular survival or death.

5.2   Future studies

Since the following issues were beyond the scope of this study, it is suggested to investigate

- the effect of a higher dose of the protective effect of the exogenous AO NAC which will prove cysteine as a substrate for GSH and therefore protect against H_2O_2 toxicity and GSH depletion;
- whether the inaccessible level of GSH (at high H_2O_2/SO) was because of the cell not having sufficient substrate to form additional GSH.

In future studies the higher doses of Trolox on conferring greater levels of protection to a cell exposed to a high level of OS.

5.3 References

Abbott, N. J. (2002). Astrocyte–endothelial interactions and blood–brain barrier
permeability. *Journal of Anatomy*, *200*(**5**), 523–534.

Abbott, N. J., Rönnbäck, L., & Hansson, E. (2006). Astrocyte-endothelial
interactions at the blood-brain barrier. *Nature Reviews. Neuroscience*,
7(**1**), 41–53.

Abbott, N. J., Patabendige, A. A., Dolman, D. E., Yusof, S. R., & Begley, D. J.
(2010). Structure and function of the blood–brain barrier. *Neurobiology of
Disease*, *37*(**1**), 13–25.

Abegg, M. A., Alabarse, P. V. G., Schüller, Á. K., & Benfato, M. S. (2012).
Glutathione levels in and total antioxidant capacity of Candida sp. cells
exposed to oxidative stress caused by hydrogen peroxide. Revista Da
Sociedade Brasileira de Medicina Tropical, **45**(**5**), 620–626.

Abramov, A. Y., Scorziello, A., & Duchen, M. R. (2007). Three distinct
mechanisms generate oxygen free radicals in neurons and contribute to
cell death during anoxia and reoxygenation. *The Journal of Neuroscience*,
27(**5**), 1129–1138.

Agarwal, R., & Shukla, G. S. (1999). Potential Role of Cerebral Glutathione in the Maintenance of Blood-Brain Barrier Integrity in Rat. *Neurochemical Research*, *24*(**12**), 1507–1514.

Aoyama, K., Watabe, M., & Nakaki, T. (2008). Regulation of neuronal glutathione synthesis. *Journal of Pharmacological Sciences*, *108*(**3**), 227–238.

Aoyama, K., & Nakaki, T. (2013). Impaired glutathione synthesis in neurodegeneration. *International Journal of Molecular Sciences*, *14*(**10**), 21021–21044.

Argaw, A. T., Gurfein, B. T., Zhang, Y., Zameer, A., & John, G. R. (2009). VEGF-mediated disruption of endothelial CLN-5 promotes blood-brain barrier breakdown. *Proceedings of the National Academy of Sciences of the United States of America*, *106*(**6**), 1977–1982.

Ashtiani, H. R. A., Bakhshandi, A. K., Rahbar, M., Mirzaei, A., Malekpour, A., & Rastegar, H. (2013). Glutathione, cell proliferation and differentiation. *African Journal of Biotechnology*, *10*(**34**), 6348–6363.

Ballabh, P., Braun, A., & Nedergaard, M. (2004). The blood–brain barrier: an overview: structure, regulation, and clinical implications. *Neurobiology of Disease*, *16*(**1**), 1–13.

Ballatori, N., Krance, S. M., Marchan, R., & Hammond, C. L. (2009). Plasma membrane glutathione transporters and their roles in cell physiology and pathophysiology. *Molecular Aspects of Medicine, 30*(**1**), 13-28.

Baxter, P. S., Bell, K. F., Hasel, P., Kaindl, A. M., Fricker, M., Thomson, D., … Hardingham, G. E. (2015). Synaptic NMDA receptor activity is coupled to the transcriptional control of the glutathione system. *Nature Communications*, ***6***.613-226.

Bernacki, J., Dobrowolska, A., Nierwiñska, K., & Malecki, A. (2008). Physiology and pharmacological role of the blood-brain barrier. *Pharmacol Rep*, ***60*(5)**, 600–622.

Betteridge, D. J. (2000). What is oxidative stress? *Metabolism*, ***49*(2, Supplement 1)**, 3–8.

Brechbuhl, H. M., Gould, N., Kachadourian, R., Riekhof, W. R., Voelker, D. R., & Day, B. J. (2010). Glutathione transport is a unique function of the ATP-binding cassette protein ABCG2. *J Biol Chem, 285*(**22**), 16582-

Brooks, T. A., Hawkins, B. T., Huber, J. D., Egleton, R. D., & Davis, T. P. (2005). Chronic inflammatory pain leads to increased blood-brain barrier permeability and tight junction protein alterations. *American Journal of Physiology-Heart and Circulatory Physiology*, ***289*(2)**, H738–H743.

Brown, R. C., & Davis, T. P. (2002). Calcium Modulation of Adherens and Tight Junction Function A Potential Mechanism for Blood-Brain Barrier Disruption After Stroke. *Stroke*, *33*(**6**), 1706–1711.

Cardoso, F. L., Brites, D., & Brito, M. A. (2010). Looking at the blood–brain barrier: molecular anatomy and possible investigation approaches. *Brain Research Reviews*, *64*(**2**), 328–363.

Cecchelli, null, Dehouck, null, Descamps, null, Fenart, null, Buée-Scherrer, null, Duhem, null, … Dehouck, null. (1999). In vitro model for evaluating drug transport across the blood-brain barrier. *Advanced Drug Delivery Reviews*, *36*(**2–3**), 165–178.

Chang, H.-X., Yang, L., Li, Z., Chen, G., & Dai, G. (2011). Age-related Biological Characterization of Mesenchymal Progenitor Cells in Human Articular Cartilage, *34(8),* e382-e388.

Chatterjee, S., Noack, H., Possel, H., Keilhoff, G., & Wolf, G. (1999). Glutathione levels in primary glial cultures: Monochlorobimane provides evidence of cell type-specific distribution. *Glia*, *27*(**2**), 152–161.

Choi, Y.-K., & Kim, K.-W. (2008). Blood-neural barrier: its diversity and coordinated cell-to-cell communication. *BMB Reports*, *41*(**5**), 345–352.

Coisne, C., Dehouck, L., Faveeuw, C., Delplace, Y., Miller, F., Landry, C., …
others. (2005). Mouse syngenic in vitro blood–brain barrier model: a new
tool to examine inflammatory events in cerebral endothelium. *Laboratory
Investigation*, **85**(**6**), 734–746.

Cuadrado, A., García-Fernández, L. F., González, L., Suárez, Y., Losada, A.,
Alcaide, V., Muñoz, A. (2003). AplidinTM induces apoptosis in human
cancer cells via glutathione depletion and sustained activation of the
epidermal growth factor receptor, Src, JNK, and p38 MAPK. *Journal of
Biological Chemistry*, **278**(**1**), 241–250.

Daneman, R., & Prat, A. (2015). The blood-brain barrier. *Cold Spring Harbor
Perspectives in Biology*, **7**(**1**), a020412.

Day, R. M., & Suzuki, Y. J. (2005). Cell Proliferation, Reactive Oxygen and
Cellular Glutathione. *Nonlinearity in Biology, Toxicology, Medicine*, **3**(**3**),
1559-3258.

Deane, R., & Zlokovic, B. V. (2007). Role of the blood-brain barrier in the
pathogenesis of Alzheimer's disease. *Curr Alzheimer Res,* **4**(**2**), 191-197.

Dickinson, D. A., & Forman, H. J. (2002). Cellular glutathione and thiols
metabolism. *Biochemical Pharmacology*, **64**(**5–6**), 1019–1026.

Dringen, R. (2000). Metabolism and functions of glutathione in brain. *Progress in Neurobiology*, *62***(6)**, 649–671.

Ellman, G. L. (1959). Tissue sulfhydryl groups. *Archives of Biochemistry and Biophysics, 82***(1)**, 70-77.

Elmore, S. (2007). Apoptosis: A Review of Programmed Cell Death. *Toxicologic pathology, 35***(4)**, 495-516.

Emerit, J., Edeas, M., & Bricaire, F. (2004). Neurodegenerative diseases and oxidative stress. *Biomedicine & Pharmacotherapy*, *58***(1)**, 39–46.

Engelhardt, B., & Sorokin, L. (2009). The blood–brain and the blood–cerebrospinal fluid barriers: function and dysfunction. In *Seminars in immunopathology*, **31**, 497–511.

Findley, M. K., & Koval, M. (2009). Regulation and roles for claudin-family tight junction proteins. *IUBMB Life*, *61***(4)**, 431–437.

Fisher, D., Gamieldien, K., & Mafunda, P. S. (2015). Methamphetamine is not Toxic but Disrupts the Cell Cycle of Blood–Brain Barrier Endothelial Cells. *Neurotoxicity Research*, *28***(1)**, 8–17.

Freeman, L. R., & Keller, J. N. (2012). Oxidative stress and cerebral endothelial cells: regulation of the blood–brain-barrier and antioxidant-based

interventions. *Biochimica et Biophysica Acta (BBA)-Molecular Basis of Disease*, *1822***(5)**, 822–829.

Furuse, M., & Tsukita, S. (2006). Claudins in occluding junctions of humans and flies. *Trends in Cell Biology*, *16***(4)**, 181–188.

Gabathuler, R. (2010). Approaches to transport therapeutic drugs across the blood–brain barrier to treat brain diseases. *Neurobiology of Disease*, *37***(1)**, 48–57.

Garcia-Ruiz, C., & Fernandez-Checa, J. C. (2006). Mitochondrial glutathione: hepatocellular survival–death switch. *Journal of Gastroenterology and Hepatology*, *21***(s3)**, S3–S6.

Gilgun-Sherki, Y., Melamed, E., & Offen, D. (2001). Oxidative stress induced-neurodegenerative diseases: the need for antioxidants that penetrate the blood brain barrier. *Neuropharmacology, 40***(8)**, 959-975.

Gipp, J. J., Bailey, H. H., & Mulcahy, R. T. (1995). Cloning and Sequencing of the cDNA for the Light Subunit of Human Liver γ-Glutamylcysteine Synthetase and Relative RNA Levels for Heavy and Light Subunits in Human Normal Tissues. *Biochemical and Biophysical Research Communications*, *206***(2)**, 584–589.

Grant, G. A., Abbott, N. J., & Janigro, D. (1998). Understanding the Physiology of the Blood-Brain Barrier: In Vitro Models. *Physiology*, *13*(**6**), 287–293.

Guilford, F. T., & Hope, J. (2014). Deficient Glutathione in the Pathophysiology of Mycotoxin-Related Illness. *Toxins*, *6*(**2**), 608–623.

Hardin, B., Valentine, W. N., Follette, J. H., & Lawrence, J. S. (1954). Studies on the sulfhydryl content of hyman leukocytes and erythrocytes. *Am J Med Sci,* *228*(**1**), 73-82.

Hartmann, T. N., Fricker, M. D., Rennenberg, H., & Meyer, A. J. (2003). Cell-specific measurement of cytosolic glutathione in poplar leaves. *Plant, Cell & Environment*, *26*(**6**), 965–975.

Hawkins, B. T., & Davis, T. P. (2005). The blood-brain barrier/neurovascular unit in health and disease. *Pharmacological Reviews*, *57*(**2**), 173–185.

Hawkins, R. A., O'Kane, R. L., Simpson, I. A., & Viña, J. R. (2006). Structure of the blood–brain barrier and its role in the transport of amino acids. *The Journal of Nutrition*, *136*(**1**), 218S–226S.

Huber, J. D., Egleton, R. D., & Davis, T. P. (2001). Molecular physiology and pathophysiology of tight junctions in the blood-brain barrier. Trends Neurosci, **24(12)**, 719-725.

Huber, J. D., Hau, V. S., Borg, L., Campos, C. R., Egleton, R. D., & Davis, T. P. (2002). Blood-brain barrier tight junctions are altered during a 72-h exposure to λ-carrageenan-induced inflammatory pain. *American Journal of Physiology-Heart and Circulatory Physiology*, *283*(**4**), H1531–H1537.

Itoh, A., Uchiyama, A., Taniguchi, S. i., & Sagara, J. (2014). Phactr3/Scapinin, a Member of Protein Phosphatase 1 and Actin Regulator (Phactr) Family, Interacts with the Plasma Membrane via Basic and Hydrophobic Residues in the N-Terminus (Vol. 9).

Kaur, C., & Ling, E. A. (2008). Blood brain barrier in hypoxic-ischemic conditions. *Current Neurovascular Research*, *5*(**1**), 71–81.

Konstantoulaki, M., Kouklis, P., & Malik, A. B. (2003). Protein kinase C modifications of VE-cadherin, p120, and β-catenin contribute to endothelial barrier dysregulation induced by thrombin. *American Journal of Physiology-Lung Cellular and Molecular Physiology*, *285*(**2**), L434–L442.

Lash, L. H., Putt, D. A., & Jankovich, A. D. (2015). Glutathione Levels and Susceptibility to Chemically Induced Injury in Two Human Prostate Cancer Cell Lines. *Molecules, 20*(**6**), 10399-10414.

Lawther, B. K., Kumar, S., & Krovvidi, H. (2011). Blood–brain barrier. *Continuing Education in Anaesthesia, Critical Care & Pain*, **11**,128-132

Lee, F. Y. F., Siemann, D. W., Allalunis-Turner, M. J., & Keng, P. C. (1988). Glutathione Contents in Human and Rodent Tumor Cells in Various Phases of the Cell Cycle. *Cancer Research*, **48(13)**, 3661-3665.

Lee, H., Lee, K., Jung, J.-K., Cho, J., & Theodorakis, E. A. (2005). Synthesis and evaluation of 6-hydroxy-7-methoxy-4-chromanone- and chroman-2-carboxamides as antioxidants. *Bioorganic & Medicinal Chemistry Letters*, *15*(**11**), 2745–2748.

Lehner, C., Gehwolf, R., Tempfer, H., Krizbai, I., Hennig, B., Bauer, H. C., & Bauer, H. (2011). Oxidative stress and blood-brain barrier dysfunction under particular consideration of matrix metalloproteinases. *Antioxid Redox Signal, 15*(**5**), 1305-1323.

Leier, I., Jedlitschky, G., Buchholz, U., Center, M., Cole, S. P., Deeley, R. G., & Keppler, D. (1996). ATP-dependent glutathione disulphide transport mediated by the MRP gene-encoded conjugate export pump. *Biochem J, 314 (Pt 2)*, 433-437.

Li, W., Busu, C., Circu, M. L., & Aw, T. Y. (2012). Glutathione in cerebral microvascular endothelial biology and pathobiology: implications for brain homeostasis. *International Journal of Cell Biology*, *2012*, 256-260.

Liebner, S., Czupalla, C. J., & Wolburg, H. (2011). Current concepts of blood-brain barrier development. *International Journal of Developmental Biology*, **55(4)**, 467.

Lippmann, E. S., Azarin, S. M., Kay, J. E., Nessler, R. A., Wilson, H. K., Al-Ahmad, A., … Shusta, E. V. (2012). Derivation of blood-brain barrier endothelial cells from human pluripotent stem cells. *Nature Biotechnology*, **30(8)**, 783–791.

Lossinsky, A. S., & Shivers, R. R. (2004). Structural pathways for macromolecular and cellular transport across the blood-brain barrier during inflammatory conditions. Review. *Histology and Histopathology*, **19(2)**, 535–564.

Lu, S. C. (1999). Regulation of hepatic glutathione synthesis: current concepts and controversies. *The FASEB Journal*, **13(10)**, 1169–1183.

Lu, S. C. (2009). Regulation of glutathione synthesis. *Molecular Aspects of Medicine*, **30(1)**, 42–59.

Lum, H., & Malik, A. B. (1994). Regulation of vascular endothelial barrier function. *Am J Physiol, **267(3 Pt 1)**, L223-241.

Lum, H., & Roebuck, K. A. (2001). Oxidant stress and endothelial cell dysfunction. *American Journal of Physiology-Cell Physiology*, *280*(**4**), C719–C741.

Lundquist, S., Renftel, M., Brillault, J., Fenart, L., Cecchelli, R., & Dehouck, M.-P. (2002). Prediction of Drug Transport Through the Blood-Brain Barrier in Vivo: A Comparison Between Two in Vitro Cell Models. *Pharmaceutical Research*, *19*(**7**), 976–981.

Machado, M. D., & Soares, E. V. (2012). Assessment of cellular reduced glutathione content in Pseudokirchneriella subcapitata using monochlorobimane. *Journal of Applied Phycology*, *24*(**6**), 1509–1516.

Malaeb, S. N., Cohen, S. S., Virgintino, D., & Stonestreet, B. S. (2012). Core Concepts Development of the Blood-Brain Barrier. *NeoReviews*, *13*(**4**), e241–e250.

Markovic, J., Mora, N. J., Broseta, A. M., Gimeno, A., de-la-Concepción, N., Viña, J., & Pallardó, F. V. (2009). The Depletion of Nuclear Glutathione Impairs Cell Proliferation in 3t3 Fibroblasts. PLoS ONE, **4(7),** e6413.

Malorni, W., Iosi, F., Mirabelli, F., & Bellomo, G. (1991). Cytoskeleton as a target in menadione-induced oxidative stress in cultured mammalian cells:

Alterations underlying surface bleb formation. *Chemico-Biological Interactions, 80*(**2**), 217-236.

McClain, D. E., Kalinich, J. F., & Ramakrishnan, N. (1995). Trolox inhibits apoptosis in irradiated MOLT-4 lymphocytes. *The FASEB Journal*, *9*(**13**), 1345–1354.

Mentor, S., & Fisher, D. (2017). Aggressive Antioxidant Reductive Stress Impairs Brain Endothelial Cell Angiogenesis and Blood Brain Barrier Function. *Current Neurovascular Research*, *14*(**1**), 71–81.

Mirabelli, F., Salis, A., Marinoni, V., Finardi, G., Bellomo, G., Thor, H., & Orrenius, S. (1988). Menadione-induced bleb formation in hepatocytes is associated with the oxidation of thiol groups in actin. *Archives of Biochemistry and Biophysics, 264*(**1**), 261-269.

Moinova, H. R., & Mulcahy, R. T. (1998). An Electrophile Responsive Element (EpRE) Regulates β-Naphthoflavone Induction of the Human γ-Glutamylcysteine Synthetase Regulatory Subunit Gene CONSTITUTIVE EXPRESSION IS MEDIATED BY AN ADJACENT AP-1 SITE. *Journal of Biological Chemistry*, *273*(**24**), 14683–14689.

Monticone, M., Taherian, R., Stigliani, S., Carra, E., Monteghirfo, S., Longo, L., … Castagnola, P. (2014). NAC, Tiron and Trolox Impair Survival of Cell

Cultures Containing Glioblastoma Tumorigenic Initiating Cells by
Inhibition of Cell Cycle Progression. *PLOS ONE*, *9*(**2**), e90085.

Moosmann, B., & Behl, C. (2002). Antioxidants as treatment for
neurodegenerative disorders. *Expert Opinion on Investigational Drugs,*
11(**10**), 1407-1435.

Nakagawa, S., Deli, M. A., Nakao, S., Honda, M., Hayashi, K., Nakaoke, R., …
Niwa, M. (2007). Pericytes from brain microvessels strengthen the barrier
integrity in primary cultures of rat brain endothelial cells. *Cellular and*
Molecular Neurobiology, *27*(**6**), 687–694.

Ortega, A. L., Mena, S., & Estrela, J. M. (2011). Glutathione in cancer cell death.
Cancers (Basel), 3(**1**), 1285-1310.

Paolinelli, R., Corada, M., Ferrarini, L., Devraj, K., Artus, C., Czupalla, C. J., …
Dejana, E. (2013). Wnt Activation of Immortalized Brain Endothelial
Cells as a Tool for Generating a Standardized Model of the Blood Brain
Barrier In Vitro. *PLOS ONE*, *8*(**8**), e70233.

Pardridge, W. M. (1995). Transport of small molecules through the blood-brain
barrier: biology and methodology. *Advanced Drug Delivery Reviews*,
15(**1**), 5–36.

Pardridge, W. M. (2003). Blood-brain barrier drug targeting: the future of brain drug development. *Molecular Interventions*, *3*(**2**), 90.

Pfeiffer, F., Schäfer, J., Lyck, R., Makrides, V., Brunner, S., Schaeren-Wiemers, N., … Engelhardt, B. (2011). Claudin-1 induced sealing of blood–brain barrier tight junctions ameliorates chronic experimental autoimmune encephalomyelitis. *Acta Neuropathologica*, *122*(**5**), 601–614.

Plateel, M., Dehouck, M.-P., Torpier, G., Cecchelli, R., & Teissier, E. (1995). Hypoxia increases the susceptibility to oxidant stress and the permeability of the blood-brain barrier endothelial cell monolayer. *Journal of Neurochemistry*, *65*(**5**), 2138–2145.

Popescu, B. O. (2013). Triggers and effectors of oxidative stress at blood-brain barrier level: relevance for brain ageing and neurodegeneration. *Oxidative Medicine and Cellular Longevity*, *2013*, 786-798.

Rahman, K. (2007) Studies on free radical, antioxidants and co-factors. *Clinical Intervention in Aging* **2**(**20**), 219-236.

Rao, A. V., & Balachandran, B. (2002). Role of Oxidative Stress and Antioxidants in Neurodegenerative Diseases. *Nutritional Neuroscience,* *5*(**5**), 291-309.

Reiss, Y., Hoch, G., Deutsch, U., & Engelhardt, B. (1998). T cell interaction with ICAM-1-deficient endothelium in vitro: essential role for ICAM-1 and ICAM-2 in transendothelial migration of T cells. *European Journal of Immunology*, *28*(**10**), 3086–3099.

Röhnelt, R. K., Hoch, G., Rei\s s, Y., & Engelhardt, B. (1997). Immunosurveillance modelled in vitro: naive and memory T cells spontaneously migrate across unstimulated microvascular endothelium. *International Immunology*, *9*(**3**), 435–450.

Romanitan, M. O., Popescu, B. O., Spulber, Ş., Băjenaru, O., Popescu, L., Winblad, B., … others. (2010). Altered expression of claudin family proteins in Alzheimer's disease and vascular dementia brains. *Journal of Cellular and Molecular Medicine*, *14*(**5**), 1088–1100.

Sambuy, Y. (2009). A sideways glance. Alcoholic breakdown of barriers: how ethanol can initiate a landslide towards disease. *Genes & Nutrition*, *4*(**2**), 77–81.

SCHERER, C., CRISTOFANON, S., DICATO, M., DIEDERICH, M., & others. (2008). Homogeneous luminescence-based assay for quantifying the glutathione content in mammalian CELLS. EDITOR'S DESK. Retrieved from.

Schreibelt, G., Kooij, G., Reijerkerk, A., van Doorn, R., Gringhuis, S. I., van der Pol, S., … others. (2007). Reactive oxygen species alter brain endothelial tight junction dynamics via RhoA, PI3 kinase, and PKB signaling. *The FASEB Journal*, *21*(**13**), 3666–3676.

Schrot, S., Weidenfeller, C., Schäffer, T. E., Robenek, H., & Galla, H.-J. (2005). Influence of hydrocortisone on the mechanical properties of the cerebral endothelium in vitro. *Biophysical Journal*, *89*(**6**), 3904–3910.

Shelton, P., & Jaiswal, A. K. (2013). The transcription factor NF-E2-related factor 2 (Nrf2): a protooncogene? *The FASEB Journal*, *27*(**2**), 414–423.

Song, J., Kang, S. M., Lee, W. T., Park, K. A., Lee, K. M., & Lee, J. E. (2014). Glutathione protects brain endothelial cells from hydrogen peroxide-induced oxidative stress by increasing nrf2 expression. *Experimental Neurobiology*, *23*(**1**), 93–103.

Stadtman, E. R., & Levine, R. L. (2000). Protein Oxidation. *Annals of the New York Academy of Sciences*, *899*(**1**), 191–208.

Steiner, O., Coisne, C., Engelhardt, B., & Lyck, R. (2011). Comparison of immortalized bEnd5 and primary mouse brain microvascular endothelial cells as in vitro blood-brain barrier models for the study of T cell extravasation. *Journal of Cerebral Blood Flow and Metabolism: Official*

Journal of the International Society of Cerebral Blood Flow and

Metabolism, *31***(1)**, 315–327.

Steiner, O., Coisne, C., Engelhardt, B., & Lyck, R. (2011b). Comparison of

immortalized bEnd5 and primary mouse brain microvascular endothelial

cells as in vitro blood–brain barrier models for the study of T cell

extravasation. *Journal of Cerebral Blood Flow & Metabolism*, *31***(1)**, 315–

327.

Stolp, H. B., & Dziegielewska, K. M. (2009). Review: role of developmental

inflammation and blood–brain barrier dysfunction in neurodevelopmental

and neurodegenerative diseases. *Neuropathology and Applied*

Neurobiology, *35***(2)**, 132–146.

Strober, W. (2001). Trypan blue exclusion test of cell viability. Curr Protoc

Immunol, Appendix 3, Appendix 3B. doi:10.1002/0471142735.ima03bs21

Tietze, F. (1969). Enzymic method for quantitative determination of nanogram

amounts of total and oxidized glutathione: applications to mammalian

blood and other tissues. *Anal Biochem, 27***(3)**, 502-522.

Tobwala, S., Wang, H.-J., Carey, J. W., Banks, W. A., & Ercal, N. (2014). Effects

of Lead and Cadmium on Brain Endothelial Cell Survival, Monolayer

Permeability, and Crucial Oxidative Stress Markers in an in Vitro Model

of the Blood-Brain Barrier. *Toxics*, *2***(2)**, 258–275.

Tousoulis, D., Kampoli, A.-M., Tentolouris Nikolaos Papageorgiou, C., & Stefanadis, C. (2012). The role of nitric oxide on endothelial function. *Current Vascular Pharmacology*, *10*(**1**), 4–18.

Traverso, N., Ricciarelli, R., Nitti, M., Marengo, B., Furfaro, A. L., Pronzato, M. A., Domenicotti, C. (2013). Role of Glutathione in Cancer Progression and Chemoresistance. *Oxidative Medicine and Cellular Longevity, 2013*, 875-885.

Turrens, J. F. (2003). Mitochondrial formation of reactive oxygen species. *The Journal of Physiology*, *552*(**2**), 335–344.

Vorbrodt, A. W., & Dobrogowska, D. H. (2003). Molecular anatomy of intercellular junctions in brain endothelial and epithelial barriers: electron microscopist's view. *Brain Research Reviews*, *42*(**3**), 221–242.

Weidenfeller, C., Schrot, S., Zozulya, A., & Galla, H.-J. (2005). Murine brain capillary endothelial cells exhibit improved barrier properties under the influence of hydrocortisone. *Brain Research*, *1053*(**1–2**), 162–174.

Weiss, N., Miller, F., Cazaubon, S., & Couraud, P.-O. (2009). The blood-brain barrier in brain homeostasis and neurological diseases. *Biochimica et Biophysica Acta (BBA)-Biomembranes*, *1788*(**4**), 842–857.

Wild, A. C., & Mulcahy, R. T. (2000). Regulation of gamma-glutamylcysteine synthetase subunit gene expression: insights into transcriptional control of antioxidant defenses. *Free Radical Research*, *32*(**4**), 281–301.

Wilhelm, I., Fazakas, C., & Krizbai, I. A. (2011). In vitro models of the blood-brain barrier. *Acta Neurobiol Exp (Wars)*, *71*(**1**), 113–28.

Wolburg, H., & Lippoldt, A. (2002). Tight junctions of the blood–brain barrier: development, composition and regulation. *Vascular Pharmacology*, *38*(**6**), 323–337.

Wu, D., Cederbaum, A. I., & others. (2003). Alcohol, oxidative stress, and free radical damage. *Alcohol Research and Health*, *27*, 277–284.

Wu, G., Fang, Y.-Z., Yang, S., Lupton, J. R., & Turner, N. D. (2004). Glutathione Metabolism and Its Implications for Health. *The Journal of Nutrition*, *134*(**3**), 489–492.

Yang, T., Roder, K. E., & Abbruscato, T. J. (2007). Evaluation of bEnd5 cell line as an in vitro model for the blood-brain barrier under normal and hypoxic/aglycemic conditions. *Journal of Pharmaceutical Sciences*, *96*(**12**), 3196–3213.

Yuan, Y., Zhang, J., Wang, M., Mei, B., Guan, Y., & Liang, G. (2013). Detection
of glutathione in vitro and in cells by the controlled self-assembly of
nanorings. *Anal Chem, 85***(3)**, 1280-1284.

Zhang, D. X., & Gutterman, D. D. (2007). Mitochondrial reactive oxygen species-
mediated signaling in endothelial cells. *American Journal of Physiology-
Heart and Circulatory Physiology*, *292***(5)**, H2023–H2031.

Zhao, Y., Cui, J.-G., & Lukiw, W. J. (2006). Natural secretory products of human
neural and microvessel endothelial cells. *Molecular Neurobiology*, *34***(3)**,
181–192.

Zlokovic, B. V. (2008). The blood-brain barrier in health and chronic
neurodegenerative disorders. *Neuron*, *57***(2)**, 178–201.
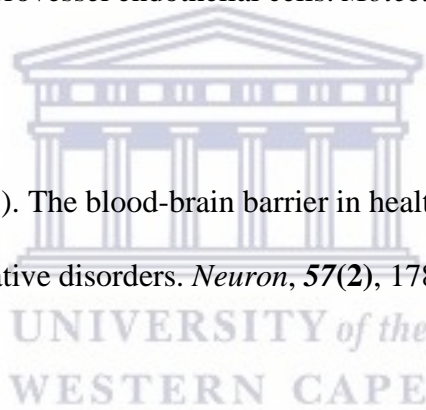
5.4 Web-based references

Figure 2.3 Chapter: 2 2.7 Protective effect of Trolox against H₂O₂ toxicity and GSH depletion

http://www.lookchem.com/Trolox-C/ [Accessed 29 September 2017]

Figure 2.2: Chapter: 2 2.5.3.1 Description for GSH-Glo^{TM} Glutathione assay

https://worldwide.promega.com [Accessed 29 September 2017]

Table 1. Series concentration of H_2O_2 (0.05-5 mM) was prepared for the ROS neutralising capacity of bEnd5 cells by marking 12 conical tubes A-L. The stock solution was diluted as follows to make a series concentration of H_2O_2 in the table below:

Tube	H_2O_2 stock solution (µl)	Media (ml)	Concentration (mM)
A	0	32ml	Ctrl
B	25.5	49.975	5
C	9000	9	2.5
D	7200	10.8	2
I	5400	12.6	1.5
F	3600	14.4	1
G	1800	16.2	0.5
H	500	17.5	0.25
I	750	17.28	0.2
J	240	17.76	0.15
K	360	17.64	0.1
L	180	17.82	0.05

Table 2. Effect of exposure to selected concentrations of H_2O_2 (50 -2500 µM) on the GSH_T, GSH and GSSG levels in bEnd5 cells by using the GSH-Glo Assay Kit method and the modified GSH recycling method of Tietze respectively (Tietze, 1969) at selected time intervals (24 hours) (mean±SEM; n=4).

H_2O_2 concentrations in µM	GSH_T	GSH	GSSG
Ctrl	1028619±3828.5	971323±24885.5	57296.0±23914.
50	1368827±20967	1228695±9985	140132±30452
150	1406145±18925	1215764±28793.5	190381.5±39718.5
250	1337500±17940	1130065±29075	207435±8935
500	1276680±18719.5	1087735±30535	188944.5± 49254.5
1500	662193±14000	327243±43590	334950±36590
2500	634640±3710	300535±5935.	334105±3025

Table 3. Effect of exposure to selected concentrations of H_2O_2 (50 -2500 µM) on the GSH_T, GSH and GSSG levels in bEnd5 cells by using the GSH-Glo Assay Kit method and the modified GSH recycling method of Tietze respectively (Tietze, 1969) at selected time intervals (48 hours) (mean±SEM; n=4).
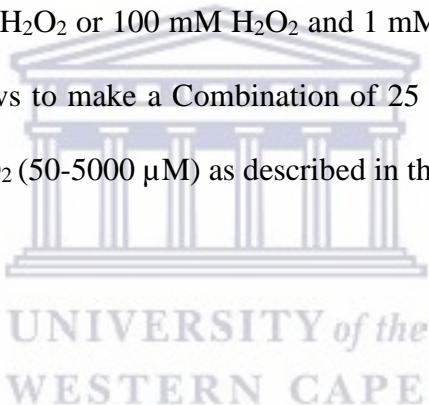
H_2O_2 concentrations in µM	*GSH_T*	*GSH*	*GSSG*
Ctrl	1142251±30358	1183658±100760	
50	1826510±99960	1644086±99914	182424±4666
150	1993515±193988	1471091±101100	522424.5±92888
250	1964906±204880	1408606±200091	681309±4789
500	1757661±210285	1231263±199895	526398± 41010
1500	722286±199584	368366±70004	353920±26988
2500	722031±101199	370546.5±100172	351484.5±20171

123

APPENDIX C

Table 4. Combination of 25 µM Trolox and increasing concentrations of H_2O_2 (50-5000 µM) was prepared for the protective effect of Trolox against H_2O_2 toxicity and GSH depletion in bEnd5 cells was prepared. the first 1 mM of Trolox was prepared by dissolving 0.0025g in 1 ml of DMSO and then made it up to 10 ml with the medium. 1.9 ml of 100 mM H_2O_2 stocks were prepared by added 19.4µl of H_2O_2 stock to 1.881 ml of the medium. 15 ml of 1 mM H_2O_2 was prepared by added 150µl of 100 mM H_2O_2 to 14,85 ml of the medium. Then 25 µM Trolox and increasing concentrations of H_2O_2 (50-5000 µM) was prepared by marking 11 conical tubes A-K tube. The 1 mM H_2O_2 or 100 mM H_2O_2 and 1 mM of Trolox stocks solution were diluted as follows to make a Combination of 25 µM Trolox and increasing concentrations of H_2O_2 (50-5000 µM) as described in the table below:

+

Tube	H_2O_2 concentrations (µM)	Medium (ml)	1 mM of H_2O_2 stock solution (µl)	100 mM of H_2O_2 stock solution (µl)	1 mM Trolox stock solution (µl)
A	50	14.8	0.8	-	400
B	100	14	1.6	-	400

124

C	150	13.2	2.4	-	400
D	200	12.4	3.2	-	400
E	250	11.6	4	-	400
F	500	15.52	-	80	400
G	1000	15.44	-	160	400
H	1500	15.36	-	240	400
I	2000	15.28	-	320	400
J	2500	15.2	-	400	400
K	5000	14.8	-	800	400
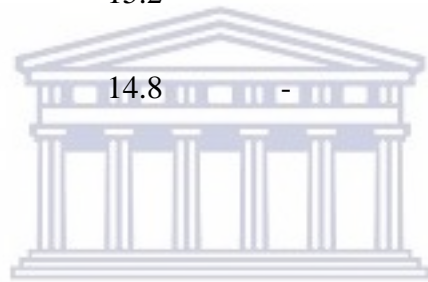
APPENDIX D

Table 5. Effect of exposure to combination of 25 µM Trolox and increasing concentrations of H_2O_2 (50-2500 µM) against H_2O_2 toxicity and GSH depletion in bEnd5 cells by using the GSH-Glo Assay Kit method and the modified GSH recycling method of Tietze respectively (Tietze, 1969). At selected time intervals (24 hours) (mean±SEM; n=4).

H_2O_2 concentrations in µM	GSH_T	GSH	GSSG
Ctrl	1028619 ± 3528.5	971323±24385	57296±27914
Ctrl T	1026139±11868.5	978791±18800.5	47348±6932
50	1368827±19967	1228695±9485	140132±29452
50 T	1331785±53765	1218248±5772	113537±59537
150	1406145±13925	1215764±23793	190382±37718.5
150 T	1372835±6675	1214671±70981	158164±7765
250	1337500±12940	1130065±21075	207435±8135
250 T	1330443±3797	1151780±29300	178663±33097
500	1276680±17719.5	1087735±29535	188945±47254.5
500 T	1257932±5738.5	1076575±24285	181357±30023.5
1500	662193±10000	334950±43590	327243±33590
1500T	638287±392.5	303725±33600	334562±44190

H2O2			
2500	634640±3410	300535±2125	334105±5535
2500T	633412±5441.844	308170±17155.840	325242±11714

Table 6. Effect of exposure to combination of 25 µM Trolox and increasing concentrations of H_2O_2 (50-2500 µM) against H_2O_2 toxicity and GSH depletion in bEnd5 cells by using the GSH-Glo Assay Kit method and the modified GSH recycling method of Tietze respectively (Tietze, 1969). At selected time intervals 48 hours (mean±SEM; n=4) (Chatterjee, Noack, Possel, Keilhoff, & Wolf, 1999).

H_2O_2 concentrations in µM	GSH_T	GSH	GSSG
Ctrl	1183658±88449	1142251±92672.6	41407±323.5
Ctrl T	1217255±96425	1153622±90648.5	63634±3450
50	1815710±154970	1630075±138126	185635±15944
50 T	1826510±159844	1644086±138126	182424±3420
150	1993515±49075	1471091± 64959.5	522425±15684.5
150 T	1993525±120365	1483390±83767.6	510136±5430
250	1964906±164880	1408606±104146	556301±7760
250 T	1977610±242790	1417759±103335	559852±2360
500	1757661±150286	1231263±10959	526398±5420
500 T	1746176±150505	1220244±15505	525933±5430

127

1500	722286±47066.	353920± 3402	368366±6870
1500T	710195±45299	340894±12326.5	369302±7050
2500	722031±49801	351485±6522	370547±6820
2500T	713154±46824	343634±13185.5	369521±3440